Soil Carbon Dioxide dynamics and Nitrogen cycling in an Eastern Amazonian Rainforest, Caxiuanã, Brazil

Dissertation

Submitted for the Degree of

Doctor of Forestry and Forest Ecology

of Georg-August-University of Göttingen

by

Eleneide Doff Sotta

From Curitiba, Brazil

Göttingen, June 2006

Referee: Prof. Dr. Edzo Veldkamp

Coreferee: Prof. Dr. Gode Gravenhorst

Day of Oral Examination: 11.07.2006

Table of Contents

Table of Contents iii

List of Figures vii

List of Tables viii

List of Abbreviations and Symbols ix

1. Introduction 1

1.1. Problem analysis 1

1.2. Future projections 3

Intensification of ENSO in the Amazon region *3*

Increase in N_2O emissions to the atmosphere from Amazon soils *5*

1.3. Objectives of the study 6

1.4. Site description 7

Characteristics of Amazon forest soils, vegetation and climate *7*

General design of the study *8*

1.5. Overview of the thesis 9

2. Landscape and climatic controls on spatial and temporal variation in soil CO_2 efflux in an Eastern Amazonian Rainforest, Caxiuanã, Brazil. 10

2.1. Introduction 10

2.2. Materials and Methods 12

Study site *12*

Design of experiment to measure effect of soil texture *13*

Design of experiment to measure effect of topography *14*

Design of experiment to measure contribution of litter layer *14*

Measurements of soil CO_2 efflux *15*

Complementary measurements *15*

Calculations and Statistical analyses *17*

2.3. Results 17

Variation in soil CO_2 efflux caused by differences in soil texture *17*

Spatial variation in soil CO_2 efflux caused by topography *18*

Temporal variation in soil CO_2 efflux caused by the litter layer *21*

Correlations with environmental factors *23*

2.4. Discussion 23

Magnitude of CO_2 efflux and spatial variation *23*

Temporal variation in CO_2 efflux *25*

Estimating annual landscape scale CO_2 efflux *26*

3. Effects of an induced drought on the soil CO_2 production and soil CO_2 efflux in an Eastern Amazonian Rainforest, Brazil. 28

3.1. Introduction 28

3.2. Materials and Methods 29

Study site *29*

Experimental design *31*

Measurements of soil CO_2 efflux *31*

Measurements of CO_2 concentration profiles *33*

Measurements of soil radon activity and radon production *33*

Calculation of CO_2 production *34*

Environmental measurements *38*

Statistical analyses *39*

3.3. Results 39

Magnitude and seasonality of soil CO_2 efflux and CO_2 production *39*

Soil CO_2 concentrations *43*

Environmental parameters 43

Effects of environmental parameters on soil CO_2 efflux and on CO_2 production 45

3.4. Discussion 47

Effects of seasonality on soil CO_2 production and emission 47

Effects of throughfall exclusion on soil CO_2 efflux and CO_2 production 48

Comparison with the drought experiment in Santarém and consequences for drought sensitivity 50

4. Mechanisms of soil N retention in an Eastern Amazonian Rainforest, Caxiuanã, Brazil. 52

4.1. Introduction 52

4.2. Methods 54

Site Description 54

Sampling design 55

^{15}N pool dilution for measurement of gross rates of N mineralization and nitrification 57

N concentration and ^{15}N analyses 58

Dissimilatory nitrate reduction to ammonium (DNRA) 60

NH_4^+ and NO_3^- immobilization rates and microbial biomass C and N by chloroform fumigation 60

Calculation of mean residence time (MRT) 62

Other supporting parameters 62

Statistical Analyses 64

4.3. Results 64

^{15}N recovery from intact cores 10 minutes (T_0) after ^{15}N injection 64

Gross rates of NH_4^+ transformation, microbial biomass, and available C 65

$\delta^{15}N$ signals and enrichment factor (ε) 67

Gross rates of NO_3^- transformation, dissimilatory nitrate reduction to ammonium (DNRA), and N_2O emissions *69*

4.4. Discussion 71

Implications of Rapid Reactions of injected $^{15}NH_4^+$ and $^{15}NO_3^-$ to organic N *71*

Gross rates of NH_4^+ transformation processes, enrichment factor (ε) and implications to soil N status *72*

Gross rates of NO_3^- transformation, dissimilatory nitrate reduction to ammonium (DNRA), and implications for N losses *74*

Mean residence time (MRT) and implication for N losses *76*

4.5. Conclusions 77

5. Summarizing synthesis 79

5.1. Landscape and climatic controls on spatial and temporal variation 79

5.2. Effects of induced drought on soil CO_2 production and soil CO_2 efflux 81

5.3. Mechanisms of soil N retention 82

5.4. Belowground CO_2 dynamics and N cycling 83

6. Zusammenfassung 87

7. Summary 90

8. References 93

9. Appendix 115

Acknowledgements 119

List of Figures

2.1 Soil CO_2 efflux, soil water content and soil temperature in sandy and clay sites.

2.2 Measurements of soil CO_2 efflux, soil temperature at 0.05 m depth and soil water content at 0.30 m depth in topographic positions.

2.3 Soil CO_2 efflux from forest floor without litter, with normal amount of litter and double the normal amount of litter.

2.4 Relationship between soil water content and soil CO_2 efflux and between soil water content and soil temperature at 0.05 m depth in sandy and clay sites.

3.1 Depth profiles of simulated and measured radon activity.

3.2 Temporal variation of soil CO_2 efflux, soil water content at 0.3 m depth in control and TFE plots and bi-weekly rainfall.

3.3 Temporal variation in CO_2 production rates.

3.4 Isopleths of CO_2 concentration in soil air.

3.5 Relationship between soil water potential and soil CO_2 efflux and between soil water potential and soil temperature in control and TFE plots.

4.1 Percent recovery of ^{15}N in soil N pools.

4.2 Means of gross rates of microbial N cycling, of N pools, and of mean residence time.

4.3 Variation in natural abundance of ^{15}N for clayey and sandy soil.

5.1 Diagrammatic representation of the carbon and nitrogen cycles

List of Tables

2.1 Characterization of chemical and physical properties of the sand and clay soil.

2.2 Correlation among sites, seasons, CO_2 efflux and environmental factors.

3.1 Characterization of chemical and physical properties of the soil of the TFE experiment.

3.2 Contribution of the subsoil (0.6-3.0 m depth) to the total CO_2 production.

4.1 Main characteristics of the forest sites in Caxiuana, Brazil.

4.2 Microbial C, available C, water filled pore space (WFPS) and rates of N_2O emission.

A1 Soil CO_2 efflux, soil temperature at 0.05 m depth (*Ts*) and soil water content (*swc*) at 0.3 m depth in sand and clay soil textures

A2 Soil CO_2 production (P_{CO2}), soil temperature (*Ts*) and soil water content (*swc*) in control and throughfall exclusion (TFE) plot

List of Abbreviations and Symbols

C	carbon
C:N	carbon : nitrogen ratio
CO_2	carbon dioxide
DNRA	dissimilatory nitrate reduction to ammonia
DOC	dissolved organic carbon
ECEC	effective cation exchange capacity
ENSO	El Nino Southern Oscillation
FDR	frequency domain reflectometry
IRMS	isotope ratio mass spectrometry
LAI	leaf area index
LBA	Large Scale Biosphere Atmosphere Experiment in Amazonia
Mg	Megagrams
MPEG	Museu Paraense Emilio Goeldi
MRT	mean residence time
N	nitrogen
N_2O	nitrous oxide
NEE	net ecosystem exchange
NH_4^+	ammonia
NO_3^-	nitrate
NPP	net primary productivity
PAR	photosynthetically active radiation
Pg	Petagrams
SOC	soil organic carbon
T_0	core extracted 10 minutes after the injection

T_1	core extracted 1-2 days after the injection	
TCD	thermal conductivity detector	
TDR	time domain reflectometry	
TFE	through-fall exclusion	
Tg	Tones	
WFPS	water filled pore space	
x	determined from the relation $a^{2x} + (1-a)^x = 1$	
y	exponent usually between 0.6 and 0.8	
z	exponent usually between 0.6 and 0.8	
a	air-filled porosity	m^3m^{-3}
a_{100}	air-filled porosity at -100 cm H_2O	m^3m^{-3}
a_{er}	inter-aggregated air-filled pore space	m^3m^{-3}
a_{ra}	intra-aggregated air-filled pore space	m^3m^{-3}
b	pore-size distribution	
D_o	diffusion coefficient of the same gas in free air	
D_s	diffusion coefficient of a gas in soil air	
δs	$\delta^{15}N$ value at different depths in the soil profile	‰
δso	$\delta^{15}N$ value of the input substrate	‰
E	soil CO_2 efflux	µmol CO_2 m^{-2} s^{-1}
ε	total porosity	m^3m^{-3}
ε	enrichment factor	‰
$\varepsilon_{\rho\varepsilon}$	inter-aggregated total pore space	m^3m^{-3}
$\varepsilon_{\alpha\rho}$	intra-aggregated total pore space	m^3m^{-3}
f	remaining fraction of total N	‰

P_{CO2}	soil CO_2 production	µmol CO_2 m^{-2} s^{-1}
θ	volumetric water content.	m^3m^{-3}
swc	soil water content	m^3m^{-3}
Ts	Soil temperature	° C
Ψ	water potential	kPa
$\delta^{15}N$	delta^{15}N	‰

k_C	0.45
k_N	0.68

1. Introduction

1.1. Problem analysis

At the present, there is no doubt that the composition of the atmosphere and reactions among atmospheric constituents are changing as a result of human activities (Schlesinger 1997). Atmospheric concentrations of greenhouse gases have grown significantly since pre-industrial time (IPCC 1992). The concentration of CO_2 has increased from about 280 to almost 360 ppmv and N_2O from about 275 to about 310 ppbv. These trends can be attributed largely to human activities, mostly fossil fuel use, manufacturing and industrial processes, such as production of iron, steel, aluminium, ammonia, cement and other materials, land use change and agriculture (IPCC 1997). This increase of greenhouse gas concentrations leads to an additional warming of the atmosphere and the Earth's surface, and consequently a likely global rise in soil temperature. As a response to the higher soil temperature, soil respiration is expected to increase, in a rate of about 2.0 per 10° C rise in temperature (Schimel et al. 1994, McGuire et al. 1995). However, the effect of the higher temperature in the soil biochemical dynamics is yet not clear and it may differ between temperate and tropical areas.

The global carbon cycle is closely linked with climate, the water cycle, nutrient cycles, and the production of biomass through photosynthesis on land and in the oceans. Soil carbon is a major component of the terrestrial carbon cycle. Nearly all models of global climate change predict a loss of carbon from soils as a result of global warming (Schimel et al. 1994, McGuire et al. 1995). Global soil organic carbon storage in the top 3 m of soil is 2344 Pg C (Jobaggy and Jackson 2000), which is three times the amount of carbon in the atmosphere and five times the carbon stored in vegetation (Schlesinger et al. 2000). Thus small increases or decreases in the amount of carbon in soils could have a large impact on the atmospheric CO_2 concentration (Trumbore 2000). Soil CO_2 efflux is the major path by which carbon is lost

from the soil system. Soil CO_2 flux is a major flux in the global C cycle (60 Pg C yr^{-1}), second in magnitude to the fixation of carbon by land plants (120 Pg C yr^{-1}; Schlesinger et al. 2000). As a result of burning of fossil fuels (6 Pg C yr^{-1}) and deforestation (2 Pg C yr^{-1}) there is currently an anthropogenic input to the atmosphere of about 8 Pg of carbon each year as CO_2 (IPCC 2000). Of the 8 Pg C yr^{-1} emitted, only about 3 Pg of carbon remains in the atmosphere. The remaining carbon is dissolved in the ocean or taken up by photosynthesis and sequestered as biomass or organic matter in soil.

Additionally to the unknown soil C feedbacks to the increase of global temperature, the increase in N deposition may also affect soil CO_2 emissions (Brumme and Beese 1992, Gallardo and Schlesinger 1994). Apart from the influence on CO_2 emissions, N deposition may also have an effect on N_2O emissions. Current rates of atmospheric N deposition are in some cases large enough to saturate the biological demand for N within many ecosystems over time (Aber et al. 1995, Dise and Wright 1995) resulting in losses of N as soil gases.

N deposition has been of great concern, already for some time, in the industrialized world, primarily associated with N-oxide and ammonia emissions from combustion processes and agricultural activity (Hall and Matson 2003). However, the intensification of fossil fuel use and agricultural practices worldwide, including many tropical areas, has raised the concern of N deposition also in the developing world (Galloway et al. 1994, Matson et al. 1999). As well as in carbon cycle, nitrogen cycle is also linked to the rate of net primary production on land and in the sea (Vitousek and Howarth 1991). About 240 Tg of newly fixed N is delivered from the atmosphere to the Earth's land surface each year, 40 % by natural and 60 % by human-derived sources. Each year rivers carry about 36 Tg N from land to the sea (Wollast 1993), and humans additions of fixed nitrogen to the terrestrial biosphere have also resulted in marked increases in the nitrogen content of groundwater, especially in many agricultural areas (Spalding and Exner 1993). The remaining nitrogen is assumed to be lost by

denitrification in terrestrial soils and in wetlands, and during forest fires. Estimates of global denitrification in terrestrial ecosystems range from 13 to 233 Tg N yr^{-1} (Bowden 1986). Most of the loss occurs as N_2, but the small fraction that is lost as N_2O during nitrification and denitrification contributes significantly to the global budget of this gas.

N_2O is an effective greenhouse gas, and its concentration in the atmosphere is increasing by 0.25 % yr^{-1} due to human activity (IPCC 1996). This long-lived greenhouse gas has a per molecule radioactive forcing strength 200-300 times greater than CO_2 (Shine et al. 1990, 1995, Prather and Ehalt 2001). N_2O also contributes to stratospheric ozone destruction (Cicerone 1987). Recent estimates suggest that soil emissions of N_2O from humid tropical forests account for 20-50 % of all global sources of atmospheric N_2O (Prather et al. 1995, Potter et al. 1996). As these ecosystems are generally N saturated the N availability may exceed biological demand very rapidly and the excess of N will possibly result in even larger and more immediate losses of N (Verchot et al. 1999, Hall and Matson 2003).

Natural systems and biogeochemical cycles have historically maintained their pools in dynamic equilibrium. However with the current anthropogenic activities it is already possible to observe large shifts among terrestrial, oceanic and atmospheric pools (IPCC 1995). The disruption of the global C and N cycle by human activity in both developed and developing countries is one of the key environmental issues facing human populations as we move into the 21st century (Rustad et al. 2000).

1.2. Future projections

Intensification of ENSO in the Amazon region

Many global climate change models (Foley et al. 1996, Cramer et al. 2001) suggest strong reductions in precipitation in some tropical regions, particularly in Amazonia (Prentice

et al. 2000). As a result of the lower recirculation of water between the deforested biosphere and the atmosphere, the regional climate in the Amazon Basin may become drier (Shukla et al. 1990, Nobre at al. 1991, Costa and Foley 2000, Werth and Avisar 2002) with consequent reduction in forest area and net primary productivity (NPP). Added to that the development in the Amazon region has been accompanied by increasing forest fragmentation and poorly managed logging activities. Both fragmentation and logging increase the likelihood of fire escaping from managed systems into forest, especially during dry years often associated with El Nino (Keller et al. 2004). El Nino Southern Oscillation (ENSO) is responsible for a large part of the climate variability at interannual scales in Latin America (Foley et al. 2002). ENSO-related drought can desiccate large areas of Amazonian forest, creating the potential for large-scale forest fires. Such episodes are increasing in frequency and intensity, possibly in response to the accumulation of greenhouse gases in the atmosphere (Nepstad et al.1999, Timmermann et al. 1999).

Changes in precipitation could also affect emissions of carbon dioxide (CO_2) from the remaining forested soils (Davidson et al. 2004). However, besides the precipitation, changes in CO_2 concentration and soil temperature also play important roles in finding the equilibrium on the soil C pool. The full consequences of these changes are not yet well known. Increasing temperature may cause a net loss of soil organic carbon, increasing CO_2 concentration can stimulate NPP, thus adding extra carbon to the system and increasing total soil carbon storage (e.g. Kirschbaum 1993, King et al. 1997). Model results point to the existence of a positive feedback from warming to increased CO_2 concentration on decade to century time scales that to some extent counteracts the negative feedback due to the physiological effects of CO_2 (Prentice et al. 2000). Increased storage of carbon in soils could help offset further anthropogenic emissions of CO_2, whereas a release could significantly exacerbate the atmospheric increases (Eswaran et al. 1993).

Ecosystem models which include soil carbon and nitrogen cycling predict carbon turnover times of less than a decade for most of the carbon in the upper 20 to 30 cm of moist tropical forest soils (Potter et al. 1993, Schimel et al. 1994). It is also expected that increased flux of CO_2 from soils resultant from disturbance or global warming will largely derive from labile pools with the fastest turnover times. Hence, the greatest losses of soil carbon will probably be seen in tropical regions (Trumbore et al. 1996). This is of concern as the amount of carbon stored in the upper meter of tropical soils is estimated to be 13-17 % of global soil carbon storage (Sombroek et al.1993), and the Amazon forest in Brazil alone contains ~210 Pg of this carbon (Houghton et al. 2001).

Increase in N_2O emissions to the atmosphere from Amazon soils

Nitrogen availability is especially high in clay-rich, weathered tropical soils where N does not limit plant growth (Martinelli et al. 1999). The rapid cycling on nitrogen supports large emissions of the greenhouse gas nitrous oxide (N_2O) (Keller et al. 2004). Emissions of N_2O from the forests of the Amazon Basin account for ~0.8-1.3 Tg N yr^{-1}, or nearly 10-15 %, of the global natural emissions of that gas (Melillo et al. 2001). Because increased anthropogenic N deposition (as is projected for large areas in the tropics) may result in larger and more immediate losses of N as soil gases (nitrous oxide, nitric oxide, dinitrogen) or as NO_3^- in solution (Hall and Matson 2003), perturbations of the Amazon tropical forest may be expected to have a major impact on global concentrations of N_2O, with consequent effects on the chemistry of the stratosphere and on the heat budget of the atmosphere (Myers 1980, Fearnside 1986, Keller et al. 1988).

However, mechanisms of soil N retention may exert a strong influence on the size and timing of these losses. Despite the high denitrification potential of humid tropical forests, N retention may be favoured in the presence of high C-to-NO_3^- ratio (Silver et al. 2005). The

relative balance between NO_3^- reduction to NH_4^+ via dissimilatory nitrate reduction to ammonia (DNRA) and losses via N_2O emissions is likely to be sensitive to a variety of ecosystem properties, particularly soil redox status and soil C and NO_3^- pools (Silver et al. 2005). Hence, the predicted loss of C from soils with the change in climate may also have unknown feedbacks in the N cycle in the soil of these ecosystems.

1.3. Objectives of the study

The significance of climate changes to the interaction of both carbon and nitrogen cycles in tropical soils is still unknown and deserves more attention. For that, it is important to identify individual processes and their consequences to changes in the climate. The overall goal of this study was to quantify spatial and seasonal variation in soil CO_2 dynamics as a function of soil properties and climate variability as well as to determine the effectiveness of N retention mechanism in the main soil types in the Amazon basin.

This main goal was subdivided in several objectives:

- to quantify and compare the soil CO_2 efflux rates in two soil textures from the dominant soil type in the eastern Amazon.
- to estimate CO_2 production rates as a function of depth
- to evaluate how soil and environmental factors control CO_2 production and soil CO_2 efflux
- to investigate how an artificially imposed drought affects depth and amount of soil CO_2 production and transport
- to quantify the gross rates of mineralization, nitrification, and microbial and abiotic N immobilization in a low N availability and a high N availability tropical forest soil.

1.4. Site description

Characteristics of Amazon forest soils, vegetation and climate

All studies were conducted in the National Reserve of Caxiuanã (1°43'3.5''S, 51°27'36''W), approximately 400 km west of the city of Belem, Para, Brazil (Lisboa 1997). The site is administered by the Ferreira Penna Scientific Station which belongs to Museu Paraense Emilio Goeldi (MPEG). Caxiuana Tropical Forest is located in the north-eastern Brazilian Amazon. The terrain around Caxiuana site consists mainly of Cretaceous sedimentary rocks (Alter do Chao Formation of the Amazon basin) geomorphologically remodelled in various periods during Pleistocene (Kern 1996). These sediments were deeply weathered giving rise to lateritic profiles which extend deeply down to the saprolite, locally exposing fine kaolinite zones. Near and at the surface, the lateritic profiles have been converted into Oxisols (Yellow Latosols in the Basilian classification), which are widespread over the region. These Oxisols have clay to sand texture, are deep, acidic and oligotrophic (Almeida et al. 1993). Topography is gentle to steep and the additional erosion and leaching has reduced even further the fertility of the soils of these terraces.

The climate of the region is classified as humid tropic of the type Am (at Köppen classification; Moraes et al. 1997). Annual mean precipitation is about 2200 mm, with the peak of the rainy period registering on average 300 mm month^{-1} occurring from February to April. The period with least precipitation is September to November, and less than 100 mm of rain are received on average per month (Lourdes Pinheiro Ruivo et al. 2002). Based on monthly rainfall observed during the study period (November 2001 – November 2003; Caxiuanã Meteorological Station), two seasons were distinguished. Months with more than 100 mm rainfall were assigned to the wet season (December to June), and the dry season consists of the period of months with less than 100 mm rainfall (July to November). Mean annual incoming short wave radiation is around 350 W m^{-2} and mean annual temperature is

25.7 ºC. Average daily minimum temperatures remains the same (23.0-23.1°C), but maximum temperature is higher in the dry season (31.2 °C) than the wet season (29.6 °C) (Fisher et al. in review a). The height of the canopy is about 35 meters, and the aboveground biomass is 200 m^3 ha^{-1} (Lisboa 1997, Lisboa and Ferraz 1999). The forest presents considerable diversity and big trees, as *Dinizia excelsa* (angelim-vermelho), *Marmaroxylon racemosum* (Angelim-rajado), *Couratari guianensis* (tauari), *Bucheniavia grandis* (tanimbuca), *Swartzia racemosa* (pitaíca), *Dipteryx odorata* (cumaru), among others (Almeida et al. 1993).

General design of the study

This thesis presents an analysis including the CO_2 dynamics and the nitrogen cycle in two different soil textures analyzing the potential feedback mechanisms in these soils generated by the climate change. Data on the throughfall exclusion experiment in Caxiuanã is part of the Large Scale Biosphere Atmosphere Experiment in Amazonia (LBA) project. The objective of the LBA project is to understand the changes in the water recirculation, solar energy, carbon and nutrients with local changes of the vegetation and global climate changes (Avissar and Nobre 2002). Two experimental rainfall manipulations were implemented by LBA project (Avissar and Nobre 2002) in order to investigate the role of drought in constraining forest gas exchange. Two sites, Santarém and Caxiuanã, were selected in Eastern Amazonia, the area most at risk from reduced rainfall (Cox et al. 2000, 2004). At both sites, a system of plastic panels and guttering intercepts the rainfall at 2 m height, and channels the intercepted water away from the plot, thereby reducing the quantity of water hitting the soil by ~ 50 % (Fisher et al. 2006).

1.5. Overview of the thesis

This thesis is divided into 5 chapters, according to the different objectives. Chapter 2 deals with the quantification of soil CO_2 efflux, in particular the spatial and temporal variation of CO_2 emissions in different soil types, landscape and litter input together with climatic controls. In Chapter 3, the estimates of CO_2 productions rates are presented and the effects of an induced drought on soil CO_2 production and soil CO_2 efflux are discussed. Diffusion coefficients, which are needed to calculate the CO_2 production rates, are derived from empirical formulas and validated using radon measurements. In addition, two years data on soil air CO_2 concentration, soil temperature and soil water content are shown and compared with a similar throughfall exclusion experiment results. Chapter 4 focuses on the quantification of gross rates of mineralization, nitrification, and microbial and abiotic N immobilization in a tropical forest soil with low N availability and one with high N availability. Measurement of gross rates of N mineralization and nitrification were made using ^{15}N pool dilution technique, as well as estimates of NH_4^+ and NO_3^- immobilization rates using chloroform fumigation extraction technique and the characterization of soil physical and chemical properties. These rates were used to evaluate if the mechanisms of soil N retention (biotic and abiotic immobilization and DNRA) are more effective in tropical rain forest soils with a low N availability than in tropical rain forest soils with a high N availability. All results are compiled in Chapter 5 to reach some general conclusions.

2. Landscape and climatic controls on spatial and temporal variation in soil CO_2 efflux in an Eastern Amazonian Rainforest, Caxiuanã, Brazil.

2.1. Introduction

In recent years, the recognition that old-growth forests of Amazonia play an important role in the global carbon cycle, has led to the establishment of several sites across the Amazon basin where net ecosystem exchange (NEE) of CO_2 is measured (Grace et al. 1995a, Malhi and Grace 2000, Saleska et al. 2003). In the absence of fire, NEE is the net result of CO_2 uptake through photosynthesis and CO_2 losses through autotrophic and heterotrophic respiration. A major part of the respired CO_2 originates from the soil and quantifying the size and variation of this CO_2 source is critical for the correct interpretation of NEE measurements.

In contrast to tower-based NEE measurements, there are no standard methods to measure soil CO_2 efflux (or soil respiration) over larger areas; chambers which normally cover only a fraction of a square meter are used. At the same time, soil CO_2 efflux is highly variable, both spatially and temporally (Hanson et al. 1993, Xu and Qi 2001). As a result, estimates of the mean soil CO_2 efflux, even within homogeneous vegetation are uncertain. Spatial variability of soil CO_2 efflux, typically caused by variations in landscape, soils and vegetation (Xu and Qi 2001, Schwendenmann et al. 2003) introduces a considerable level of uncertainty in modelling soil respiration at landscape and larger regional scales (Gough and Seiler 2004). Temporal variability, mainly caused by climatic variables (Davidson et al. 2000a), is a major source of error when estimating the cumulative annual soil CO_2 efflux (Janssens et al. 2000, Gough and Seiler 2004).

Although the vast majority of soils in Amazonia have in common that they are heavily weathered, there is considerable spatial heterogeneity in soil texture both at local and regional

scales (Sombroek 1966, Jordan 1985) and along topographic gradients (e.g. Silver et al. 2000). Furthermore, topographically induced microclimates and variations in soil water content can also cause spatial heterogeneity by affecting the ability to retain carbon, water, and nutrients (Running et al. 1987, Kang et al. 2000). Apart from soil texture and topography, the litter layer may also contribute to spatial and temporal variation of soil CO_2 efflux. Although litter input and turnover are frequently studied, the influence of the litter layer on temporal variation of soil CO_2 efflux has to our knowledge not been studied for tropical forests.

Because NEE measurements are done at high frequency and later integrated for longer time periods (hours to days), there is an increasing tendency to also collect soil CO_2 efflux at high frequency, with a limited amount of (automated) chambers (e.g. Goulden and Crill 1997, Drewitt et al. 2002). While this approach leads to an excellent characterization of temporal variation, spatial variation can only be quantified between the few deployed chambers. As a result, soil CO_2 efflux is normally modelled using climatic parameters as input (most often soil temperature and sometimes soil moisture) thereby ignoring landscape variations in soil CO_2 efflux. This may lead to serious errors because the 'footprint' of tower-based measurements is normally large enough to cover considerable variation in landscape and soils (Grace et al. 1995b). An additional problem may be that soil temperature and soil moisture co-vary, even in tropical forest ecosystems, making it impossible to separate their effect on soil CO_2 efflux (Davidson et al. 2000a, Schwendenmann et al. 2003).

Our goal was to quantify the spatial and seasonal variation in soil CO_2 efflux and its environmental controls in the old-growth forest of Caxiuanã in the eastern Amazon. Using manually deployed flux chambers, we monitored soil CO_2 efflux from two Oxisol sites with contrasting soil texture over the course of two years. Furthermore we aimed to quantify the contribution of the litter layer to soil CO_2 efflux and to evaluate the effect of landscape

position on CO_2 efflux. As the climate of the eastern Amazon is characterized by small fluctuations in temperature throughout the year, we expected that changes in soil water content would control the seasonal variation in soil CO_2 efflux.

2.2. Materials and Methods

Study site

The experimental site was located in Caxiuanã National Forest, Pará, Brazil, (1°43'3.5''S, 51° 27'36''W). The forest is a lowland *terra firme* rainforest. Mean annual temperature is 25.7 ºC. Mean annual rainfall is 2272 mm (± 193 mm), with a dry season when only 555 mm (± 116 mm) of rainfall occurs on average (Fisher et al. 2006). Months with more than 100 mm rainfall were assigned to the wet season (December to June), and the dry season consisted of the period of months with less than 100 mm rainfall (July to November).

Most soils (65 % of the experimental site, Costa 2002) are yellow Oxisols (Brazilian classification Latossolo), but there are large differences in texture. Our study was on two Oxisols with contrasting soil texture: clay and sand (Table 2.1). Both soils have a broken laterite layer (0.3-0.4 m thick) at 3-4 m depth. The texture of the top 0.5 m of the sand is 75 % sand and 25 % clay + silt, while the topsoil of the clay had 31 % sand and 69 % clay + silt (Ruivo and Cunha 2003). Mineralogy of both soils is mainly kaolinite in the clay fraction and quartz in the sand fraction (Ruivo and Cunha 2003). The sites are located about 15 m above river level, and the water table has occasionally been observed at a depth of 10 m during the wet season (Fisher et al. in review b). The forest structure does not vary much among soil types: 419 trees ha^{-1} with a basal area of 25.1 m^2 ha^{-1} and leaf area index (LAI) of 5.5 m^2m^{-2} on the clay soil and 434 trees ha^{-1}, a basal area of 23.9 m^2 ha^{-1} and LAI of 5.2 m^2m^{-2} for the sand site (unpublished data. D. Metcalfe). The height of the canopy is about 35 meters, and

the aboveground biomass is 200 m^3 ha^{-1} (Lisboa et al. 1997). The forest presents considerable diversity, with species like *Dinizia excelsa* (angelim-vermelho), *Marmaroxylon racemosum* (Angelim-rajado), *Couratari guianensis* (tauari), *Bucheniavia grandis* (tanimbuca), *Swartzia racemosa* (pitaíca), *Dipteryx odorata* (cumaru), among others (Almeida et al. 1993).

Table 2.1 - Characterization of chemical and physical properties of the soil of our study area in Caxiuanã, Para, Brazil.

Texture/ Depth	**Clay (%)**	**Silt (%)**	**Sand (%)**	**pH (H_2O)**	**ECEC (cmol dm^{-3})**	**Total P (mg kg^{-1})**	**Total C (g kg^{-1})**	**Total N (g kg^{-1})**	**SOC (g kg^{-1})**	**Bulk density (Mg m^{-3})**
Sand										
0-10cm	14	10	77	4.5	3.1	3.4	9.6	0.40	9.5	1.49
10-100cm	23	7	70	4.4	2.2	1.2	4.3	0.38	4.8	1.53
Clay										
0-10cm	38	23	40	3.9	5.7	4.4	13.7	0.57	15.1	1.20
10-100cm	56	20	24	4.2	2.4	2.0	6.7	0.68	5.9	1.22

Design of experiment to measure effect of soil texture

Using a systematic design, 16 chambers were deployed on a 1 ha plot at the sand site, and 8 chambers on a 0.5 ha plot at the clay site. While 8 chambers was enough to get a good estimate of soil CO_2 efflux, we used more chambers on the sand site because of an additional throughfall exclusion experiment which is not described here (Fisher et al. 2006). In June 2001, PVC rings (0.296 m in diameter, 0.20 m tall) were inserted to a depth of 0.02 m into the soil. Once inserted, the rings were left in place throughout the period of measurements. Chambers were kept free of seedlings. Each of the two sites was sampled every two weeks from December 2001 to November 2002 and monthly from December 2002 to November 2003. It took two days to measure all sites, and all measurements were made between 8 AM and 2 PM local time.

Design of experiment to measure effect of topography

In February 2002, we installed chambers along four topographic transects which were between 30 and 40m apart. Average slope length was 108 ± 11 m and average inclination was 5.4° ± 0.2°. At each transect three chambers were installed at four different positions: plateau, upper slope, lower slope and valley. The chambers in the valley were installed about 0.5 m above the flood plain level. Measurements were made every three months from April 2002 to July 2003.

Design of experiment to measure contribution of litter layer

Adjacent to the sandy site twelve chambers were systematically installed within an area of 36 m^2 to minimize spatial variation. The following three treatments were imposed on four replicated chambers each: in treatment one ('no litter'), the chamber was placed directly on the mineral soil and litter was removed, and a small litter trap of 0.40 by 0.40 m was placed directly above each chamber. In treatment two ('normal litter'), the litter was not manipulated (it was used as control treatment). In the third treatment ('double litter'), the litter collected from treatment one was deposited in the chambers every two weeks. Measurements of CO_2 efflux were made every three months from July 2002 to October 2003. Contribution of litter layer was the average of the difference between 'double litter' and 'no litter' soil CO_2 efflux, and 'normal litter' and 'no litter' soil CO_2 efflux. Soil water content and soil temperature from 'no litter' and 'double litter' treatment did not differ from control ('normal litter').

Measurements of soil CO_2 efflux

Dynamic, closed chambers were used to determine soil CO_2 efflux (Parkinson 1981). Flux chambers were closed for about 5 minutes using a PVC cover. The volume of the chamber was about 13 L. Air was circulated at a flow rate of 0.8 L min^{-1} between an infrared CO_2 gas analyzer (LI-6262, Li-Cor, Inc., Lincoln, Nebraska, USA) and the flux chambers. To prevent pressure differences between the chamber and the atmosphere, the chamber was vented to the atmosphere through a 0.25 m long stainless steel tube (3.2 mm outer diameter). CO_2 concentrations were recorded at 5 second intervals with a datalogger (Campbell CR10X, Campbell Scientific, Inc., Logan, Utah, USA). CO_2 flux (μmol CO_2 m^{-2} s^{-1}) was calculated from linear regression of CO_2 concentration within the chamber versus time, usually between 2 and 4 min after placing the cover over the ring. The coefficient of determination (r^2) of the regression was typically greater than 0.99. The infrared gas analyzer was calibrated in the laboratory using a loop with a column containing CO_2 scrubber (Soda Lime indicating 4-8 mesh) as zero-standard and a secondary CO_2 standard (510 ppm). The secondary standard was calibrated against primary standards from the Large Scale Biosphere-Atmosphere Experiment in Amazon (LBA) project.

Complementary measurements

Three replicates of mineral soil were collected for total C, N analysis to support our measurements of the soil CO_2 efflux. Bulk density was determined using soil core method. Particle size distribution was analyzed with the pipette method using pyrophosphate as a dispersing agent. Soil pH was measured from a saturated paste mixture (1:1 ratio of soil to H_2O and to 1 M KCl). ECEC was determined from air-dried, 2-mm sieved samples, percolated with unbuffered 1 M NH_4Cl, and the percolates analyzed for exchangeable cations

using Flame-Atomic Absorption Spectrometer (Varian, Darmstadt, Germany). Total P was analyzed from air-dried, ground samples, digested under high pressure in concentrated HNO_3, and the digests were analyzed using Inductively Coupled Plasma-Atomic Emission Spectrometer (Spectro Analytical Instruments, Kleve, Germany)

In October 2001, 20 litterfall collectors were placed randomly at the sand site. The collectors were made of 2 mm mesh nylon net, had an area of 1 m^2, and were placed about 30 cm above the forest floor. From November 2001 to November 2003, litter was collected monthly, put in paper bags and dried in a ventilated oven at 80 °C for 48 hours. The material was separated in three fractions: a) leaves, b) twigs and c) reproductive organs (flower, fruit and seeds); and weighed.

Soil temperature (*Ts*) was measured adjacent to each flux chamber at approximately 0.05 m depth from soil surface (litter layer was normally insignificant) using a thermocouple T-probe and a handheld thermocouple meter (HI 93551, Hanna Instruments, Ann Arbor, MI, USA). Soil water content (*swc*) was determined using frequency domain reflectometry (FDR). The probe (CS 615, Campbell Scientific Ltd, Lougborough, UK) consists of 0.3 m long stainless steel rods that were placed vertically into the soil. The sensor output was converted to estimates of volumetric soil water content (m^3 m^{-3}) using the standard calibration curve from the sensor. For the sand soil, the *swc* values were corrected by the calibration equation from Fisher et al. (in review a). Soil temperature and soil water content probes were inserted into the soil each time. Half-hourly meteorology data was measured by a tower-based automatic weather station in the vicinity of the study site (Carswell et al. 2002). This weather station provided measurements for wet and dry bulb temperature, incoming and outgoing short-wave radiation, photosynthetically active radiation (PAR), and long-wave radiation, wind speed and direction and rainfall (unpublished data from Y. Malhi).

Calculations and Statistical analyses

For each of the sites, the average CO_2 efflux rate was calculated from the chamber flux measurements. Daily mean soil efflux was calculated by averaging the sampling dates for each site in both years. Coefficient of variation was the standard deviation of all chambers in each measurement date divided by the average soil CO_2 efflux of the given measurement for each site in both years.

Spatial (between soil types and treatments) and temporal differences as well as differences in topography were analysed by repeated measure ANOVA. Progressive decrease in soil CO_2 efflux was evaluated by testing (t-test) the average of the beginning (for the wet season from December to March, and for the dry season from July to September) and the end (for the wet season April to June, and for the dry season from October to November) of each season. Multiple regression analysis was used to examine relationships between soil CO_2 efflux, soil water content, soil temperature and other factors. Significant effects were determined at $P < 0.05$. All statistical analyses used STATISTICA 6 software package (StatSoft Inc., Tulsa, OK, USA).

2.3. Results

Variation in soil CO_2 efflux caused by differences in soil texture

Spatial variation, for both sites, among soil chambers within the two-year measurements ranged from 13 to 52 % and was on average 23 % for the sand soil and 25 % for the clay soil. The two-year average CO_2 efflux rates were 21 % higher ($P < 0.001$) for the sand (3.9 ± 0.1 μmol CO_2 $m^{-2}s^{-1}$) than for the clay (3.1 ± 0.1 μmol CO_2 $m^{-2}s^{-1}$). No difference was detected for soil temperature between sites (24.1 ± 0.1 °C for sand and 24.2 ± 0.1 °C for

clay; $P < 0.05$), while soil water content in sandy soil (23.2 ± 0.3 %) was much lower ($P < 0.001$) than the clay soil (34.5 ± 1.0 %), for the two-year period.

Temporal variation ranged from 16.4 to 30.7 % and with an average coefficient of variation (CV) of 16.4 % for sand and 21.8 % for clay soil. Soil CO_2 efflux decreased progressively during the first wet season ($P < 0.05$, $n = 6$) in both sites. Towards the transition from the wet to the dry season, soil CO_2 efflux increased, followed by a progressive decrease observed during the dry season. Soil CO_2 efflux recovered with the onset of heavy rainfalls at the beginning of the wet season (Fig. 2.1). There was no difference in soil CO_2 efflux between the two years of measurement for both soils ($P > 0.05$). The magnitude of soil CO_2 efflux on both soils did not differ significantly between dry season (4.0 ± 0.1 for sand and 3.1 ± 0.1 μmol CO_2 $m^{-2}s^{-1}$ for clay) and wet season (3.9 ± 0.1 for sand and 3.1 ± 0.1 μmol CO_2 $m^{-2}s^{-1}$ for clay), probably due to the within season variation.. Soil temperature and water content did differ between seasons on both sites ($P < 0.001$).

Spatial variation in soil CO_2 efflux caused by topography

Coefficient of variation among landscape position and soil chambers ranged from 17.2 to 32.8 % and were on average 26.3 %. On average, soil CO_2 efflux did not differ between the plateau, valley and upper and lower slope positions. Time of the year and the interaction between time and position did however have a significant effect on CO_2 efflux ($P < 0.01$). April (peak wet season) was generally the month with lowest CO_2 efflux while July and January (transition months) were the months with highest efflux rates, independent of topographic position (Fig. 2.2). Soil water content and soil temperature differed as a function of topographical position.

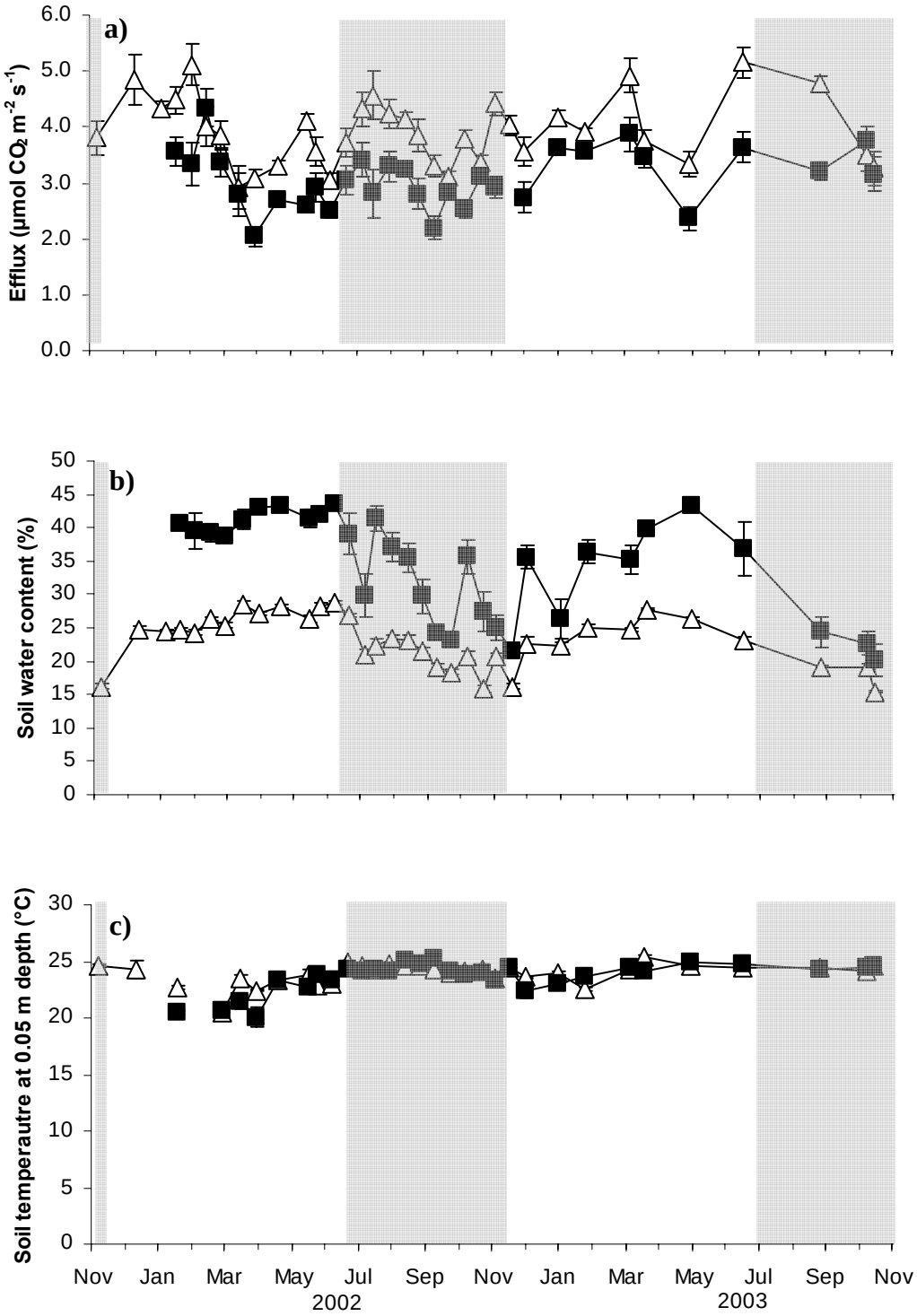

Figure 2.1 - Soil CO_2 efflux (a) , soil water content (b) and soil temperature (c) from November 2002 to November 2003 in sandy (-△-) and clay (-■-) sites. Shaded area mark the dry season; white background indicates the wet season. Each point is the mean of sixteen chambers for sand and eight chambers for clay. Error bars represent ± standard error of the mean.

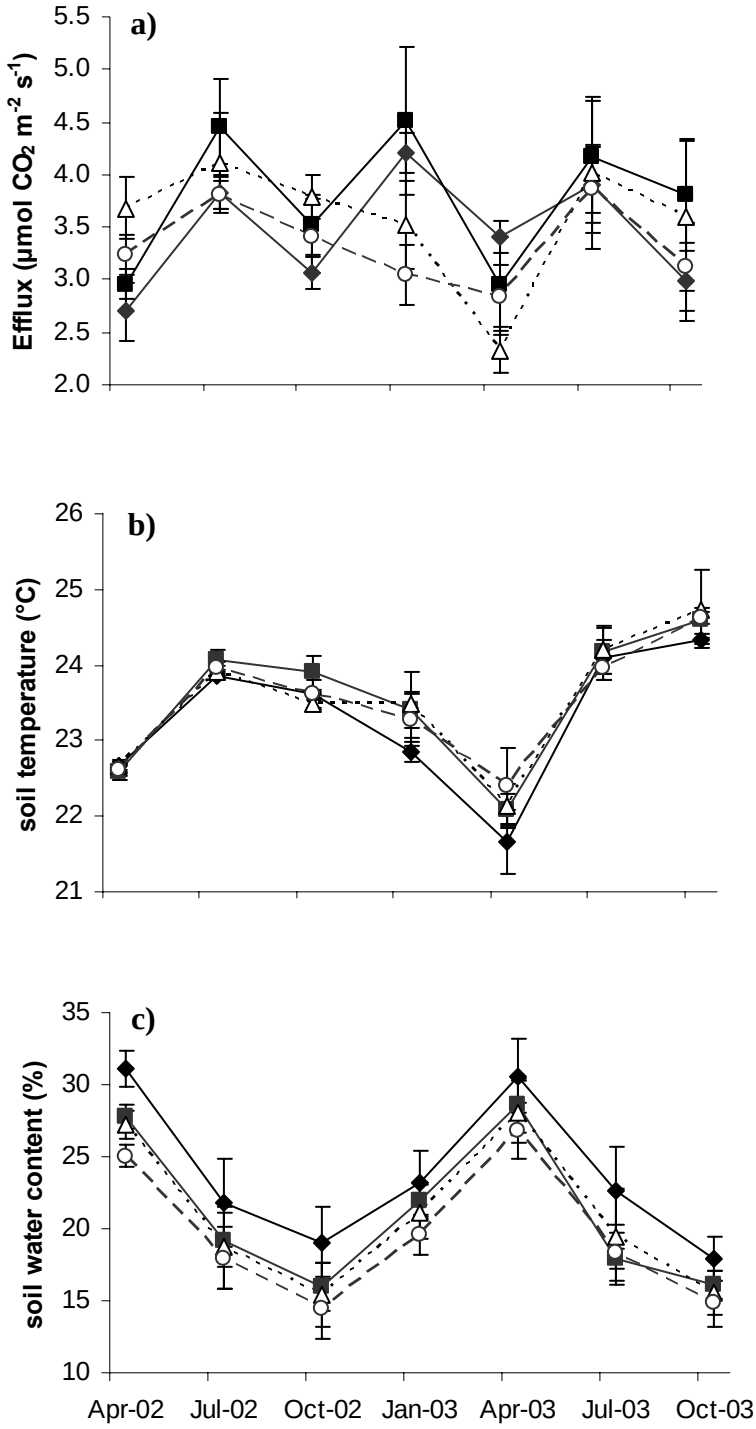

Figure 2.2 - Measurements of (a) soil CO_2 efflux, (b) soil temperature at 0.05 m depth and (c) soil water content at 0.30 m depth in the valley (–◆–), low slope (–■–), upper slope (····△····) and plateau (- -○- -). Each point is the mean of four sites (with three chambers measurements at each site). Error bars represent ± standard error of the mean.

Temporal variation in soil CO_2 efflux caused by the litter layer

Throughout the year the contribution of the litter layer to CO_2 efflux was about 20 %, varying from 25 % to almost zero depending on the seasonal conditions. In the wet season (Jan-03) the higher rates of soil CO_2 efflux (6.1 ± 0.6 µmol CO_2 m^{-2} s^{-1}, $P < 0.05$, $n = 4$) were measured in the double litter treatment, while at the onset of the dry season (July) soil CO_2 efflux rates were similar in all treatments (Fig. 2.3). Total litterfall was higher during the end (May and Jun) of the wet season and lower at the peak (Jan-Feb) of the wet season (data not shown). Soil temperature and soil water content did not differ among treatments ($P > 0.05$).

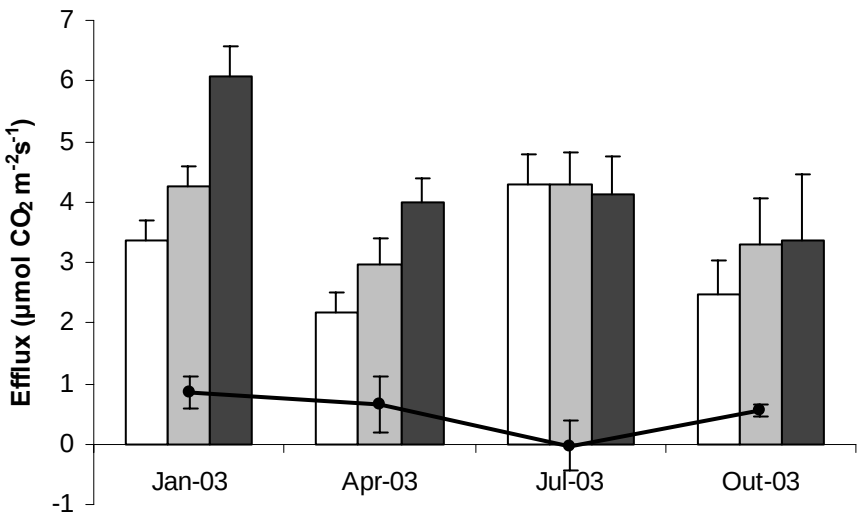

Figure 2.3 - Soil CO_2 efflux from forest floor without litter (white background), with normal amount of litter (gray background) and double the normal amount of litter (black background) at different time of the year, and the estimates of average seasonal contribution of the litter layer (–●–) to soil CO_2 efflux. Each point is the mean of four chambers. Error bars represent ± standard error of the mean.

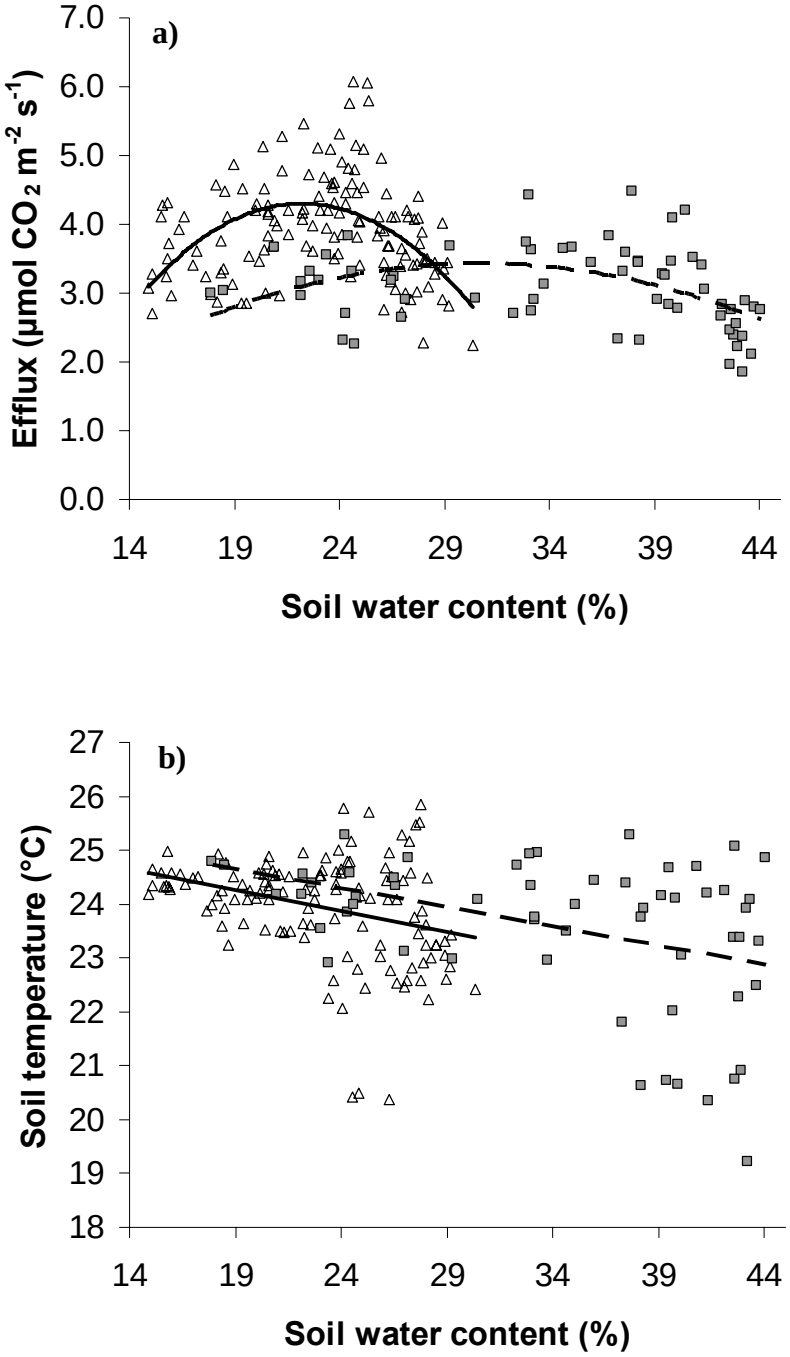

Figure 2.4 - Relationship between (a) soil water content (*swc*) and soil CO_2 efflux (*E*) and (b) between soil water content and soil temperature at 0.05 m depth (*Ts*) in sand (△) and clay (■) soil texture. The regression curves in (a) are for sand (solid line) $E_{sand} = -0.0226(swc)^2 + 1.0053(swc) - 6.8602$, $r^2 = 0.23$ and for clay (dashed line) $E_{clay} = -0.0046(swc)^2 + 0.2842(swc) - 0.9443$, $r^2 = 0.18$. The regression lines in (b) are for sand $Ts = -0.0771(swc) + 25.718$, $r^2 = 0.10$ and for clay $Ts = -0.0708(swc) + 25.984$, $r^2 = 0.16$.

Correlations with environmental factors

Soil CO_2 efflux was correlated with soil moisture and temperature but did not correlate with any other environmental factor (Table 2.2). As expected, soil temperature was positively correlated with air temperature and radiation and negatively correlated with rainfall. For both soils, the relationship between soil water content and soil CO_2 efflux could be described with a quadratic function ($r^2 = 0.23$ for sand and $r^2 = 0.18$ for clay soil, $P < 0.01$). The optimal soil water content, at which CO_2 efflux was highest, was greater for the clay than for the sand (Fig. 2.4a). A multiple regression for soil water content including both soil textures explained 22 % of the soil CO_2 efflux ($P < 0.001$; not shown). Soil water content and soil temperature co-varied in both soil types ($r^2 = 0.09$ for sand and $r^2 = 0.16$ for clay, $P < 0.001$, Fig. 2.4b).

Table 2.2 - Correlation among sites, seasons, CO_2 efflux and environmental factors using Spearman *r* coefficient ($n = 18$). Bold values are significant at $P < 0.05$.

	Soil CO_2 efflux	**Soil temperature**	**Soil water content**	**Air temperature**	**Solar radiation**
Soil temperature	**0.5**				
Soil water content	**-0.5**	0.1			
Air temperature	0.1	**0.3**	-0.2		
Solar radiation	0.1	**0.4**	-0.1	**0.8**	
Rainfall	-0.1	**-0.4**	0.3	**-0.7**	**-0.7**

Monthly average, across all chambers and both soil types, was used for soil CO_2 efflux, soil temperature and soil water content. Monthly average was also used for air temperature and solar radiation, while for rainfall was used the monthly sum.

2.4. Discussion

Magnitude of CO_2 efflux and spatial variation

Our annual CO_2 effluxes are similar to those reported for clay Oxisols in Manaus, Santarém and Costa Rica (Chambers et al. 2004, Davidson et al. 2004, Schwendenmann et al.

2003). However, higher CO_2 effluxes have been reported for a clay Oxisol in Paragominas (Davidson et al. 2000a) and Manaus (Sotta et al. 2004). The lower CO_2 efflux from the clay soil, compared to the sand soil may have different causes. The lower water holding capacity and capacity to retain nutrients (Table 2.1) of the sandy Oxisol may stimulate this forest to invest more in roots, reflected in a higher root respiration. In Santarém, it was shown that forest on a sandy soil had a higher fine root biomass and total root biomass than an adjacent forest on clay (Silver et al. 2000). Additionally, during the wet season the soil water content of the clay was frequently close to or at saturation level (estimated at ~40 %) which may have prevented diffusion of CO_2 out of the soil. This effect is illustrated by the low soil CO_2 efflux that we measured at high soil water contents which has also been shown for Oxisols in Costa Rica (Schwendenmann et al. 2003).

Although the effect of topographic position was not significant on a year basis, the significant interaction of topographic position and time shows that soil CO_2 efflux from different topographic positions have different seasonal variations (Fig. 2.2). These variations may be caused by water redistribution in the landscape and by different amounts of litter and soil organic matter at different positions. That water redistribution takes place is likely given the systematic difference in soil water content along the topographical gradient (Fig. 2.2c). A study on the effect of topographical position on soil CO_2 efflux in a forest close to Manaus also reported a high soil CO_2 efflux from the slope and a low value from the plateau and valley (Souza 2004). Although variations in topography are relatively small, spatial variation in soil CO_2 efflux due to topography was comparable to temporal variation in soil CO_2 efflux, illustrating its importance.

Temporal variation in CO_2 efflux

Temporal variability of soil CO_2 efflux was comparable to other studies, and depended mainly of soil water content (Davidson et al. 2000a, Schwendenmann et al. 2003). The quadratic function fitted to the plot of soil water content against soil CO_2 efflux is comparable to the influence of soil moisture detected in a tropical wet forest of Costa Rica (Schwendenmann et al. 2003). As was the case in Costa Rica, in our study soil temperature could not explain additional variation of soil CO_2 efflux beyond soil moisture alone. The weak positive correlation that we found between soil CO_2 efflux and soil temperature we therefore explain by the covariance of soil temperature and soil moisture (Fig. 2.4b) combined with the small variations in temperature that occur throughout the year (Fig. 2.1). Covariation of temperature and soil moisture has been detected in several ecosystems, including tropical rainforests (Davidson et al. 2000a, Schwendenmann et al. 2003).

Seasonal variation in the contribution of the litter layer to CO_2 efflux (Fig. 2.4) may be caused by variations in the amount of decomposing litter on the forest floor and in conditions influencing litter decomposition. Our results show that in July during the dry season the contribution of the litter layer to CO_2 emissions was negligible, even though in May and June the peak of litter production occurs (data not shown). The low moisture content of litter is probably responsible for this small contribution (Toledo 2002). The highest contribution was measured in January, about one month after the onset of the rainy season when there is both a considerable amount of litter on the forest floor and a high moisture content of litter. Although our results cannot be used to calculate the contribution of the litter layer to total soil CO_2 efflux (due to the relatively low frequency of measurements), they do illustrate that the dynamics of litter production and litter decomposition exert quite a strong influence on the observed temporal variation in soil CO_2 efflux.

Although we measured some seasonal variation in soil temperature and soil water content, the seasonality of the soil CO_2 efflux was not strong (Fig. 2.1). A drought mediated reduction in CO_2 produced from microbial respiration in the topsoil and litter layer may be (partly) compensated by higher CO_2 production from deeper root activity (Liu et al. 2004) which may explain the weak seasonality. Under normal rainfall conditions, Amazonian forests are able to sustain high evapotranspiration rates throughout the majority of the dry season (Nepstad et al. 1994, Davidson et al. 2004, Fisher et al. in review b) and water stress is not strong enough to affect root respiration. The somewhat lower fluxes for the dry season may also be related to a reduction in leaf area index and ecosystem photosynthetic capacity (Meir and Grace 2005), because of the peak in litterfall associated with the onset of the dry season (Chambers et al. 2004). Seasonality of soil CO_2 efflux in a Costa Rican rain forest was also minimal; however the dry season in this forest was much shorter compared to many areas in the Amazon Basin (Schwendenmann et al. 2003).

Estimating annual landscape scale CO_2 efflux

To illustrate how extrapolation methods affect estimates of annual soil CO_2 efflux we use an area of 581 ha in Caxiuanã which includes the area where the tower based NEE measurements are being done. In the first approach we used measurements done at the base of the tower to scale up the results for the whole area during one year. This approach is often found in literature using monthly or less frequent measurements (e.g. Fan et al. 1990, Chambers et al. 2004). We calculated the monthly mean plus or minus one standard error and added the results to an annual soil CO_2 efflux which was then calculated for the whole area. The result of this approach was 6953 (± 623) Mg C yr^{-1}. In the second approach, we first stratified the area in the different landscape unit. Contribution of the different landscape units were: valley: 14 %; lower slope: 15 %; upper slope: 15 %; plateau with sand: 20 % and

plateau with clay: 36 %. For each of these units we calculated the annual soil CO_2 efflux plus or minus one standard error, including the seasonal variation and this value was multiplied with the area of the landscape unit. Finally the total soil CO_2 efflux was calculated by adding the contributions of the different landscape units. This approach resulted in an annual soil CO_2 efflux of 7594 (± 621) Mg C yr^{-1} which was almost 10 % higher than the first estimate.

The results of our study illustrate that successful extrapolation of soil CO_2 efflux for larger areas needs inclusion of complex spatial and temporal controls. Soil temperature and moisture are important drivers of temporal variations in soil CO_2 efflux at a specific location, however to detect non-linear relationships (like we found e.g. between soil moisture and soil respiration) it is necessary to do measurements under a wide range of conditions. Had we limited our measurements to the wettest part of the wet season and the driest part of the dry season only, we would not have detected the non-linearity between soil water and soil CO_2 efflux. Furthermore, our extrapolation example shows that soil texture, litter stocks and the significant interaction of topographical position and time make it necessary to include some of the complexity of landscapes when extrapolating soil CO_2 efflux over landscapes.

3. Effects of an induced drought on the soil CO_2 production and soil CO_2 efflux in an Eastern Amazonian Rainforest, Brazil.

3.1. Introduction

In the next few decades, climate of the Amazon basin is expected to change, as a result of regional deforestation and rising global temperatures (Nobre et al. 1991, Costa and Foley 2000, Werth and Avisar 2002). Several climate scenarios predict a warming trend of 1.5 – 2.5 °C in annual mean temperature for a large part of the tropics (Cox et al. 2000, Hulme and Viner 1998) and some of these scenarios predict more frequent occurrence of ENSO droughts of increasing severity (Timmermann et al. 1999) induced by global warming. These changes in climate may lead to feedback mechanisms in global biogeochemical cycles that are presently unknown. For example climate changes may affect C stocks in vegetation as well as shifts in total soil C and belowground C allocation (Davidson et al. 2004).

One third of the global soil carbon storage (to 3 m depth) is in the upper meter of tropical soils (Jobbagy and Jackson, 2000). Moreover, a large portion of the soil organic carbon (SOC) in tropical soils has a short residence time (Amundson 2001), which implies a high potential for rapid changes in soil carbon stocks (Trumbore et al. 1995). Increasing temperature may therefore lead to additional CO_2 release, especially in the tropics (Trumbore et al. 1996). Until the early 1990's carbon fluxes in soil below 1 m depth were often thought to be insignificant compared to C fluxes in the upper meter (e.g. Sombroek et al. 1993). However, many forest soils in the Brazilian Amazon are very deep, strongly weathered and contain significant live-root biomass below 1 m depth (Nepstad et al. 1994). For these Amazonian ecosystems (but also e.g. for deeply weathered forest soils in Costa Rica) it has been shown that the deep part of the soil contributes considerable amounts to the CO_2 efflux (Davidson and Trumbore 1995, Schwendenmann and Veldkamp 2006).

Given the expected intensification of ENSO events, which will probably lead to an increasing frequency of droughts and higher temperatures, an experiment was set up in which throughfall was experimentally reduced to create and artificial drought (Fisher et al. 2006). This experiment was part of the Large Scale Biosphere Atmosphere Experiment in Amazon (LBA). Using this throughfall exclusion experiment, our goal was to study how an artificially imposed drought affects depth and amount of soil CO_2 production and transport in a deeply weathered soil of the Eastern Amazon. Our hypothesis is that soils with lower capacity to maintain water in the root zone will be more promptly affected by the reduced precipitation. A similar experimental rainfall manipulation was implemented in another site in Eastern Amazon, Santarém (Nepstad et al. 2002, Stokstad 2005). In this replicate the throughfall exclusion of three rain seasons did not lead to significant differences in soil CO_2 efflux (Davidson et al. 2004). However, Amazon region has high variability in soil and vegetation and different responses to drought may be expected. Over the course of two years, we monitored soil CO_2 efflux and soil CO_2 concentrations, soil temperature and soil moisture in pits down to 3 m depth in a sandy Oxisol. Using a simple one-dimensional gas diffusion model which was calibrated using naturally occurring ^{222}Rn profiles, we calculate CO_2 production with depth and we relate this to a range of environmental controls that can potentially affect the production and emission of CO_2 in the soil.

3.2. Materials and Methods

Study site

The experimental site was located in Caxiuanã National Forest, Para, Brazil, (1° 43’ 3.5’’S, 51° 27’ 36’’W). The forest is a lowland *terra firme* rainforest. Mean annual rainfall is 2272 mm, with a pronounced dry season between July and December, when on average only

555 mm of rainfall occurs (Fisher et al. 2006). Months with more than 100 mm rainfall were assigned to the wet season (December to June), and the dry season consisted of the period of months with less than 100 mm rainfall (July to November).

The studied soil is a yellow Oxisol (Brasilian classification: Latosol), which has a broken ironstone layer (0.3-0.4 m thick) at 3-4 m depth. On average, the top 0.5 m of the soil contains 75 % sand, 15 % clay and 10 % silt (Table 3.1). Mineralogy of the clay fraction is dominantly Kaolinite while the sand fraction consists mainly of quartz (Ruivo and Cunha 2003). The location of the experiment is about 15 m above river level, and during wet season, the water table has been observed at a depth of 10 m (Fisher et al. 2006). The forest structure is formed by 434 trees ha^{-1}, a basal area of 23.9 m^2 ha^{-1} and leaf area index (LAI) of 5.2 m^2m^{-2} (unpublished data. D. Metcalfe). The height of the canopy is about 35 meters, and the aboveground biomass is 200 m^3 ha^{-1} (Lisboa et al. 1997).

Table 3.1 - Characterization of chemical and physical properties of the soil of our study area in Caxiuana, Para, Brazil.

Depth (cm)	**Clay (%)**	**Silt (%)**	**Sand (%)**	**pH H_2O**	**ECEC (cmol dm^{-3})**	**P (mg dm^{-3})**	**Total C (g kg^{-1})**	**Total N (g kg^{-1})**	**C/N**
Control									
0-10	18	5	77	4.0	4.4	3.0	9.1	0.4	22.7
10-25	21	6	73	4.1	4.3	1.8	8.8	0.4	22.0
25-50	19	8	73	4.2	4.4	1.2	5.2	0.4	13.7
50-100	22	10	68	4.4	2.8	1.0	5.1	0.4	13.8
100-200	28	9	63	4.5	2.0	0.6	4.0	0.3	12.5
200-300	20	10	70	4.6	1.4	0.7	4.9	0.3	15.8
TFE									
0-10	13	4	83	4.0	5.2	3.1	11.7	0.3	35.4
10-25	15	7	78	3.0	4.3	2.3	10.1	0.3	33.7
25-50	20	10	70	4.1	3.2	1.2	6.7	0.4	18.6
50-100	23	9	68	4.3	2.7	0.7	4.1	0.3	12.8
100-200	26	10	64	4.4	2.0	0.5	4.9	0.3	16.3
200-300	20	10	70	4.7	1.4	0.5	6.1	0.3	21.8

Experimental design

The experiment consists of two plots of 1 ha (100m x 100m), one control plot and one experimental throughfall exclusion (TFE) plot. Both plots are located about 800 m north of the research station. In the TFE plot, a roof of transparent plastic sheeting and wooden guttering was installed at approx. 2 m height above the soil, with the purpose of displacing part of the throughfall from the plot to impose an artificial drought. Both control plot and the TFE plot were trenched to a depth of 1 m around their borders to reduce the lateral flow of water in roots and soil across plot boundaries. Throughfall exclusion started in January 2002, ~ 50 % of the rainfall was excluded from the soil of the TFE plot. During the peak dry season (from mid September to mid November) only 50 % of the plastic panels were left on the TFE plot in order to have a better aeration under the covered area. At each plot four pits (0.8 m by 1.8 m with 5 m depth) were established at randomly chosen locations. The plots were further divided into four quadrants in order to facilitate the systematic placement of soil CO_2 efflux chambers.

Measurements of soil CO_2 efflux

Sixteen respiration chambers were deployed systematically forming a cross in the TFE and control plot of the drought experiment, four at each quadrant. Systematic sampling was chosen to cover the plots uniformly, which allows a better overview of the soil CO_2 efflux spatial variation. In June 2001, PVC rings (0.296 m in diameter, 0.20 m tall) were inserted to a depth of about 0.02 m into the soil. Once inserted, the rings were left in place throughout the time investigated. Chambers were kept free of seedlings throughout the whole study period. Dynamic, closed chambers were used to determine soil CO_2 efflux (Parkinson 1981, Norman et al. 1992). Average chamber volume was about 13 L. Flux chambers were closed with a PVC cover for about 5 minutes. Air was circulated at a flow rate of about 0.8 L min^{-1} between

an infrared CO_2 gas analyzer (LI-6262, Li-Cor, Inc., Lincoln, Nebraska, USA) and the flux chambers. To prevent pressure differences between chamber and atmosphere, chambers were vented to the atmosphere through a 0.25 m long stainless steel tube (3.2 mm outer diameter). CO_2 concentrations were recorded at 5 second intervals with a datalogger (Campbell CR10X, Campbell Scientific, Inc., Logan, Utah, USA). CO_2 flux (μmol CO_2 m^{-2} s^{-1}) was calculated from the linear change in CO_2 concentration multiplied by the density of air and the ratio of chamber volume to soil surface area. Air density was adjusted for air temperature measured at the time of sampling. A linear increase in CO_2 concentration usually occurred between 2 and 4 min after placing the cover over the ring. The coefficient of determination (r^2) of the regression was typically better than 0.99. The infrared gas analyzer was calibrated in the lab using a loop with a column with CO_2 scrubber (Soda Lime indicating 4-8 mesh) as zero-standard and a secondary CO_2 standard (510 ppm). The secondary CO_2 standard was calibrated against primary standards from the LBA project.

Each plot was measured every two weeks from December 2001 to November 2002 and monthly from December 2002 to November 2003. It took two days to measure both plots. All measurements were conducted between 8 AM to 2 PM local time. For each plot, the average CO_2 efflux rate was calculated from the sixteen chamber flux measurements on a sampling day. Daily mean soil efflux for each plot was calculated by linear interpolation between sampling dates. Daily CO_2 flux rates were then summed up to estimate annual flux rates. Soil temperature at 0.05 m depth was measured with a thermocouple probe (HI 93551, Hanna Instruments, Ann Arbor, MI, USA) and soil water content was measured with a soil moisture probe (CS 615, Campbell Scientific Ltd, Lougborough, UK).

Measurements of CO_2 concentration profiles

In December 2001, all eight pits were instrumented for sampling of soil air. Stainless steel gas sampling tubes (3.2 mm outer diameter) were inserted horizontally at 0.10, 0.25, 0.50, 1.00, 2.00 and 3.00 m depth. The tubes were perforated at one end and closed with a septum holder with septum at the other end to allow sampling of soil air (Davidson and Trumbore 1995). Tubes at depths of 0.10 m to 1.00 m were 0.90 m long; tubes at greater depth were 1.80 m long. Samples at 0.05 m depth were collected using a 0.10 m stainless steel tubing adapted to a syringe, which was vertically inserted in the top soil every sampling date. Soil air samples were collected in polypropylene syringes which were closed with a three-way stopcock. Before a sample was taken, 10 to 20 ml of soil air was withdrawn and discarded.

Gas samples were analyzed for CO_2 concentration in the lab within 8 hours using a gas chromatograph (GC 11, Delsi Instruments, France) with a thermal conductivity detector (TCD). Soil air CO_2 concentration was calculated by comparison of integrated peak areas of samples with standard gases (0.051 % and 3 % CO_2), which were used to make a two point calibration. The coefficient of variation for replicate injections of standard gases was < 1 %. Storage tests indicated that on average 9-12 % of CO_2 was lost between time of sampling and analysis. Soil CO_2 concentration measurements were made in all pits every two weeks in 2002 and monthly in 2003.

Measurements of soil radon activity and radon production

To validate the gas diffusion model we measured ^{222}Rn activity and ^{222}Rn production rates as described by Mathieu et al. (1988) and Davidson and Trumbore (1995). Soil air samples were withdrawn from the stainless steel gas sampling probes to determine soil air ^{222}Rn concentration (also called radon activity). Soil air (90 to 120 mL) was dried using a $CaCl_2$ column and introduced into pre-evacuated 150 mL scintillation cells (110A Lucas Cell,

Pylon Electronics Inc., Ottawa, ON, Canada). Impulses were measured using a Pylon AB-5 radiation monitor (Pylon Electronics Inc., Ottawa, ON, Canada). Radon production rates were measured for each site and depth interval individually, for both dry and wet conditions following the procedure described by Davidson and Trumbore (1995).

Calculation of CO_2 production

The diffusive properties of a soil media are usually characterized by means of relative diffusion coefficient D_s/D_o. D_s is the diffusion coefficient of a gas in soil air and D_o is the diffusion coefficient of the same gas in free air at standard conditions, e.g. 0.158 $cm^2\ s^{-1}$ for CO_2 at 20 °C and standard pressure of 1013 hPa (Mason and Monchick 1962). The gas diffusion coefficient in soil (D_s) is a fraction of the gas diffusion coefficient in free air (D_o), as diffusivity depends not only on gas pressure and temperature but also on the amount of air-filled pores and on their continuity and shape. The relationship between D_s/D_o, and soil properties have been investigated in multiple studies and several empirical formulas have been developed to describe soil gas diffusivity. In our experiment we tested the gas diffusion models with three different approaches:

a) the model described by Millington and Quirk (1961) for non-aggregated media,

$$\frac{D_s}{D_o} = a^{2x}\left(\frac{a}{\varepsilon}\right)^2; \qquad (1)$$

where:

a	air-filled porosity	m^3m^{-3}
ε	total porosity	m^3m^{-3}

b) the model developed by Millington and Shearer (1971) for aggregated media,

$$\frac{D_s}{D_o} = \left[\frac{\left(\frac{a_{ra}}{\varepsilon_{ra}}\right)^2 \left(\frac{a_{ra}}{1-\varepsilon_{er}}\right)^{2x} \left(1-\varepsilon_{er}^{2y}\right)\left(a_{er}-a_{er}^{2z}\right)}{\left(\frac{a_{ra}}{\varepsilon_{ra}}\right)^2 \left(\frac{a_{ra}}{1-\varepsilon_{er}}\right)^{2x} \left(1-\varepsilon_{er}^{2y}\right)+\left(a_{er}-a_{er}^{2z}\right)} \right] + \left[a_{er}^{2z}\left(\frac{a_{er}}{\varepsilon_{er}}\right)^2 \right]; \qquad (2)$$

where:

a_{ra}	intra-aggregated air-filled pore space	m^3m^{-3}
ε_{ra}	intra-aggregated total pore space ($\varepsilon_{ra} = \theta_W$ at field capacity)	m^3m^{-3}
a_{er}	inter-aggregated air-filled pore space	m^3m^{-3}
ε_{er}	inter-aggregated total pore space ($\varepsilon_{er} = \varepsilon - \varepsilon_{ra}$)	m^3m^{-3}
x	determined from the relation $a^{2x} + (1-a)^x = 1$	
y	exponent usually between 0.6 and 0.8	
z	exponent usually between 0.6 and 0.8	

and c) the model described by Moldrup et al. (2000) based on the soil water characteristic curve,

$$\frac{D_s}{D_o} = \left(2a_{100}^3 + 0.04a_{100}\right)\left(\frac{a}{a_{100}}\right)^{2+3b} \qquad (3)$$

where:

a_{100}	air-filled porosity at -100 cm H_2O (porosity with the soil tension at -10 kPa)	m^3m^{-3}
b	pore-size distribution characterized by the slope of the line determined from the water retention curve, which is: $\log -\psi = a + b\theta$ where Ψ is the water potential and θ is volumetric water content.	

To calculate diffusivity we estimated total porosity (ε) from measurements of bulk density and an assumed particle density of 2.65 Mg m^{-3}. Air-filled porosity (a) was calculated by the difference between total porosity and water-filled porosity (θ). Water-filled porosity is the volumetric soil water content determined from the TDR probes on a given sampling date.

For the aggregated soil model the pore space is divided into intra-aggregated porosity (estimated from volumetric water content at field capacity) and inter-aggregated porosity (calculated as the difference between total porosity and volumetric water content at field capacity).

A 1-dimensional model developed by Schwendenmann and Veldkamp (2006) was used to predict ^{222}Rn activity throughout the soil profile. Input parameters are measured radon production rates and the diffusion coefficient calculated by the three approaches. These predicted values were compared with measured ^{222}Rn activities from the profile to test the diffusion models for their applicability. The estimated diffusion values from the Millington and Quirk (1961) soil model (M&Q) provided better agreement with the observed ^{222}Rn activities (Fig. 3.1). Millington and Shearer (1971) model overestimated diffusivity resulting in an underestimation of ^{222}Rn activities, while Moldrup et al. (2000) model underestimated diffusivity which resulted in an overestimation of ^{222}Rn activities. We thus decided to use M&Q model to estimate the diffusion coefficients for Caxiuanã soils. Fluxes of CO_2 were estimated at each sampling depth, based on Fick's law (Trumbore et al. 1990, Uchida et al. 1997).

Because a uniform diffusion coefficient in the soil is unlikely, a multi-box model was used (De Jong and Schapert 1972, Davidson and Trumbore 1995) to calculate soil CO_2 production (P_{CO2}). CO_2 production was calculated for each 0.1 m layer, but as the P_{CO2} rate for these individual layers may not be reliable, we summed the P_{CO2} estimates for larger depth intervals (0.6 – 1.0, 1.0 – 2.0, 2.0 – 3.0 m; Schwendenmann and Veldkamp 2006). For the topsoil (0-0.5 m depth) CO_2 production was estimated as the difference between the measured soil CO_2 efflux and the sum of the CO_2 production rates for all individual 0.1 m layers between 0.6 and 3.0 m (subsoil) on a given date. This approach avoids negative production

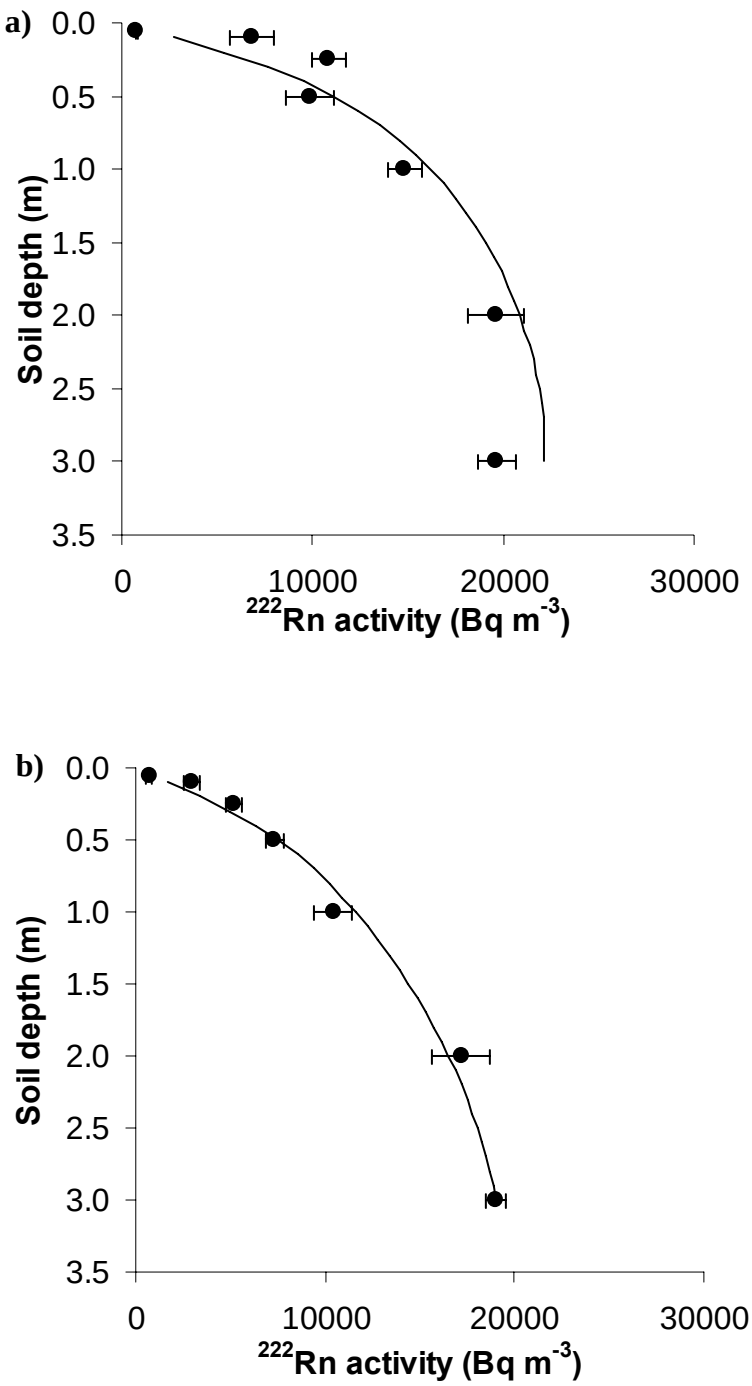

Figure 3.1 - Depth profiles of simulated and measured radon activity in (a) control and (b) TFE plots. Solid lines (—) show the calculated values using the Millington and Quirk (1961) model. The closed circles (●) are the measured radon activity, where each point is the mean (± standard error) of four profiles.

values, in case soil constituents are not uniformly distributed and the soil CO_2 gradient near the surface is not smooth (Davidson and Trumbore 1995).

Environmental measurements

Thermocouple T-probes were installed at the same depths attached to the end of the stainless steel tubes inserted in the soil for sampling CO_2 concentration. Soil temperature was measured with a handheld thermometer (HI 93551 Microprocessor K, J, T-Type Thermocouple Thermometer, Hanna Instruments Deutschland GmbH, Kehl/Rhein, Germany). At 0.05 m depth the temperature was measured with a T-type thermocouple penetration tip probe (HI 766 Thermocouple probe, Hanna Instruments GmbH, Kehl/Rhein, Germany).

For soil moisture monitoring, Time Domain Reflectometry (TDR) sensors (Soil Moisture Corp, Santa Barbara, CA, USA) were installed vertically at the soil surface (0-0.30 m depth) and horizontally at 0.50, 1.00, 2.00 and 3.00 m depth (Fisher et al. in review b). TDR were inserted 1.5 m into the walls, with connections sticking out of the re-packed soil wall. Measurements were made at the same time as CO_2 concentration. Water retention curves of intact soil cores were determined on pressure plates by Dr E. J. M. Carvalho in the soil physics laboratory of Embrapa Amazonia Oriental in Belém, Brazil. The water retention curve for each plot was then used to transform soil water content in soil water potential (Ψ). Half-hourly meteorology data was measured by a tower-based automatic weather station in the vicinity of the study site (Carswell et al. 2002). This weather station provided measurements for wet and dry bulb temperature, incoming and outgoing short-wave radiation, photosynthetically active radiation (PAR), and long-wave radiation, wind speed and direction and rainfall (unpublished data from Y. Malhi).

From November 2001 to November 2003, litter was collected monthly, put in paper bags and dried in a ventilated oven for 48 hours at 80° C. The material was separated into three fractions: a) leaves, b) twigs and c) reproductive organs (flower, fruit and seeds); and weighted.

In October 2002 (nine month after the start of the throughfall exclusion), 12 pits of 0.40 x 0.40 x 0.50 m depth were excavated in control and in TFE plot (24 holes in total). All roots were sieved and separated by layers (0-0.05, 0.05-0.10, 0.10-0.25 and 0.25-0.50 m depth). Roots were than separated into two classes: fine (< 5 mm diameter) and coarse (> 5 mm diameter) roots.

Statistical analyses

Repeated measure ANOVA was used to examine differences in season and treatment. Regression analysis was used to examine relationships between CO_2 production rates and environmental variables. Significant effects were determined at $P < 0.05$. All statistical analyses were carried out using the STATISTICA 6 software package (StatSoft Inc., Tulsa, Oklahoma, USA).

3.3. Results

Magnitude and seasonality of soil CO_2 efflux and CO_2 production

The coefficient of variation among soil chambers within plots was on average 23 % for control plot and 26 % for TFE plot, and typically ranged from 13 to 40 %. The two-year average CO_2 efflux rates were higher ($P < 0.01$, $n = 32$) for the control plot (4.3 ± 0.1 µmol CO_2 m^{-2} s^{-1}) than the TFE (3.2 ± 0.1 µmol CO_2 m^{-2} s^{-1}; Fig. 3.2). Although we detected seasonal changes in soil CO_2 efflux, the CO_2 efflux of the control plot did not differ

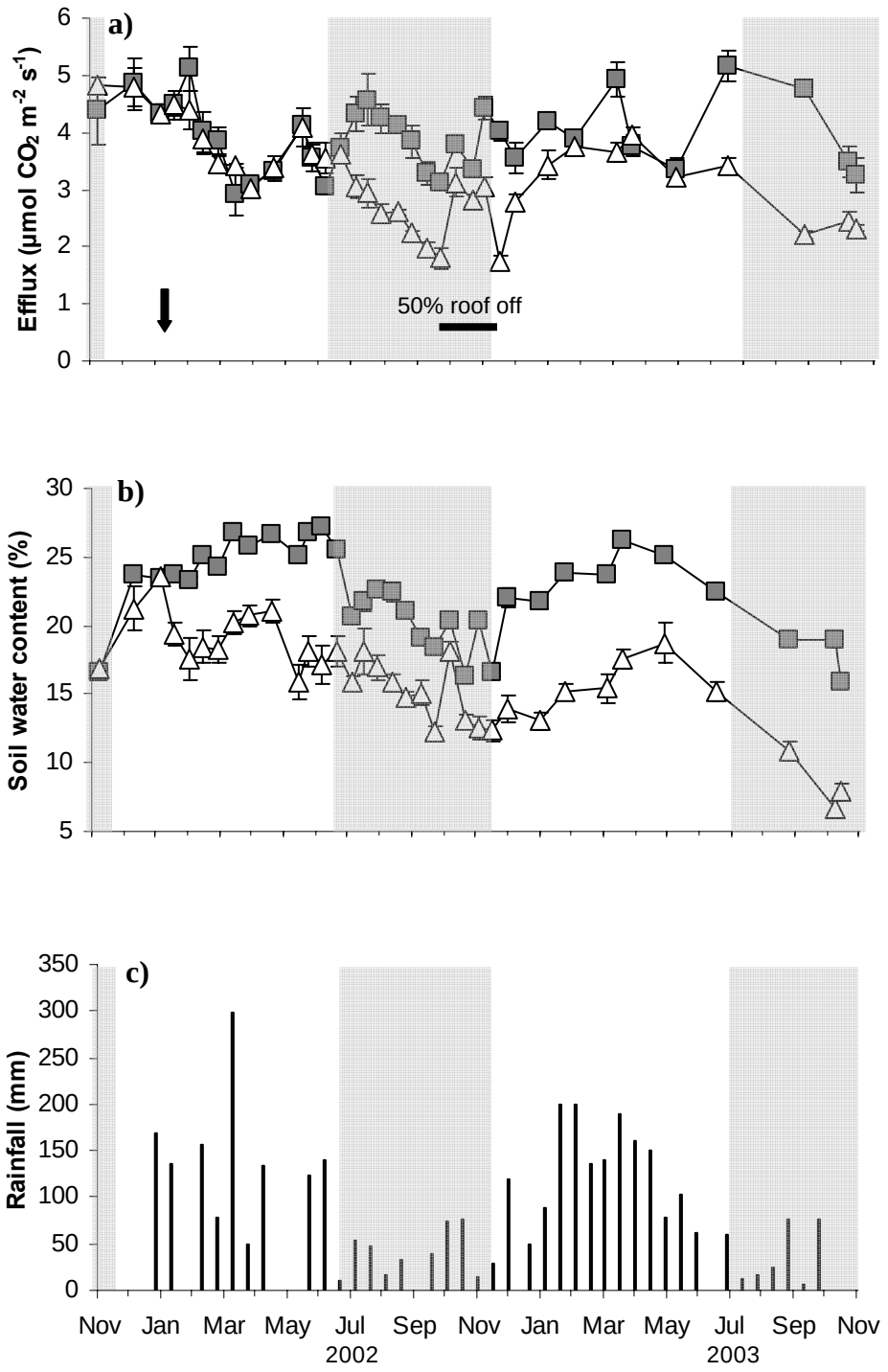

Figure 3.2 – Temporal variation of (a) soil CO_2 efflux, (b) soil water content (VWC) at 0.3 m depth in control (–■–) and TFE (–△–) plots and (c) bi-weekly rainfall from November 2002 to November 2003. Each point is the mean (± standard error) of 16 chambers per treatment. Shaded area mark the dry season and white background indicates wet season. The arrow shows when the throughfall exclusion began.

significantly between wet season (4.2 ± 0.2 μmol CO_2 m^{-2} s^{-1}) and dry (4.5 ± 0.1 μmol CO_2 m^{-2} s^{-1}) season. During the wet season the TFE (3.7 ± 0.1 μmol CO_2 m^{-2} s^{-1}) did not differ ($P > 0.05$) from the control plot, however during the dry season CO_2 efflux from the TFE was lower (2.6 ± 0.1 μmol CO_2 m^{-2} s^{-1}) than the control ($P < 0.01$). CO_2 efflux in the TFE plot significantly differ between wet and dry season ($P < 0.001$).

The importance of the topsoil (0-0.5 m) for soil CO_2 production (P_{CO2}) is illustrated by the following numbers: between 71 % and 73 % of soil CO_2 production in both plots occurred within the top 0.5 m of the soil including the forest litter layer. In the topsoil (0-0.5 m including litter layer) the TFE (2.3 ± 0.1 μmol CO_2 m^{-2} s^{-1}) had a significantly lower CO_2 production than the control plot (3.1 ± 0.1 μmol CO_2 m^{-2} s^{-1}; Fig. 3.3a). At the onset of the dry season in July 2002 CO_2 production at 0-0.5 m decreased by approximately 0.8 μmol CO_2 m^{-2} s^{-1}. The CO_2 production in this layer dropped by another 0.8 μmol CO_2 m^{-2} s^{-1} between Sep-Nov 2002.

The production of CO_2 in the subsoil (0.6-3.0 m depth) in both plots was on average 0.8 μmol CO_2 m^{-2} s^{-1}. But during the first two months of throughfall exclusion (Feb-Mar 2002) the P_{CO2} from 0.6-2.0 m layer was significantly higher in the TFE plot as compared to the control plot ($P < 0.05$; Fig. 3.3b). The higher P_{CO2} was also observed in the 2.1-3.0 m layer of the TFE plot in the subsequent months (May-Jun 2002; Fig. 3.3c). During the dry season there was no difference in P_{CO2} between plots at the subsoil (0.6-3.0 m depth).

In the control plot, soil CO_2 production at 0-0.5 m depth was negatively correlated ($r = -0.45$, $P < 0.01$) to 0.6-3.0 m CO_2 production for the whole experiment, which was not observed for the TFE plot. Nonetheless the P_{CO2} at 2.1-3.0 m depth in the TFE plot did have a negative correlation ($r = -0.70$, $P < 0.000$) with the P_{CO2} of the top 0.5 m. The contribution of subsoil (0.6-3.0 m) to the total soil CO_2 efflux was higher in the TFE plot (28 %) compared to the control plot (17 %, $P < 0.000$; Table 3.2), and it did not differ between seasons and years.

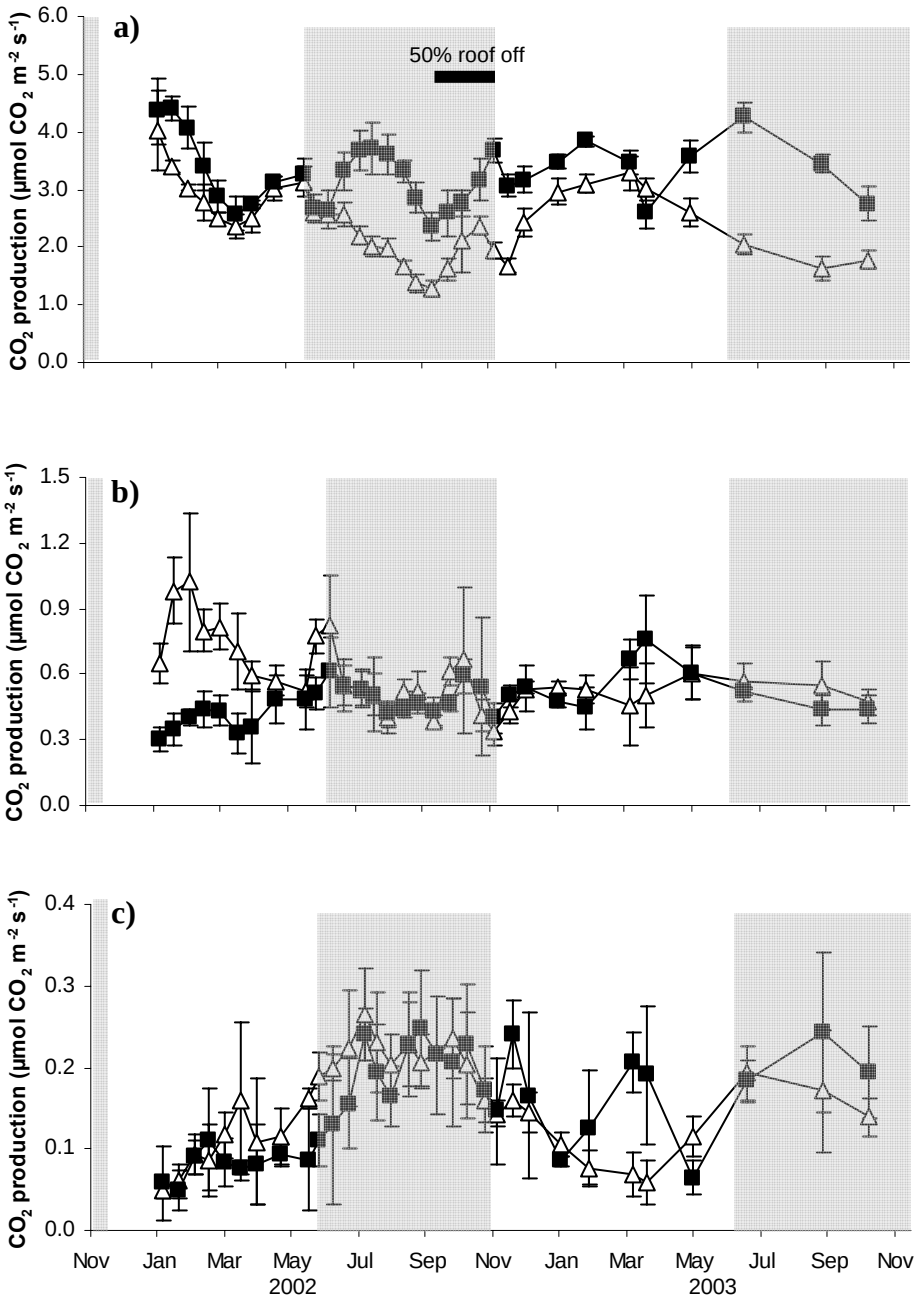

Figure 3.3 - Temporal variation in CO_2 production rates from January 2002 to November 2003 in both control (–■–) and TFE (–△–) plot. (a) CO_2 production of the 0-0.5 m layer; (b) CO_2 production of the 0.6-2.0 m layer; and (c) CO_2 production of the 2.1-3.0 m layer. Each point is the average (± standard error) of four profiles. Shaded area mark the dry season and white background indicates wet season. The arrow shows when the throughfall exclusion began.

Table 3.2 - Contribution of the subsoil (0.6-3.0 m depth) to the total CO_2 production by seasons for both plots. Letters indicate difference between treatments (ANOVA, $P < 0.05$).

Relative contribution of deep soil (%)	**2002**		**2003**	
	Wet season	**Dry season**	**Wet season**	**Dry season**
Control plot	16 A	19 A	19	17 A
TFE plot	27 B	32 B	20	31 B

Soil CO_2 concentrations

Soil CO_2 concentration profiles (at 0-3.0 m depth) changed with season in both plots. CO_2 concentrations increased over the course of the wet season and decreased soon after the beginning of the dry season (Fig 3.4a, b). Up to 2 % CO_2 were measured in the upper layers (0.05 m and 0.10 m depth) of control plot during periods of high precipitation and high soil water contents. This observation corroborates with our observations of soil CO_2 efflux which tends to be lower towards the end of the wet season (Fig. 3.2a). During the two-year period the average soil CO_2 concentration measured in the control plot (3.2 %) was higher than the concentration in the TFE (1.0 %).

Environmental parameters

Soil water content at 0-0.3 m depth differed significantly between plots ($P < 0.01$). The two year average for the control plot was 22.4 ± 0.6 % and for TFE was 16.2 ± 0.6 % (Fig. 3.2b) with the correspondent soil water potential of -47 ± 8 kPa and -201 ± 29 kPa respectively. In the control, soil water potential reached a maximum of -184 kPa in the dry season and a minimum of -8 kPa in the wet season, while in the TFE plot soil water potential varied between -744 kPa in the dry and -22 kPa in the wet season. Soil water content was also significantly different for control and TFE at all depths in the soil profile and in dry and wet

period. We did not measure differences in soil temperature at 0.05 m depth between control (23.9 ± 0.2 °C) and TFE plot (24.0 ± 0.2 °C), nor at greater depth in the soil profile.

Total fine root biomass (<5 mm diameter) in the 0-0.50 m layer recorded in Oct 2002 (after nine months of throughfall exclusion) was not different between control (13.9 ± 1.3 Mg ha^{-1}) and TFE plot (15.2 ± 2.1 Mg ha^{-1}).

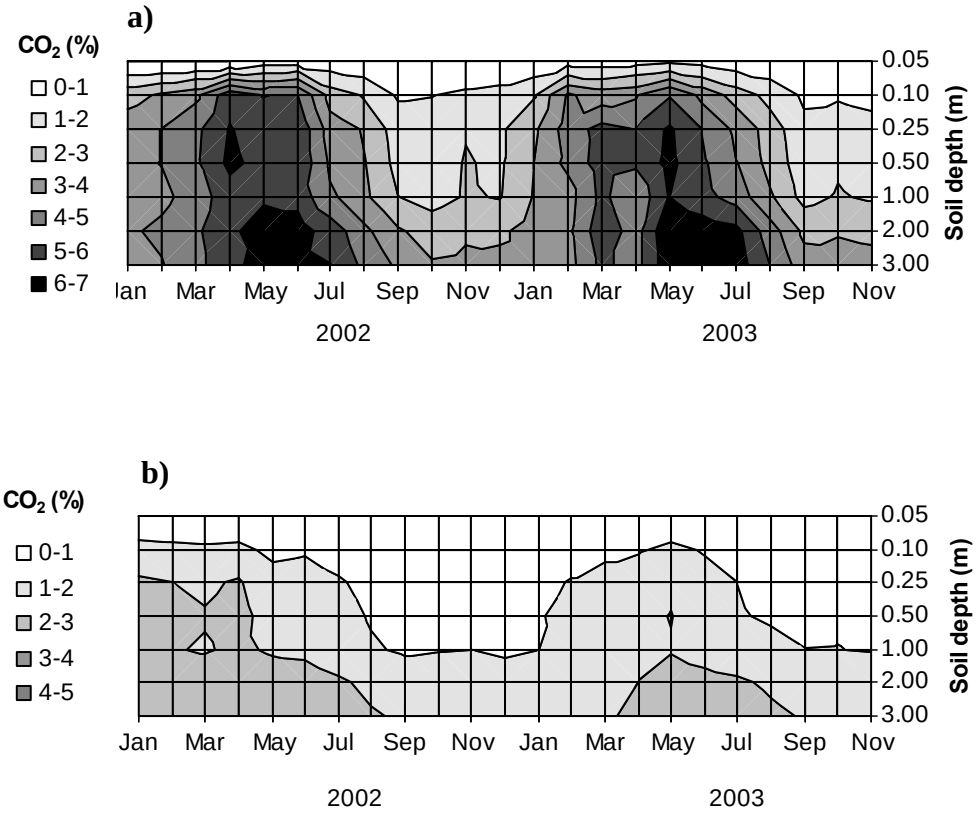

Figure 3.4 - Isopleths of CO_2 concentration in soil air as a function of soil depth and time in (a) control and (b) TFE plot. Each measurement is the mean of four profiles per plot.

Effects of environmental parameters on soil CO_2 efflux and on CO_2 production

For both control and TFE plot, the relationship between soil CO_2 efflux and soil water potential (at 0-30 cm depth) could be described with a parabolic function (r^2 = 0.43, P < 0.001). The shape of the curves from both plots was complementary (Fig. 3.5a) with the higher water potential from the TFE plot and lower from the control. Taking only the values from the TFE plot we observed a linear relationship between soil water potential and CO_2 efflux (r^2 = 0.36, P < 0.001). We did not find any significant effect of temperature on soil CO_2 efflux, but there was a positive covariation between soil temperature and soil water potential (r^2 = 0.07, P < 0.05; Fig. 3.5b).

Total litter biomass for both plots had a significant polynomial relationship with soil CO_2 efflux (r^2 = 0.13, P < 0.05) which is probably explained by the positive linear relationship between total litter and soil water content (r^2 = 0.25, P < 0.001). The reproductive part of the litter (~15 % of total litter biomass) also had a high relationship with soil CO_2 efflux and co-varied with soil water content. A positive linear relationship was found between reproductive part of the litter and soil water content for the TFE plot (r^2 = 0.35, P < 0.01), but for the control plot the linear relationship was negative and only marginally significant (r^2 = 0.16, P = 0.05).

For the control plot at 0-0.5 m and 0.6-1.0 m depth there was no correlation with P_{CO2}. At 1.1-2.0 m depth soil temperature correlated positively with P_{CO2} (r = +0.41), while at 2.1-3.0 m depth soil water content (r = -0.52), soil temperature (r = +0.41) and PAR (r = +0.46) correlated with P_{CO2}. For the TFE plot at 0-0.5 m depth soil water content (r = +0.63) and soil temperature (r = -0.35) correlated with P_{CO2}. At 0.6-1.0 m soil water content (r = +0.41), soil temperature (r = -0.44) and air temperature (r = -0.56) also had significant correlations. There was no significant correlation at 1.1-2.0 m depth with P_{CO2} rate but at 2.1-3.0 m depth soil water content (r = -0.48) and PAR (r = +0.47) correlated with P_{CO2} rate.

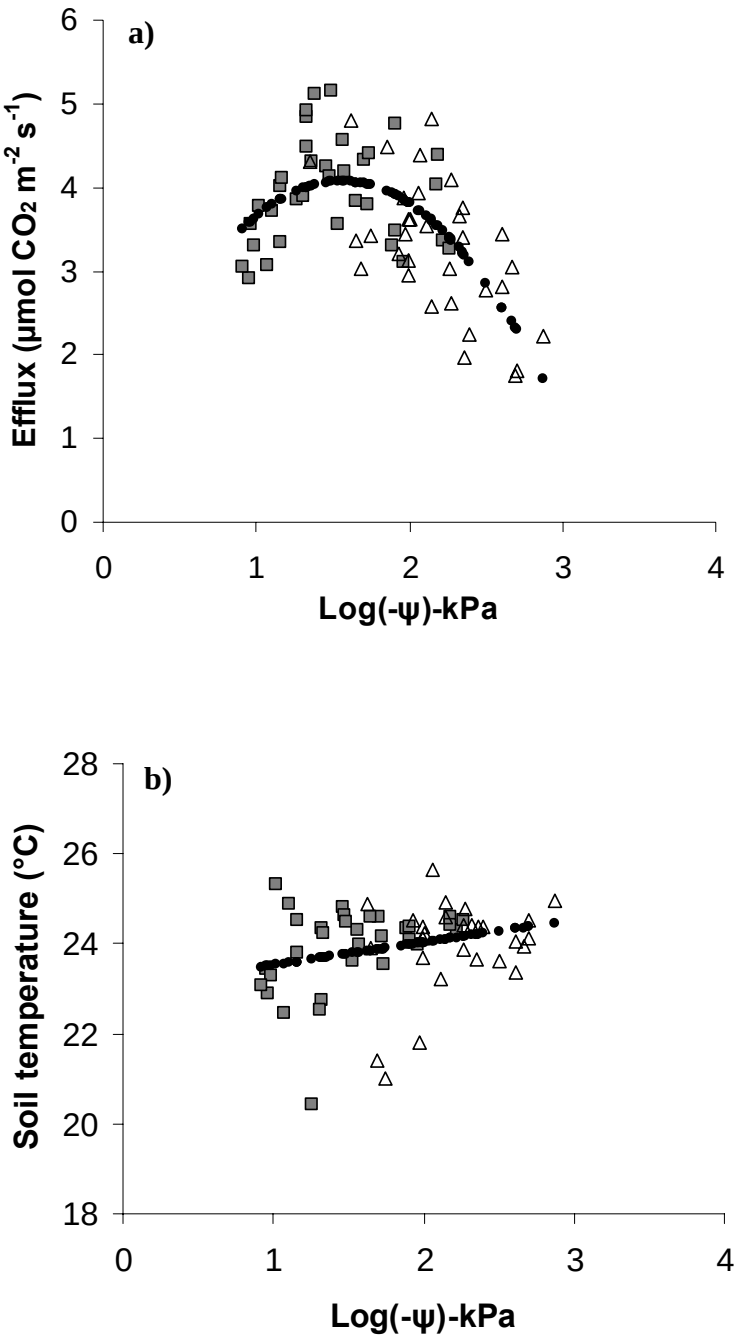

Figure 3.5 - Relationship between (a) soil water potential and soil CO_2 efflux and (b) between soil water potential and soil temperature with data from both control (■) and TFE (△) plot. The regression equation for (a) is Efflux = -1.3664 (log ψ)^2 + 4.2622 (log ψ) + 0.7486 (r^2 = 0.43, P < 0.001) and for (b) is Soil temperature = 0.5051(log ψ) + 23.008 (r^2 = 0.07, P < 0.05).

3.4. Discussion

Effects of seasonality on soil CO_2 production and emission

Soil CO_2 efflux in the control plot was strongly affected by seasonality. Although on average no difference was detected in soil CO_2 efflux between dry and wet season, this masks the strong seasonal response that we observed as a result of changes in soil moisture content (Fig. 3.2). At the onset of the rainy season, soil CO_2 efflux was high, and tended to decrease during the course of the wet season when soil water content increased. This was especially clear during the first year. The low soil CO_2 efflux at the end of the wet season corresponded with high CO_2 concentrations in the topsoil (Fig. 3.4) which suggests that low gas diffusivity may have contributed to the low soil CO_2 efflux. A similar pattern in soil CO_2 efflux during the wet season in Costa Rica was also explained with reduced gas diffusivity (Schwendenmann et al. 2003). However, as was the case in Costa Rica, this cannot be the only explanation as soil CO_2 *production* rates (calculated with the gas diffusion model) in the top 0.5 m of our study were also reduced at the end of the wet season (Fig. 3.3). The high water content at the end of the wet season may have reduced microbial activity and root activity which may have resulted in lower CO_2 production. Reduced soil CO_2 efflux from an Amazonian forest during the wet season has also been attributed to lower solar flux rates, which could affect photosynthesis rates and indirectly also root respiration (Wofsy et al. 1988).

At the beginning of the dry season the observed increase in soil CO_2 efflux corresponded with a strong decrease in CO_2 concentrations (Fig. 3.2a a 3.4). A similar increase in CO_2 efflux has been observed in a study in Paragominas (Davidson et al. 2000a) and in Costa Rica (Schwendenmann et al. 2003). The increase may be the result of CO_2 diffusing out of the soil that had accumulated during the wet season. However, the transition of wet to dry season may also have caused high root growth as has been observed e.g. in a

Panamanian rainforest (Cavelier et al. 1999). The decrease in soil CO_2 efflux during the dry season we attribute to water stress which may have reduced root respiration as well as heterotrophic respiration. Such a decrease has been observed in the forest in Paragominas which has also a strong dry season (Davidson et al. 2000a) but not in Costa Rica, which has a very weak dry season (Schwendenmann et al. 2003). A strong increase in CO_2 production after some rainstorms at the beginning of the wet season was probably caused by the effect of rewetting. During rewetting normally a CO_2 production peak occurs which depends on the size of decomposable soil organic carbon (Franzluebbers et al. 2000). Field experiments in temperate forests have shown that this CO_2 peak occurs within minutes of rewetting and strongly depends on the amount of rain added to the ecosystem (Borken et al. 2003).

Effects of throughfall exclusion on soil CO_2 efflux and CO_2 production

During the first year we were able to distinguish three phases in the TFE experiment. The first phase started with a reduction in soil CO_2 production in the 0.0-0.5 m depth interval shortly after throughfall was excluded (Fig. 3.3a) which was accompanied by an increase in the depth interval 0.5-2.0 m until May 2002 (Fig. 3.3b) and in the depth interval 2.0-3.0 m depth from March until July 2002 (Fig. 3.3c). These features can be explained by a translocation of water uptake (and accompanying root activity) to deeper layers in the TFE plot. Roots are expected to respond to reduced water availability in the topsoil by searching for water deeper in the soil profile (Joslin et al. 2000, Norby and Jackson 2000). This is furthermore supported by the lack of difference between total soil CO_2 efflux between TFE and control in this period (Fig. 3.2a) which suggests that there was not yet enough water stress to affect microbial activity and/or total root respiration. A similar translocation of root activity to deeper layers has been observed in a Costa Rican rain forest even though the dry season in this forest is very weak (Schwendenmann and Veldkamp 2006). It should be mentioned here

that in our method to derive CO_2 production in the top 0.5 m, CO_2 production in topsoil and subsoil were not completely independent so these results should be interpreted with care.

The second phase of the drying started at the onset of the dry season (July 2002; Fig. 3.3a). The observed reduction in total soil CO_2 efflux and soil CO_2 production (0-0.5 m) in the TFE plot compared to the control was probably related to a reduction of the activity of soil- and litter decomposers, which are sensitive to water stress (Lavine et al. 2004, Li et al. 2005). At this moment a reduction in total root respiration did not yet occur because sap flow measurements from this period in the TFE plot did not show a reduction either suggesting that water stress was not yet severe enough to affect photosynthesis (Fisher et al. in review b). Further support comes from an ancillary experiment where we showed that during the wet season about 25 % of the soil CO_2 efflux originated from the litter layer, a contribution which became negligible during the dry season (Sotta et al. in review). Bacterial activity declines sharply as water potential falls from -50 to -300 kPa and is negligible at -1500 kPa (Wong and Griffin 1976). In our experiment, the decrease in soil CO_2 efflux in July 2002 was accompanied with a drop in soil water potential from -100 to -200 kPa. The lag between the start of the TFE and the reduction in soil CO_2 production and CO_2 efflux was probably related to the time necessary for the litter to dry out. In a temperate forest Salamanca et al. (2003) showed that after 12 months of partial throughfall exclusion, litter mass loss was not different from the control. However, three months of total exclusion resulted in lower litter mass loss, lower CO_2 efflux and lower microbial biomass of decomposing forest litter.

The third phase of drying was characterized by a continuing decrease in soil CO_2 production between Sep. and Nov. 2002 which was probably dominated by a water stress-induced decrease in total root respiration when soil water potential dropped from -250 to -500 kPa. This is supported by a decline in sap flow which was probably caused by the reduced stomatal conductance due to the low soil-to-leaf water supply (Fisher et al. in review b). The

reduction in stomatal conductance caused a decrease in estimated GPP suggesting a reduction in the photosynthetic supply (Fisher et al. in review b). This may also explain the high observed correlation between the reproductive parts of the litter and CO_2 efflux.

Comparison with the drought experiment in Santarém and consequences for drought sensitivity

In the control plot (no TFE) the annual estimate of soil CO_2 efflux in Santarém was about 30 % lower (10 Mg C ha^{-1} yr^{-1}, Davidson et al. 2004) than the estimate for Caxiuanã (15 Mg C ha^{-1} yr^{-1}). The higher soil CO_2 efflux in the control of Caxiuanã is probably related to soil texture as the soil CO_2 efflux from an Oxisol with a clay texture in Caxiuanã was also lower compared to the sand (Sotta et al. in review). Apart from soil texture, also rooting depth probably differs between the two sites (at least 12 m rooting depth in Santarém (Davidson et al. 2004); 10 m rooting depth in Caxiuanã with very low root density under 5 m because of coarse sands (Fisher et al. in review b)). In contrast to our results, three years of throughfall exclusion in Santarém led to a marginal increase of about 9 % (11 Mg C ha^{-1} yr^{-1}) in the annual soil CO_2 efflux while in Caxiuanã already the first year of throughfall exclusion led to a decrease of 22 % (12 Mg C ha^{-1} yr^{-1}) in annual soil CO_2 efflux. Theses different reactions of soil CO_2 efflux to throughfall exclusion are probably related to the time needed to reach a matrix potential where decomposition and photosynthesis are strongly reduced because of water stress. While with the clay texture and deep rooting zone in Santarém three years of throughfall exclusion did not reach this matrix potential, the sandy texture and less available soil water at depth, caused that this critical matrix potential was already reached in the first dry season following throughfall exclusion in Caxiuanã. This completely different effect of soil CO_2 efflux to throughfall exclusion illustrates that soil characteristics (especially soil texture, related soil water retention and rooting depth) will strongly influence the resilience of

Amazonian forests to prolonged dry periods. The more drought-sensitive ecosystems are the ones located on soils with coarse textures which cannot compensate the relatively low water holding capacity with water stored in deeper soil layers.

4. Mechanisms of soil N retention in an Eastern Amazonian Rainforest, Caxiuanã, Brazil.

4.1. Introduction

High nitrogen (N) deposition is an environmental problem recognized until recently mainly in the economically developed regions of Europe and North America (Matson et al. 1999). Projections are that rates of N deposition in the tropics will increase by several hundred percent due to demands for food and energy by a growing population with increasing per capita use of N (Galloway et al. 2002). Presently, Latin America is a region where both enhanced and low inputs of reactive N occur, and a rapid increase is predicted for this region (Galloway et al. 2004) as a consequence of continued increase in fertilizer use, fossil fuel consumption (Matson et al. 1999), and biomass burning (Cochrane 2003, Fabian et al. 2005).

European and North American studies on responses of forest ecosystems to elevated N inputs have reported forest destabilization, increased NO_3^- pollution to ground and surface water (Aber et al. 1998, Schulze 1989), increased soil acidity (Van Breemen et al. 1982), increased losses of soil nutrients that are important for long-term fertility of soils, increased emissions of N_2O (a potent greenhouse gas) and other N-oxides which drive the formation of photochemical smog (Vitousek et al. 1997), and loss of biodiversity (Bobbink et al. 1998). A condition in which N availability exceeds the capacity of plants, soil biotic and abiotic processes to accumulate N is termed as N saturation (e.g., Aber et al. 1998). The results of European and North American studies have been summarized by Aber et al. (1998) into a conceptual model of N saturation, which depicts that the rate at which a forest ecosystem moves towards N saturation is regulated by two main factors: the rate of N input and the inherent N status of the system (the latter being determined by soil type, forest types, and land-use history). The only experiment in tropical forest in which environmental

consequences of elevated N input have been investigated (in Hawaii; Vitousek and Farrington 1997) reported that N additions were processed differently in N-limited forests and forests with high N-availability, depending on the relative strength of the pathways of N-retention versus N-loss (such as leaching losses (Hedin et al. 2003) and N trace gases emissions (Hall and Matson 2003)). In contrast to N-limited forests, high-N availability forests responded to N additions with large and immediate losses of N_2O and other N-oxides (Hall and Matson 2003). This study and those from temperate forests made clear that the soil N status is the key to analyze effects of increasing anthropogenic N deposition on forest ecosystem processes.

At present, our knowledge on the N status of tropical forests is based on indirect evidence, e.g., N contents in leaves and litter (Vitousek 1984), extractable inorganic N, net rates of soil N cycling and related N oxide emissions (Matson and Vitousek 1987, Riley and Vitousek 1995, Davidson et al. 2000b), and ^{15}N isotope signals in leaves and soils (Martinelli et al. 1999). While net rates of soil N cycling provide information on N availability for plants, they do not reveal the N retention processes which are important indicators of how a forest ecosystem reacts to changes in N input. An alternative way to asses the soil N status of tropical forest is identification and quantification of pathways of N-retention versus N-production. So far there are only few studies in tropical forest soils which quantified gross rates of soil N cycling, revealing rates of N production and consumption (i.e., Puerto Rico: Silver et al. 2001; Hawaii: Hall and Matson 2003; Costa Rica: Silver et al. 2005; Indonesia: Corre et al. 2006; and only one study in the Brazilian Amazon (Rondonia): Neill et al. 1999).

From indirect evidence of the N status of tropical forests, lowland forests have higher litterfall N contents, lower dry mass/N ratios (Vitousek 1984), higher net mineralization rates and N trace gas emissions (Matson and Vitousek 1987, Riley and Vitousek 1995, Davidson et al. 2000b), and heavier $\delta^{15}N$ signals in leaves and soils (Martinelli et al. 1999) than montane forests, supporting the speculation that N in lowland forests is in relative excess. However,

within the lowland forests of Amazon basin, there is substantial evidence that soil texture influences soil NH_4^+ and NO_3^- concentrations, water and other nutrient ions availability, decomposition, soil C retention and net primary production, particularly in highly-weathered soils (Silver et al. 2000, Luizão et al. 2004). For example, Silver et al. (2000) reported that Amazonian lowland forests on clay soils have higher NO_3^- and lower NH_4^+ concentrations than those on sandy soils. Sites where extractable NO_3^- dominates over NH_4^+ have been characterized as having a 'leaky' or relative excess of N (i.e. N losses through NO_3^- leaching or gas emissions are relatively high compared to the amount of N cycling), while sites where NH_4^+ dominates have been interpreted as N-limited or having a 'closed' N cycle (Davidson et al. 2000b). Our investigation was therefore based on two contrasting soil texture on highly-weathered soil (Oxisol) in an Eastern Amazon forest. Our objectives were: 1) to assess the soil N status of a sandy and clayey, lowland forest soils by quantifying gross rates of N-production processes (N mineralization and nitrification), and 2) to evaluate their differences in N-retention processes by measuring the microbial N immobilization, dissimilatory NO_3^- reduction to NH_4^+, and abiotic N immobilization. Direct quantification of the inherent soil N status of tropical forests and processes of N retention will provide much-needed baseline information for tropical forests, which may hint how such ecosystems will react to predicted increase in N deposition.

4.2. Methods

Site Description

The experimental site was located in Caxiuanã National Forest, Pará, Brazil (1°43'3.5''S, 51° 27'36''W). The forest is an old-growth lowland *terra firme* rainforest. Mean annual temperature is 25.7 ºC. Mean annual rainfall is 2272 mm, with a pronounced dry

season between July and December, when on average only 555 mm of rainfall occurs (Fisher et al. 2006). The plateau of the Caxiuanã region belongs to Alter do Chão Formation (Costa and Kern 1999), which contains sedimentary rocks with texture varying from sand to clay. Soil of Caxiuanã are predominantly Oxisols (Brazilian classification Latosol), with large differences in texture (Kern 1996). Our study was conducted on two Oxisols with contrasting soil texture: clay and sand (Table 4.1). Both soils have a broken laterite layer (0.3-0.4 m thick) at 3-4 m depth. The texture of the top 0.5 m of the sand is 75 % sand and 25 % clay + silt, while the topsoil of the clay has 31 % sand and 69 % clay + silt. Mineralogy of both soils is mainly kaolinite in the clay fraction and quartz in the sand fraction (Ruivo and Cunha 2003).

Sampling design

Soil samples were collected from the sand and clay sites once during the dry (August 2004) and once during the wet (April 2005) season. From a randomly selected central transect four sampling points spaced 20 m apart were sampled. A 20-m sampling distance was selected because this ensured spatial independence between sampling points (see *Statistical Analyses*). At each sampling point, 5 undisturbed samples of the topsoil (0-0.05 m) were taken within a 0.30 m x 0.30 m area using stainless steel cores of 0.08 m diameter. Furthermore, soil, litter and green leaf samples were taken at each site for analysis of supporting parameters.

Table 4.1. Main characteristics of the forest sites (mean ± SE; *n* = 3) in Caxiuana, Brazil.

	Sand		Clay	
Leaves*		(SE)		(SE)
C [mg-C g^{-1}]	47.0	----	46.2	----
N [mg-N g^{-1}]	1.6	----	1.4	----
C/N ratio	29.2	----	33.9	----
$\delta^{15}N$[‰]	4.3	----	6.7	----
Litter				
C [mg-C g^{-1}]	46.8	1.7	47.5	1.0
N [mg-N g^{-1}]	1.2	0.0	1.6	0.1
C/N ratio	38.2	1.5	30.3	1.2
$\delta^{15}N$[‰]	5.0	0.5	6.4	0.4
Decomposing litter				
C [mg-C g^{-1}]	44.6	0.7	41.8	1.8
N [mg-N g^{-1}]	1.4	0.1	1.4	0.1
C/N ratio	30.9	4.9	29.6	2.4
$\delta^{15}N$[‰]	5.5	0.2	6.8	0.5
Mineral soil (0 - 5 cm depth)				
Bulk density [Mg m^{-3}]	1.4	0.5	1.2	0.6
Sand [%]	78.3	----	43.4	----
Clay [%]	13.6	----	42.2	----
Silt [%]	8.1	----	14.4	----
pH-H_2O	3.9	0.1	3.8	0.1
pH-KCl	3.3	0.1	3.4	0.0
Effective CEC [$mmol^{(+)}kg^{-1}$]	31.1	7.0	54.6	5.7
Base Saturation [%]	24.8	4.0	23.2	3.3
C [mg-C g^{-1}]	20.1	4.1	35.8	4.6
N [mg-N g^{-1}]	1.3	0.2	2.5	0.3
C/N ratio	15.5	0.5	14.0	0.2
$\delta^{15}N$[‰]	7.7	0.1	9.7	0.3
Total P [mg-P g^{-1}]	0.1	0.0	0.2	0.0

* Leaf sampling was one composite sample (*n* = 1) made of three subsamples

Soil cores were put in cases with built-in fittings to maintain their integrity and packed with blue ice during transport. They were transported from Caxiuanã, Brazil to the Institute of Soil Science and Forest Nutrition, Göttingen, Germany, where the N cycling measurements

were conducted. Samples were kept cool during the whole duration of the transport. The duration between field sampling and the start of laboratory assay was 2 weeks. Prior to measurements, the soil cores were allowed to acclimatize in the laboratory for 2 days at 24 °C (average soil temperature of the site).

^{15}N pool dilution for measurement of gross rates of N mineralization and nitrification

We used the ^{15}N pool dilution technique to estimate gross rates of soil N cycling (Davidson et al. 1991, Hart et al. 1994a). From 4 core samples at each sampling point, 2 were injected with $(^{15}NH_4)_2SO_4$ solution (for gross N mineralization) and 2 with $K^{15}NO_3$ solution (for gross nitrification), using 18 gauge side-port spinal needles. Each core received five 1-mL injections of the solutions, containing 30µg N mL^{-1} with 98 % ^{15}N enrichment. This was equivalent to a rate of 1.0-1.7 µg ^{15}N g^{-1} for the sandy soil and 1.4-2.4 µg ^{15}N g^{-1} for the clayey soil. One core of each labelled pair was immediately broken up, mixed well in a plastic bag, and subsampled for extraction with 0.5 mol L^{-1} K_2SO_4 (approx. 5:1 ratio of solution to dry mass soil). Time elapsed between injection and extraction was 10 minutes (T_0 cores). Not all of the added $^{15}NH_4$ and $^{15}NO_3$ were recovered in the labelled pool at T_0. The T_0 cores were used to correct for reactions that occur immediately after injection of $^{15}NH_4$ and $^{15}NO_3$, as recommended by Davidson et al. (1991) and Hart et al. (1994a). In the second measurement of soil N cycling rates (wet season, April 2005), we identified the fates of added ^{15}N at T_0 by measuring ^{15}N recoveries in K_2SO_4-extractable mineral N and organic N pools (by Persulfate digestion; see below *N concentration and ^{15}N analyses*) and in the total N pool (by submitting freeze-dried subsamples directly for isotope ratio mass spectrometry (IRMS)). The ^{15}N recovery in the insoluble (non-extractable) organic N pool was calculated from the difference between ^{15}N recoveries in the total N pool and in K_2SO_4-extractable N pools (NH_4^+ + NO_3^- + soluble organic N).

The other pair of labelled cores was incubated for 1 day (except for the $^{15}NO_3$ injected cores from wet-season sampling that were incubated for 2 days) in the dark at 24 ºC (T_1 cores). The $^{15}NO_3^-$-labelled wet-season cores were incubated for 2 days because our measurements in August 2004 showed very minimal change in $^{15}NO_3^-$ enrichment and NO_3^- concentration within 1 day of incubation. The T_1 cores were then extracted with 0.5 mol L^{-1} K_2SO_4. Extraction was done by shaking the samples for 1 hour and filtering the extracts through K_2SO_4-rinsed filter paper. From each core sample, gravimetric moisture content was measured in order to express gross rates on a soil dry mass basis.

Gross N mineralization and nitrification rates were estimated from cores that received $^{15}NH_4^+$ and $^{15}NO_3^-$, respectively, using the modified calculation procedure of Davidson et al. (1991) from the Kirkham and Bartholomew (1954) model. For gross nitrification rates, the method we used does not distinguish between autotrophic and heterotrophic nitrification; results presented include both these processes.

N concentration and ^{15}N analyses

NH_4^+ and NO_3^- contents of extracts were analyzed using continuous flow injection colorimetry (Cenco/Skalar Instruments, Breda, Netherlands), where NH_4^+ was determined using the Berthelot reaction method (Skalar Method 155-000) and NO_3^- was measured using the copper-cadmium reduction method (Skalar Method 461-000). Detection limits were 150 μg N L^{-1} for NO_3^- and NH_4^+. The organic N content of extracts was determined by Persulfate digestion (Cabrera and Beare 1993, Stark and Hart 1996), which involves oxidation of NH_4^+ and organic N to NO_3^- while NO_3^- remains the same. We conducted an ancillary experiment to test this method and results showed complete oxidation of NH_4^+ and organic N and no losses of NO_3^-. In short, 10 mL extract was added with 10 mL oxidizing reagent (consisting of 50 g $K_2S_2O_8$, 30 g H_3BO_3, and 100 mL of 3.75 mol L^{-1} NaOH per 1-L solution) and was

autoclaved for 1 hour at 120 °C; distilled-deionized water was added to a final volume of 100 mL and the N concentration was analyzed by colorimetry. Extractable organic N was calculated as the difference between Persulfate-N (i.e, total N) and NH_4^+ + NO_3^- concentrations.

For ^{15}N analysis from the extracts, the diffusion procedure described in detail by Corre et al. (2003) and Corre and Lamersdorf (2004) was followed. We used 5-cm wide Teflon (polytetrafluoroethylene) tape to encase the acidified filter disks (2 disks of 7-mm diameter cut from glass fiver filter paper and acidified with 20 μL of 2.5 mol L^{-1} $KHSO_4$ solution), and this Teflon-encased acid trap was placed on the mouth of the diffusion bottle. The wide Teflon tape covered the mouth of the diffusion bottle which helped fastening the lid tightly.

For the T_0 cores, part of the extracts was used for serial diffusion of NH_4^+ and NO_3^- and part was used for Persulfate digestion for determination of ^{15}N enrichment in extractable organic N pool (Stark and Hart 1996). This allowed us to detect which extractable N pools of the unrecovered portion of the added ^{15}N was converted at T_0. For NH_4^+ diffusion, 50 mL of the K_2SO_4 extract was placed in a 150-mL glass bottle. MgO was added to make the extract solution alkaline and drive off NH_3; the Teflon-encased acid trap was immediately placed on the mouth of the bottle and the lid fastened. Diffusion proceeded for 6 days in 22 °C room, during which periodic mixing of the solution was done by swirling the bottles. The bottles were left open for 5 days before diffusion of NO_3^- to completely eliminate residual NH_4^+, if any. For NO_3^- diffusion, new MgO and Devarda's alloy were added to convert NO_3^- to NH_3. For ^{15}N determination in the extractable organic N pool, 2 mL of 10 mol L^{-1} NaOH was added to 50 mL of the Persulfate digest (raising the pH to > 13) and left open for 5 days to eliminate any residual NH_4^+. Diffusion of Persulfate-N (NO_3^- form) proceeded by adding another 2 mL of 10 mol L^{-1} NaOH (maintaining the pH at >13) and Devarda's alloy, similar to the methods of Stark and Hart (1996). We calculated the ^{15}N enrichment of the extractable organic N pool

based on isotope mixing equations using the difference in ^{15}N enrichments and N concentrations between the Persulfate-N (i.e, total N) and NH_4^+ + NO_3^- pools. Our ancillary test of the Persulfate-N diffusion method, similar to the test of Stark and Hart (1996), showed that ^{15}N enrichment from extractable organic N was accurately measured. For the T_1-core extracts, only NH_4^+ was diffused from the $^{15}NH_4^+$-labeled cores (for gross N mineralization), and NH_4^+ and NO_3^- were sequentially diffused from the $^{15}NO_3^-$-labeled cores (for gross nitrification and dissimilatory nitrate reduction to ammonium (see below)). Part of the T_1-core extracts was reserved for the microbial N immobilization assay (see below). Blank correction, calculated by isotopic dilution, was carried out as recommended by Stark and Hart (1996). ^{15}N was analyzed using IRMS (Finigan MAT, Bremen, Germany).

Dissimilatory nitrate reduction to ammonium (DNRA)

We calculated rates of DNRA, using the $^{15}NO_3^-$-injected cores, as the difference in the $^{15}NH_4^+$ atom % between T_0 and T_1, multiplied by the mean NH_4 pool size during the incubation period, and corrected for isotopic composition of $^{15}NO_3^-$ source pool over the incubation interval (Silver et al. 2001, 2005). This was also corrected for any NH_4^+ transported out of the NH_4^+ pool (i.e., mean residence time of NH_4^+) over the incubation period.

NH_4^+ and NO_3^- immobilization rates and microbial biomass C and N by chloroform fumigation

We used the T_1 $^{15}NH_4^+$- and $^{15}NO_3^-$-labeled cores to assess NH_4^+ and NO_3^- immobilization rates, respectively, as described in detail by Davidson et al. (1991). About 25 g fresh samples were placed in a desiccator containing a beaker of purified $CHCl_3$ with

several boiling chips. The desiccator was evacuated and flushed with air several times to distribute $CHCl_3$ vapor, and during the final evacuation it was closed after letting the $CHCl_3$ bubble for 3 minutes. After 5 days of fumigation, the desiccator was flushed with air several times to remove $CHCl_3$ vapor, and the samples were extracted with 0.5 mol L^{-1} K_2SO_4 (approx. 5:1 ratio of solution to dry mass soil).

From these fumigated T_1-core extracts and the corresponding unfumigated T_1-core extracts, extractable organic N was determined using Persulfate digestion described earlier. The ^{15}N in the Persulfate digests was determined following the diffusion procedures mentioned above. The ^{15}N recovered in fumigated samples was subtracted with the ^{15}N recovered in corresponding unfumigated samples to estimate the ^{15}N released (presumably from microbial biomass) by fumigation. NH_4^+ and NO_3^- immobilization rates were calculated using the non-linear model described by Davidson et al. (1991), which is based on the ratio between the ^{15}N appearance in the $CHCl_3$-labile pool and the change of ^{15}N enrichments and mineral N concentrations from T_0 to T_1.

Microbial biomass C and N were determined from samples taken from the same sampling point, acclimatized at the same temperature and period as the cores used for microbial N cycling measurements. We used the fumigation-extraction method (Brookes et al. 1985, Davidson et al. 1989) for determining microbial biomass. Two 25-g fresh subsamples were taken. One pair of the subsamples was immediately extracted with 0.5 M K_2SO_4 (approx. 5:1 ratio of solution to dry mass soil) and the other pair was fumigated for 5 days and then extracted. Organic C from the extracts was analyzed by UV-enhanced persulfate oxidation using a Dohrmann DC-80 Carbon Analyzer with an infrared detector (Rosemount Analytical Division, CA, U.S.A.). Organic N was determined using Persulfate digestion described earlier. The differences in organic C and Persulfate-N extracted between the fumigated and unfumigated soils (C and N flushes) are assumed to represent the C and N

released from lysed soil microbes. The C and N flushes were converted to microbial biomass C and N, respectively, using k_C = 0.45 (Joergensen 1996) and k_N = 0.68 for 5-day fumigated samples (Shen et al. 1984, Brookes et al. 1985).

Calculation of mean residence time (MRT)

The MRT indicates the average length of time an N atom resides in a given pool; a lower MRT indicates a faster pool turnover rate and hence a more dynamic pool. The calculation of MRT (N pool ÷ flux rate; e.g. microbial N_{MRT} = microbial N pool ÷ total N immobilization rate) assumed that the NH_4^+, NO_3^-, and microbial biomass N pools were at steady state and that the fluxes were equal to gross rates of N mineralization, nitrification, and total N ($NH_4^+ + NO_3^-$) immobilization, respectively.

Other supporting parameters

Site characteristics were determined at the start of the study and are reported in Table 4.1. We collected samples of leaves, fresh litter and decomposing litter for C, N and $\delta^{15}N$ analyses to support our measurements of the soil N dynamics. Leaves from the trees were randomly collected to obtain a composite sample in each site. Three replicates of fresh litter, decomposing litter, and mineral soil (at 0-0.05, 0.05-0.10, 0.10-0.25 and 0.25-0.50 m depths) samples were also collected. All samples were oven-dried, ground and analysed for total organic C and N using CNS Elemental Analyzer (Elementar Vario EL, Hanau, Germany) and for ^{15}N natural abundance using IRMS. From $\delta^{15}N$ profile in each site, the enrichment factor (ε) of the soil was calculated following similar procedure employed by Mariotti et al. (1981) using a Rayleigh equation ($\varepsilon = \delta_s - \delta_{so} / \ln f$). δ_{so} stands for the $\delta^{15}N$ value of the input substrate, here the decomposing litter, δ_s for the $\delta^{15}N$ value at different depths in the soil

profile and *f* for the remaining fraction of total N. This fraction of total N was calculated as the total N at certain depth divided by the total N of the decomposing litter. $\delta^{15}N$ signal in forests has been used as indirect indicator of N status (Martinelli et al. 1999), soil N cycling behaviour (Nadelhoffer and Fry 1988), NO_3^- losses (Vervaet et al. 2002), and N gaseous emissions (Purbopuspito et al. 2006).

Additional soil characteristics were also measured. Bulk density was determined using soil core method. Particle size distribution was analyzed with the pipette method using pyrophosphate as a dispersing agent. Soil pH was measured from a saturated paste mixture (1:1 ratio of soil to H_2O and to 1 M KCl). Base saturation was calculated as the percentage base cations of the effective cation exchange capacity (ECEC); ECEC was determined from air-dried, 2-mm sieved samples, percolated with unbuffered 1 M NH_4Cl, and the percolates analyzed for exchangeable cations using Flame-Atomic Absorption Spectrometer (Varian, Darmstadt, Germany). Total P was analyzed from air-dried, ground samples, digested under high pressure in concentrated HNO_3, and the digests were analyzed using Inductively Coupled Plasma-Atomic Emission Spectrometer (Spectro Analytical Instruments, Kleve, Germany)

N_2O and CO_2 emissions were measured from the T_1 cores used for the measurement of gross rates of soil N cycling. The soil cores were placed for 30 minutes in a 1-L glass incubation vessels with a gas sampling port fitting on the lid, from which gas samples were drawn and analyzed for N_2O and CO_2 using a gas chromatograph (GC 14A, Shimadzu, Duisburg, Germany) equipped with an electron capture detector (Loftfield et al. 1997). Fluxes were calculated from the increase in N_2O and CO_2 concentrations during the incubation period minus the background N_2O and CO_2 concentrations (incubation vessel without a soil core). The CO_2 evolution was used to calculate total C utilized by microbes ([microbial C:N

ratio x total N immobilization rate] + CO_2-C evolution rate), which we used as an index of available C similar to that of Schimel (1988) and Hart et al. (1994b).

Statistical Analyses

First, we tested the spatial independence of our sampling points. This test can be carried out when the sampling points have uniform distance. In August 2004 sampling, we selected the sampling points in each soil type at uniform distance of 20 m and tested their spatial independence using the data on gross N mineralization rates. This test was carried out using the rank version of von Neumann's ratio test (Bartels 1982). We found that our sampling points spaced at 20 m apart were spatially independent. Earlier study on gross rates of microbial N cycling in tropical ecosystem (Corre et al. 2006) also showed sampling points at 10 m apart to be spatially independent and hence we considered the sampling points at each site as replicates in the succeeding analyses. Tests for normality using Kolmogorov-Smirnov D statistic (Sokal and Rohlf 1981) was conducted for each of the measured parameters. For parameters that were found to have non-normal distribution, log transformations were used to approximate normal distribution. Analyses were then carried out using two-way analysis of variance, with sites and sampling seasons representing treatments. Multiple comparisons of treatments were conducted using a Least Significant Difference test at $P \leq 0.05$. Means and standard errors were reported as measures of central tendency and dispersion, respectively.

4.3. Results

^{15}N recovery from intact cores 10 minutes (T_0) after ^{15}N injection

On average 88 ± 5 % of the added $^{15}NH_4^+$ was recovered in the form added when intact cores were extracted at T_0 (Fig. 4.1). We detected no difference in $^{15}NH_4^+$ recoveries

between soil types. Recoveries of ^{15}N in the NO_3^- pool were negligible (1.0 ± 0.2 %) and recoveries in the extractable organic N pool were not detectable (Fig. 4.1). ^{15}N recovery in the insoluble (not extractable by K_2SO_4) organic N was only 10 ± 3 % of the added $^{15}NH_4^+$, and no difference was detected between soil types. ^{15}N recoveries in the total N pool showed complete recovery of the injected $^{15}NH_4^+$ (Fig. 4.1).

For the $^{15}NO_3^-$-injected cores, on average 57 ± 4 % was recovered in the NO_3^- pool at T_0, and there was no difference detected between soil types (Fig. 4.1). We detected no ^{15}N above background level in the $^{15}NH_4^+$ pool, while the recovery of ^{15}N in the extractable organic N pool was on average 12 ± 5 % and did not differ between soil types. Also, ^{15}N recoveries in the insoluble organic N pool did not differ between soil types and was on average 25 ± 6 %. For the sand, higher ^{15}N recovery was measured in the insoluble organic N than in the extractable organic N, while for the clay similar ^{15}N recoveries were observed for these pools. ^{15}N recoveries in the total N pool were not significantly different from 100 % (Fig. 4.1).

Gross rates of NH_4^+ transformation, microbial biomass, and available C

High gross N mineralization rates were measured in the clay (seasonal average of 13.5 ± 3.1 mg N kg^{-1} d^{-1}), but these did not significantly differ from the rates in the sand (seasonal average of 6.0 ± 0.9 mg N kg^{-1} d^{-1}), because of the high variation. The rates also did not differ between seasons for each soil (Fig. 4.2). NH_4^+ immobilization rates were similar to gross N mineralization rates in the dry season, but were only about 50 % (sand) to 65 % (clay) in the wet season (Fig. 4.2). In the wet season, NH_4^+ immobilization rates were lower in the sand than in the clay. Mean residence time (MRT) of the NH_4^+ pool was on average 3.2 ± 1 days and there was no difference between soil types and seasons, although a noticeably high MRT

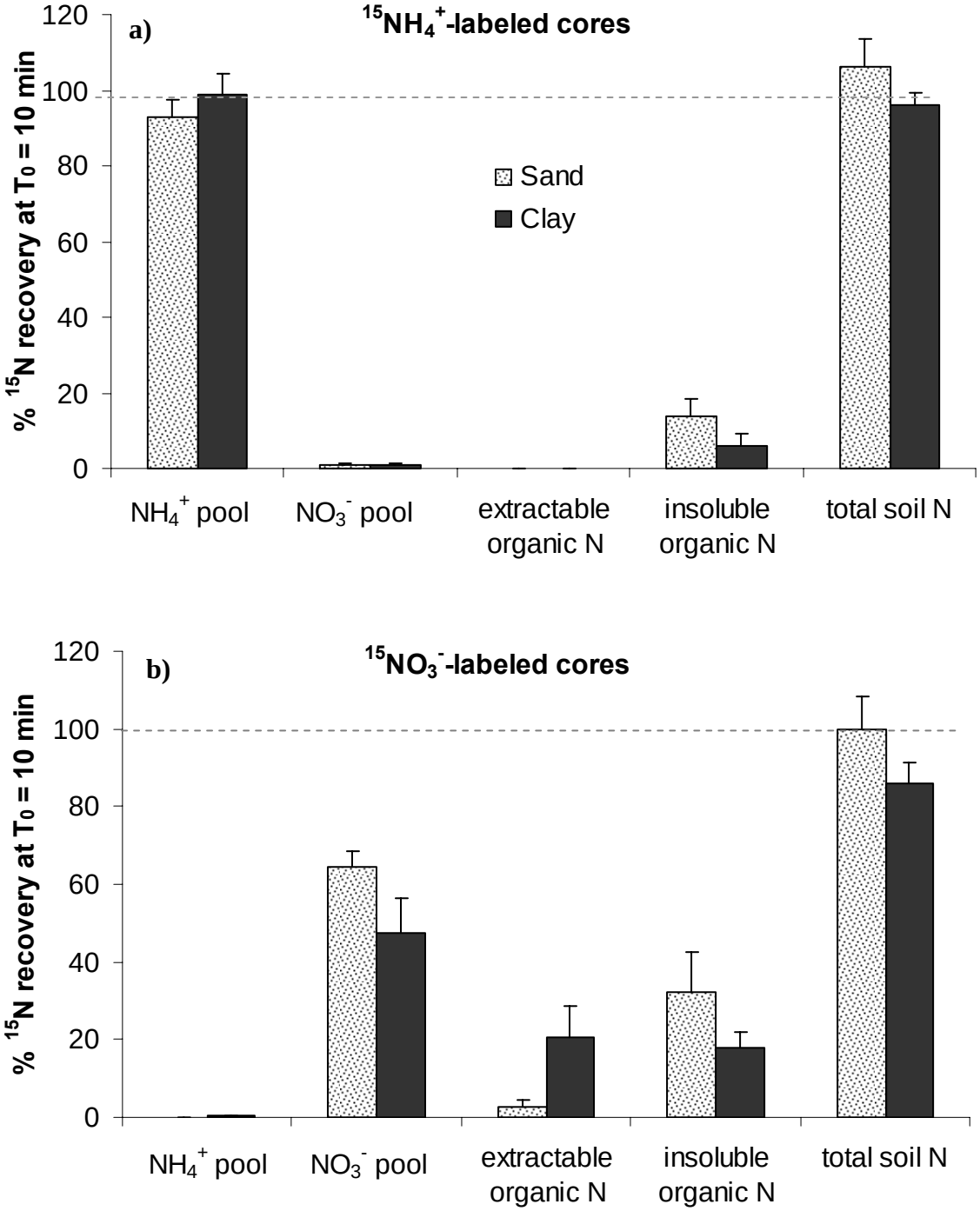

Figure 4.1 - Percent recovery (means ± 1 SE; *n* = 5) of ^{15}N in soil N pools after 10 minutes (T_0) of ^{15}N injection into the intact cores during the wet-season sampling (April 2005). (a) $^{15}NH_4^+$-labeled cores; (b) $^{15}NO_3^-$-labeled cores.

(slow turnover rates) occurred in the clayey soil during the wet season (Fig. 4.2). A similar trend was reflected in the size of the NH_4^+ pool; no difference existed between soil types and seasons, but a large NH_4^+ pool was apparent in the clayey soil during the wet season.

Microbial biomass N in the clay was more than twice as high as in the sand (Fig. 4.2), and in the sand, it was higher in the dry than in the wet season (Fig. 4.2). The MRT of microbial N pool was on average 10.1 ± 2.1 d, and no difference was observed between soil types and seasons, although a noticeably slow turnover rate was observed for the sandy soil during the wet season (Fig. 4.2). Microbial biomass C was higher in clay than in the sand and did not differ between seasons. Available C was higher in the clay than in the sand and in the clay, it was higher in the wet than in the dry season (Table 4.2).

$\delta^{15}N$ signals and enrichment factor (ε)

In both soils, $\delta^{15}N$ signals increased from leaves to litter to soil and with soil depth (Fig. 4.3). On the clay, $\delta^{15}N$ values of leaves were on average 2.4 ‰ higher and $\delta^{15}N$ values of fresh litter were 1.4 ‰ heavier than on the sand. We calculated the enrichment factor, which considers the $\delta^{15}N$ signals from the litter layer down the soil profile, to get an overall measure of the degree of ^{15}N enrichment for each soil type. A more negative enrichment factor indicates a faster mineralization of isotopically depleted organic N in the upper soil layers and an enrichment of residual soil organic matter in ^{15}N. Our calculated enrichment factors were higher for the clay than for the sand (Fig. 4.3).

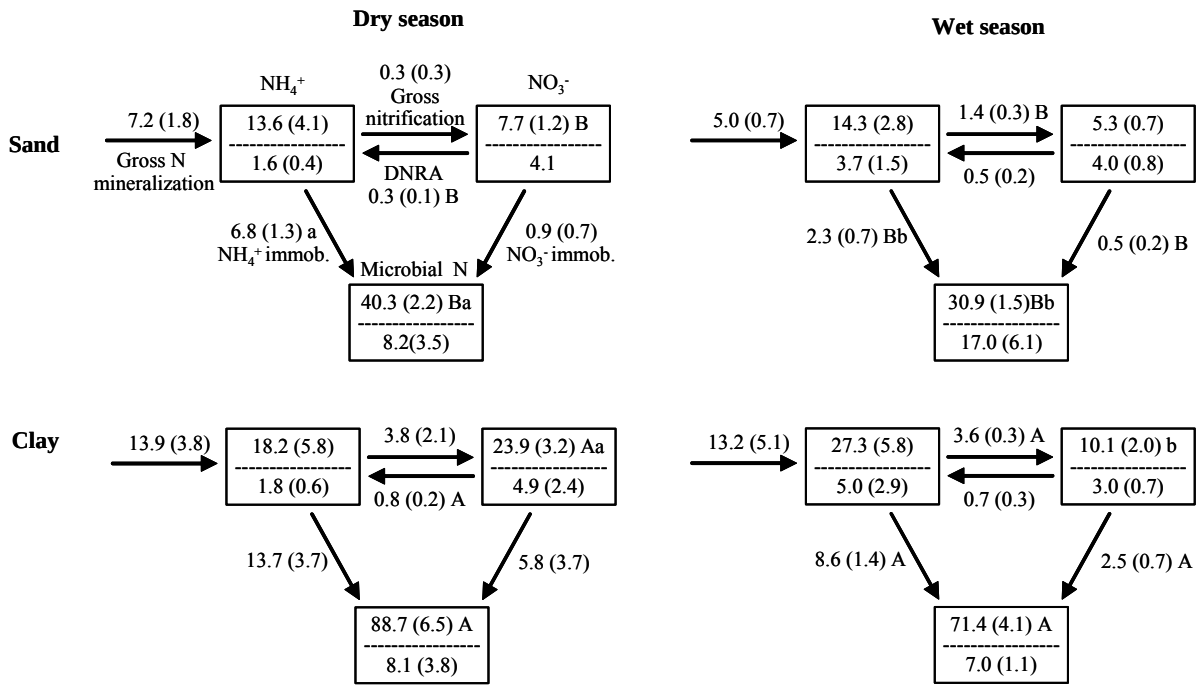

Figure 4.2 - Means ± 1 SE (n = 5) of gross rates of microbial N cycling (mg N kg^{-1} d^{-1}), of N pools (mg N kg^{-1}; upper numbers in boxes), and of mean residence time (day; lower numbers in boxes). For each parameter, means with different letters indicate significant differences between soil types at each season (upper case) and between seasons at each soil type (lower case). Arrows in sandy soil, dry season correspond to the same cycling components in clayey soil and both seasons.

Table 4.2. Microbial C, available C, water filled pore space (WFPS) and rates of N_2O emission for Oxisols with sand and clay texture at Caxiuanã National Forest, Brazil.

	Sand		**Clay**	
	Mean	SE	Mean	SE
Microbial C (mg kg^{-1})				
dry season	338 B	17	820 A	57
wet season	329 B	5	837 A	42
Available C (mg kg^{-1} d^{-1}) *				
dry season	97	46	218 b	40
wet season	163 B	11	392 Aa	62
N_2O emission (mg kg^{-1} d^{-1})				
dry season	2.9 B	2.10	19.3 Aa	5.1
wet season	0.1	0.02	6.6 b	1.8
Water-filled pore space (%)				
dry season	51 B	5.4	71 Ab	1.7
wet season	58 B	3.8	88 Aa	5.9

*Calculated using a similar index to that of Schimel (1988) and Hart et al. (1994b), where available C = ([microbial C:N ratio x total N immobilization rate] + CO_2-C evolution rate). Means ± 1 SE (n = 5) with different letters indicate significant differences between soil types at each season (upper case) and between seasons at each soil type (lower case) (two-way ANOVA, Least Significant Difference test at $P \leq 0.05$. There was no significant difference in N_2O emissions between the T_1 cores injected with $^{15}NH_4^+$ and $^{15}NO_3^-$; data for each replicate were the average from the two T_1 cores.

Gross rates of NO_3^- transformation, dissimilatory nitrate reduction to ammonium (DNRA), and N_2O emissions

Gross rates of nitrification and NO_3^- immobilization were much lower than gross rates of N mineralization and NH_4^+ immobilization in both soil types and seasons (Fig. 4.2). Both gross rates of nitrification and NO_3^- immobilization were higher in the clay than in the sand; this was particularly detectable in the wet season when the variation (as indicated by the standard

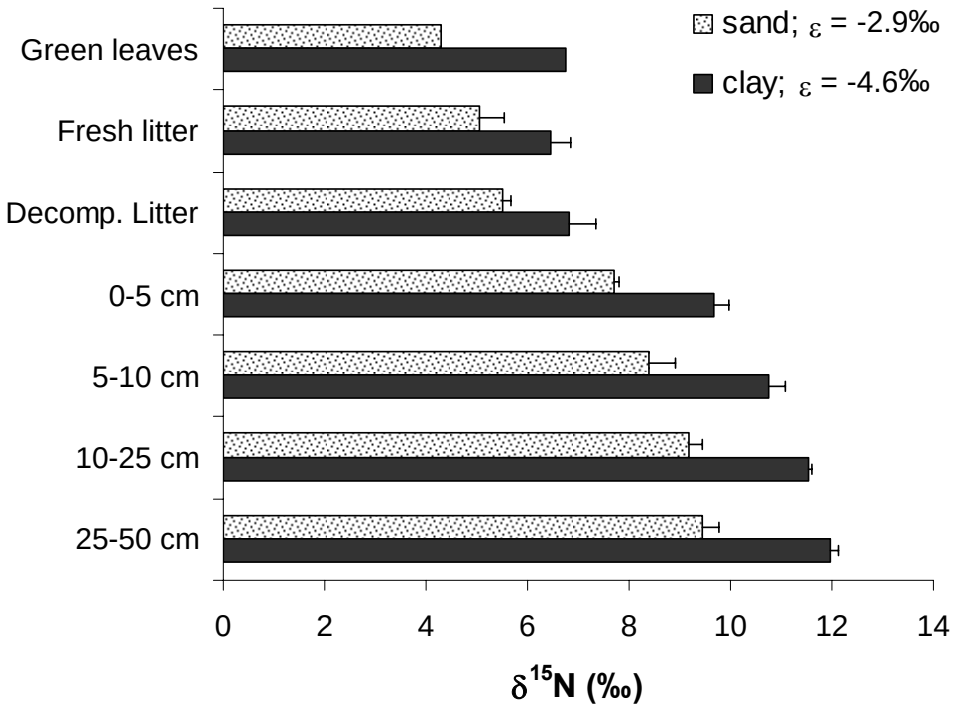

Figure 4.3 - Variation in natural abundance of ^{15}N ($\delta^{15}N$, ‰) for clayey and sandy soil. One data point represents the average of three samples (means ± 1 SE).

errors) was less (Fig. 4.2). NO_3^- immobilization rates were similar to gross nitrifications rates in the dry season (with high variation), but accounted only about 35 % (sand) to 69 % (clay) in the wet season. The NO_3^- pool was larger in the clay than in the sand during the dry season; and in the clay, the NO_3^- pool was larger in the dry than in the wet season (Fig. 4.2). MRT of the $^{15}NO_3^-$ pool was on average 3.9 ± 0.6 days and tended to be shorter in the clay during the wet season although differences were not significant between soil types or seasons (Fig. 4.2). Rates of DNRA were higher in the clay than in the sand during the dry season, and did not differ between seasons for both soil types (Fig. 4.2). For the sand, DNRA rates were similar to gross nitrification rates in the dry season but this reduced to only about 35 % in the wet season. For the clay, DNRA rates were about 20 % of the gross nitrification rates in both seasons (Fig. 4.2). When comparing their importance for NO_3^- retention, rates of DNRA and

NO_3^- immobilization were similar in the sand, but in the clay DNRA rates were only 14-28 % of NO_3^- immobilization rates (Fig. 4.2). N_2O emission rates were higher in the clay than in the sand (Table 4.2). For the sand, N_2O emission rates did not differ between seasons. For the clayey soil, rates were higher in the dry than in the wet season, possibly indicating a further reduction of N_2O to N_2 because of the more reduced conditions.

4.4. Discussion

Implications of Rapid Reactions of injected $^{15}NH_4^+$ and $^{15}NO_3^-$ to organic N

Our $^{15}NH_4^+$ recoveries at T_0 were higher than those reported for mineral soil of N-limited, tropical montane forests in Indonesia (Corre et al. 2006) and in Hawaii (Hall and Matson 1999), but comparable with high-N availability montane forest in Hawaii (Hall and Matson 1999). Our low ^{15}N recovery in the insoluble organic N pool was comparable with those measured from high N-deposition temperate forests (e.g., 8 % from a German forest with 34 kg N ha^{-1} yr^{-1} throughfall deposition (Corre and Lamersdorf 2004), and 9 % from U. S. forests with 11 kg N ha^{-1} yr^{-1} N deposition (Fitzhugh et al. 2003)). The fast reaction of added $^{15}NH_4^+$ to organic N pool is usually attributed to abiotic NH_4^+ immobilization (e.g., physical condensation reactions with phenolic compounds (Nömmik 1970, Nömmik and Vahtras 1982, Johnson et al. 2000), and fixation on clay minerals (Davidson et al. 1991)). The higher $^{15}NH_4^+$ recoveries at our sites compared to N-limited, tropical montane forests may indicate lower NH_4^+-retention capacity in these soils through rapid, abiotic NH_4^+ reactions.

Our $^{15}NO_3^-$ recoveries at T_0 from both soil types were much higher than those reported for mineral soil of N-limited, tropical montane forests in Indonesia (Corre et al. 2006). There are no other values reported for tropical forests to which we can compare our results. However, from low-N deposition (9-11 kg N ha^{-1} yr^{-1}) temperate forests, Dail et al. (2001)

reported 30 % recovery of added $^{15}NO_3^-$ in the extractable organic N and 5-8 % in the insoluble organic N fractions, while Fitzhugh et al. (2003) reported 7 % in the insoluble organic N fraction. From an N-saturated forest, Corre and Lamersdorf (2004) reported 1 % in the extractable organic N and 49 % in the insoluble organic N fractions. Such fast reaction of NO_3^- to organic N has been attributed to abiotic NO_3^- immobilization (Berntson and Aber 2000). The hypothesized reaction is that DOC reduces Fe(III) in soil minerals, producing reactive Fe(II) species that reduce NO_3^- to NO_2^- in anaerobic microsites while Fe(II) is in turn oxidize to Fe(III) (Davidson et al. 2003). NO_2^- then reacts readily and abiotically with soil organic matter (Smith and Chalk 1980, Azhar et al. 1986, Van Cleemput and Samater 1996, Thorn and Mikita 2000). The driver of these reactions is DOC, which is needed to reduce metals in the soil. The differences we found between sand and clay may be a reflection of the differences in reactive C between these soils, which may affect whether the ^{15}N is recovered in soluble or insoluble organic N. In the sand, injected $^{15}NO_3^-$ was recovered more in the insoluble organic N pool than the extractable organic N pool, while in the clay ^{15}N recoveries were similar in both pools. Until now it is however unclear whether the rapid conversion of NO_3^- to the organic N pool leads to higher NO_3^- retention. The significance of this process and its role in N retention, especially when changes N deposition in tropical areas occur, deserves more attention.

Gross rates of NH_4^+ transformation processes, enrichment factor (ε) and implications to soil N status

Gross N mineralization rates in the sand were comparable to the rates measured for a tropical lowland forest soil in Rondonia, Southern Amazon (with 23-35 % clay, which is intermediate between our sand and clay soils; Neill et al. 1999). These rates were also comparable to those reported for N-limited, tropical montane forests in Hawaii (Hall and

Matson 2003) and in Indonesia (Corre et al. 2006). On the other hand, gross N mineralization rates in the clay were comparable to the rates from a long-term (11 yr) N-fertilized, montane forest in Hawaii (Hall and Matson 2003) and from lowland forest soils (with 68-76 % clay; Veldkamp et al. 2003) in Costa Rica (Silver et al. 2005). These rates were only about half the rates measured from the high-N availability montane forest in Hawaii (Hall and Matson 2003), and much lower (more than 5 times less) than the rates reported for N-saturated temperate forests (e.g., Corre et al. 2003, Corre and Lamersdorf 2004).

The high gross N mineralization rates observed for the clay are coherent with the low C:N ratios in litter and soil, high total soil N (Table 4.1), high microbial N (Fig. 4.2), microbial C, and available C (Table 4.2). Gross N mineralization reflects both the microbial biomass size (presumably active in mineralization, e.g. chemoheterotrophs) and the amount of available substrate (indicated by available C, a similar index used by Hart et al. 1994b). The positive correlations of gross N mineralization to NH_4^+ immobilization ($r = 0.67$; $P < 0.05$), and NH_4^+ immobilization to microbial biomass N ($r = 0.59$; $P < 0.05$) attest that the high gross N mineralization rates in the clay provided high available N for microbial assimilation and hence supported a high microbial biomass. On the other hand, the low gross N mineralization rates observed in the sand are probably due to lower litter quality (high C:N ratio; Table 4.1) which was also reflected in the lower available C and microbial biomass (Table 4.2; Fig. 4.2). Lower litter quality was also reported by Silver et al. (2000) for sandy Amazonian forest soil, while nutrient and water limitations have been reported for decomposition (Cuevas and Medina 1986).

$\delta^{15}N$ signals and the ^{15}N-enrichment factor reflect the long-term behaviour of soil N cycling of an ecosystem. If N in a forest ecosystem is in relative excess (not limiting), it can be expected to be enriched in ^{15}N as many of the output pathways of N are discriminating against the heavier ^{15}N isotope. A heavier $\delta^{15}N$ signal in leaves could reflect uptake of a more

^{15}N-enriched mineral N pool, which in turn indicates high soil N cycling rates with high N losses. Our $\delta^{15}N$ values for leaves and soil were within the range reported for Amazonian forest soils (2 to 8 ‰ for leaf litter (Piccolo et al. 1994) and 8 to 23 ‰ for soil (Piccolo et al. 1996)). In our study, the clay that had high gross N mineralization rates also had heavier $\delta^{15}N$ in leaves, litter and soil compared to the sand (Fig. 4.3). $\delta^{15}N$ signals in litter and soil have been shown to correlate directly to gaseous N losses along a toposequence of montane forest soils in Indonesia (Purbopuspito et al. 2006). In addition, it has been shown in temperate forest soils that net mineralization was the main process of soil N cycle contributing largely to a high (more negative) ^{15}N-enrichment factor (Nadelhoffer and Fry 1988, Vervaet et al. 2002). Furthermore, temperate forest soils with higher enrichment factors had higher potential net N mineralization rates and higher NO_3^- losses (Vervaet et al. 2002). In Amazonian forest soils, the discrimination factor (which has similar meaning as the enrichment factor but only has an opposite sign) generally increased with increasing clay content of the soil (Piccolo et al. 1996). Our study showed that the clay that had high gross rates of N mineralization also had a higher enrichment factor (Fig. 4.3) and higher gaseous losses (i.e., N_2O emissions; Table 4.2) than the sand.

Gross rates of NO_3^- transformation, dissimilatory nitrate reduction to ammonium (DNRA), and implications for N losses

Gross rates of nitrification in sand were comparable to those reported for N-limited, montane forest in Hawaii (Hall and Matson 2003) and in Puerto Rico (Silver et al. 2001). These rates were lower than those measured from a lowland forest soil in Rondonia, Southern Amazon (with 23-35 % clay; Neill et al. 1999). However, gross nitrification rates in the clay were higher than this Rondonia site and were comparable to the rates from a lowland forest with heavy clay soil in Costa Rica, characterized by high N availability (Silver et al. 2005)

and large N losses (gaseous N losses, Keller et al. 1993, Keller and Reiners 1994, Veldkamp et al. 1999; and leaching losses, Schwendenmann and Veldkamp 2005).

Despite the high WFPS in the clay during the wet season (Table 4.2), which may limit O_2 diffusion and decrease nitrification (Paul and Clark 1996), higher gross nitrification rates were observed in the clay compared to the sand. This suggests that NH_4^+ availability limits nitrification activity rather than aeration. In the absence of root uptake, mineralized N was assimilated by micro organisms (e.g., heterotrophs) rather than nitrified (Fig. 4.2). Low gross N mineralization rates in the sand may have imposed strong competition for ammonium, resulting in low gross nitrification rates.

The low DNRA rates in the sand were comparable to the rates in lowland forest in Costa Rica (Silver et al. 2005), while the high DNRA rates in the clay were comparable to the montane forest in Puerto Rico (Silver et al. 1999). Contrary to what Silver et al. (2005) found, we did not detect correlations between DNRA rates and total C:NO_3^- ratios or to any indicators of NO_3^- availability (e.g., gross nitrification or NO_3^- pool). Instead we observed a marginal relationship between DNRA and available C (r = 0.62, P = 0.06), indicating that this NO_3^- retention process may be in part driven by the availability of C to micro organisms. High DNRA rates in the clay also signified that this process is favoured under a more O_2-reduced condition (i.e., high WFPS in the clay soil, Table 4.2). In terms of its significance for NO_3^- retention, only in the sand, where production of NO_3^- was low, DNRA was as important as NO_3^- immobilization. In the clay, where gross nitrification rates and NO_3^- pools were high, DNRA was 3-7 times lower than NO_3^- immobilization. N_2O emission rates in the clay (Table 4.2) were also higher than the combined rates of DNRA and NO_3^- immobilization (Fig. 4.2), while in the sand N_2O losses were lower than the sum of the rates of these NO_3^- retention processes. The low N_2O emissions in the sand reflect the overall low rates of soil N cycling in this soil as well as its low WFPS and C availability. In contrast, the clay typified a system

with relative excess of N - the rates of internal soil N cycling were lower than the rates of N loss (e.g. N_2O emission).

Mean residence time (MRT) and implication for N losses

MRT of NH_4^+ during the dry season was similar to the values reported for Rondonia lowland forests (Neill et al. 1999) and for Indonesian montane forests (Corre et al. 2006). We observed fast turnover rates (short MRT) of NH_4^+ in the dry season, when microbial immobilization of NH_4^+ was generally comparable to gross N mineralization (Fig. 4.2). In the wet season NH_4^+ immobilization rates were somewhat lower than gross N mineralization rates, and NH_4^+ tended to have slow turnover rates. Low N immobilization rates in the wet season were also reflected in the small microbial N pool (Fig. 4.2) and a slow turnover rate of microbial N in the sand, (Fig. 4.2). Hart et al. (1994b) have shown that fast turnover of N pools was a response to an increase in C availability that drives the internal soil N cycle. For clay, available C was higher during the wet season, whereas for sand this difference was not significant (Table 4.2). Hence, the slow turnover rates of NH_4^+ and microbial N pools during the wet season were probably not limited by available C but more likely by increased anaerobicity (higher WFPS in the wet season in the clay, Table 4.2).

The MRT of NO_3^- were comparable to values reported for Rondonia lowland forests (Neill et al. 1999), but higher than those observed from tropical montane forests where NO_3^- was sometimes even undetectable (Silver et al. 2001, Hall and Matson 2003, Corre et al. 2006). A long MRT of NO_3^- signals high potential for N losses via leaching and gaseous emissions in times of high soil water content. We do not have estimates of leaching losses from our study area, but estimates of leaching losses from lowland tropical forests were higher than from montane forests (e.g., 10 kg NO_3^--N ha^{-1} yr^{-1} from a, lowland forest in Costa Rica (Schwendenmann and Veldkamp 2005) and a similar amount from a lowland forest in

Paragominas (Klinge et al. 2004) compared to 1-5 kg N ha^{-1} yr^{-1} from N-limited, montane forest in Indonesia (Dechert et al. 2005)). It has also been shown that N-oxide emissions from most tropical lowland forests (e.g., Costa Rica: Keller et al. 1993, Keller and Reiners 1994, Veldkamp et al. 1999; Brazil: Verchot et al. 1999, Davidson et al. 2000b, Davidson et al. 2004; Australia: Breuer et al. 2000) were higher than from N-limited, tropical montane forests (e.g., Hawaii: Riley and Vitousek 1995; Indonesia: Purbopuspito et al. 2006; Australia: Kiese and Butterbach-Bahl 2002). Furthermore, we observed somewhat comparable NO_3^- immobilization rates and gross nitrification rates in the dry season while NO_3^- immobilization rates tended to be lower than gross nitrification in the wet season. However, the MRT of NO_3^- showed the opposite pattern of NH_4^+: shorter MRT of NO_3^- and lower NO_3^- in the wet than in the dry season for the clay (Fig. 4.2). In the wet season, when the sink of mineral N pool by microbial immobilization was low, NO_3^- could be more exposed to losses. The fast turnover rate of NO_3^- in the clay during the wet season could have contributed to high gaseous N losses, which could then result in low NO_3^- values. The N_2O emissions we measured do not repressent the overall gaseous N losses; in the wet season a significant part of the N_2O produced was probably reduced further to N_2 and the overall gaseous N losses were thus higher than the N_2O emissions alone.

4.5. Conclusions

This study shows that large differences exist in N cycling and N retention between heavily weathered tropical forest soils that mainly differ in texture. Our combined results suggest that some Amazonian forest soils have higher N availability than others. While the clay Oxisol in our study had high gross rates of N mineralization and nitrification, and hence high potential for N losses, the sandy Oxisol had low gross rates of N cycling and reacted more like a soil that is N-limited. $\delta^{15}N$ signals and the ^{15}N-enrichment factor, which reflect

the long-term behaviour of soil N cycling of an ecosystem, were also higher in the clay than in the sand. Our findings of faster turnover rates of NH_4^+ compared to NO_3^- signified that NH_4^+ cycles faster through microorganisms than NO_3^-, possibly contributing to better retention of NH_4^+ than NO_3^-. This was opposite to abiotic retention, which showed higher conversion of NO_3^- than NH_4^+ to the organic N pool. How this will affect long-term N retention is presently unknown and cannot be deduced from the present study, which illustrates that the importance of biotic and abiotic retention of N needs further attention. Because of the differences in N cycing and N retention, there is no doubt that the studied soils will react differently to increased anthropogenic N deposition. To make a complete analysis of these effects, however, we have to know better how abiotic and biotic N retention processes contribute to middle and long-term N sequestration and their changes with increasing N deposition in tropical forests.

5. Summarizing synthesis

The overall goal of the present study was to evaluate the soil CO_2 dynamics and the N cycle in the old-growth forest of Caxiuanã, Eastern Amazonia. Quantification of temporal and spatial variation of soil CO_2 emissions is essential for an accurate interpretation of tower-based measurements of net ecosystem exchange. This is particularly important now that climate of the Amazon basin is expected to change in the next few decades, as a result of deforestation and rising temperatures which may lead to unknown feedback mechanisms in carbon cycling. Furthermore, changes are also expected in the N cycling from tropical soils with resulting high rates of N_2O emissions. Nitrogen is in relative excess in heavily weathered lowland tropical forests soils, however within the Amazon basin soil texture may influence soil NH_4^+ and NO_3^- concentrations and hence N availability and retention in the soil.

5.1. Landscape and climatic controls on spatial and temporal variation

The chapter 2 had the goal of quantifying the spatial and seasonal variation in soil CO_2 efflux and its environmental controls in the old-growth forest of Caxiuanã, Eastern Amazonia. We measured soil CO_2 efflux from two Oxisol sites with contrasting soil texture and at different landscape positions. Using manually deployed flux chambers, we monitored soil CO_2 efflux every two weeks from the two sites with contrasting soil texture and every three months from the landscape positions, over the course of two years. The CO_2 flux was calculated from the linear regression of increasing CO_2 concentration in the chamber headspace versus time. At the same time soil water content and soil temperature were estimated.

Average CO_2 efflux was 21% higher for sand (3.93 ± 0.06 μmol CO_2 $m^{-2}s^{-1}$) than for the clay (3.08 ± 0.07 μmol CO_2 $m^{-2}s^{-1}$). No difference was detected for soil temperature

between sites (24.1 ± 0.13 °C for sand and 24.2 ± 0.15 °C for clay), while soil water content in sandy soil (23.2 ± 0.33 %) was much lower than the clay soil (34.5 ± 0.98 %), for the two-year period. Spatial difference in CO_2 efflux were related to water holding capacity and capacity to retain nutrients of each soil texture, reflecting in different root respiration. Seasonality in soil CO_2 efflux was not detectable and CO_2 efflux did not differ between dry and wet season. However, the interaction between time and topographic position had a significant effect on CO_2 efflux. The variation caused by topography was in the same order of magnitude as temporal variation, indicating the importance of considering this variation while modelling soil CO_2 efflux. Mean contribution of the litter layer to the CO_2 efflux rates was 20 % and varied from 25 % during the wet season to close to 0 % during the dry season. These seasonal variations may be caused by variations in the stock of decomposing litter on the forest floor and by the conditions influencing litter decomposition. Temporal variability of soil CO_2 efflux also depended on climatic variables. The relation between soil water content and soil CO_2 efflux showed an optimum for both soil textures but the shape and optimum of the curves were different. Soil water content explained 23 % of the soil CO_2 efflux in the sand and 18 % in the clay soil texture, and soil temperature co-varied with soil water content in both soil types. The problem of co-variation of temperature and soil moisture has been detected in several ecosystems, including tropical rainforests (Davidson et al. 2000, Schwendenmann et al. 2003). The results of our study show that soil moisture is an important driver of temporal variations in soil CO_2 efflux in this old-growth forest. But when extrapolating soil CO_2 efflux to larger areas, the significant influences of soil texture, litter, and the interaction of topographical position and time illustrate that it is necessary to include some of the complexity of landscapes.

5.2. Effects of induced drought on soil CO_2 production and soil CO_2 efflux

Given the expected intensification of ENSO events, which will probably lead to an increasing frequency of droughts and higher temperatures, in Chapter 3, we report how a throughfall exclusion (TFE) experiment affected soil CO_2 production in a deeply weathered sandy Oxisol of Caxiuanã (Eastern Amazon). Over the course of two years, we measured soil CO_2 efflux and soil CO_2 concentrations, soil temperature and moisture in pits down to 3 m depth. TFE reduced soil CO_2 efflux from 4.3 ± 0.1 µmol CO_2 m^{-2} s^{-1} (control) to 3.2 ± 0.1 µmol CO_2 m^{-2} s^{-1} (TFE) and the reduction was already evident on the first year of artificial drought. Over 70 % of soil CO_2 production in both plots occurred within the top 0.5 m of the soil including the forest litter layer, and that was the layer most affected by the soil water stress. The contribution of the subsoil (below 0.5 m depth) to the total soil CO_2 production was higher in the TFE plot (28 %) compared to the control plot (17 %), and it did not differ between years. We distinguished three phases of drying after the TFE was started. The first phase was characterized by a translocation of water uptake (and accompanying root activity) to deeper layers and not enough water stress to affect microbial activity and/or total root respiration. During the second phase a reduction in total soil CO_2 efflux in the TFE plot was related to a reduction of soil- and litter decomposers activity. The third phase of drying, characterized by a continuing decrease in soil CO_2 production was dominated by a water stress-induced decrease in total root respiration. Our results strongly contrast to results of a drought experiment on clay Oxisols which we explain with differences in water holding capacity and depth of rooting zone. We conclude in this chapter, that Amazonian forest ecosystems located on soils with coarse texture are more sensitive to drought than forests located on heavier textures because they cannot compensate the relatively low water holding capacity in the top soil with water stored in deeper soil layers.

5.3. Mechanisms of soil N retention

Direct quantification of the inherent soil N status of tropical forests and processes of N retention will provide much-needed baseline information for tropical forests, which may hint how such ecosystems will react to predicted increase in N deposition. Chapter 4 focuses on assessing the soil N status of sand and clay Oxisols, lowland forest soils by quantifying gross rates of N-production processes, and evaluating their differences in N-retention processes by measuring the microbial N immobilization, dissimilatory NO_3^- reduction to NH_4^+, and abiotic N immobilization. Soil samples were collected from the sand and clay sites once during the dry (August 2004) and once during the wet (April 2005) season. Additional soil, litter and green leaf samples were taken for analysis of other supporting parameters and the measurement of the degree of ^{15}N enrichment for each soil type. We used the ^{15}N pool dilution technique to estimate gross rates of soil N cycling (Davidson et al. 1991, Hart et al. 1994a). Gross N mineralization and nitrification rates were estimated from the cores that received $^{15}NH_4^+$ and $^{15}NO_3^-$, respectively, using the modified calculation procedure of Davidson et al. (1991) from the Kirkham and Bartholomew (1954) model.

The clay had high gross rates of N mineralization (13.5 ± 3.1 mg N kg^{-1} d^{-1}), nitrification (3.7 ± 1.1 mg N kg^{-1} d^{-1}) and ^{15}N enrichment factor (ε = -4.6 ‰) and hence high potential for N losses. The sand had low gross rates of N cycling (N mineralization was 6.0 ± 0.9 mg N kg^{-1} d^{-1} and nitrification 0.8 ± 0.3 mg N kg^{-1} d^{-1}) and ^{15}N enrichment factor (ε = -2.9 ‰), and reacted more like a soil that is N-limited. Faster turnover rates of NH_4^+ compared to NO_3^- signified that NH_4^+ cycles faster through microorganisms than NO_3^-, possibly contributing to better retention of NH_4^+ than NO_3^-. However this was opposite to abiotic retention processes, which showed higher conversion of NO_3^- to the organic N pool than NH_4^+. Our combined results suggest that some Amazonian forest soils have higher N

availability than others which will have important consequences for soil N cycling and losses when projected increases in anthropogenic N deposition will occur.

5.4. Belowground CO_2 dynamics and N cycling

The use of global climate models has become one of the most powerful tools to estimate changes in natural ecosystems due to climate, but these models are mainly based in meteorological data. Although aboveground components have been successfully modelled using basic climate data, belowground components are not yet satisfactorily assessed. While in many ecosystems temperature has described well the belowground processes (over 80 % of the variation; Janssens et al. 2001), in tropical ecosystems the temperature is not a good predictor. Modelling of belowground processes in tropical areas has therefore been led by the soil water content (Davidson et al. 2006). However, the improvement of these models depends on a better characterization of the belowground processes and their variation within the region. The Amazon region embraces a wide range of soils, vegetation and landscape and this study shows that we should expect different responses within the basin to changes in climate.

Quantification of the contribution of the litter layer, the effect of the interaction of landscape and time, and soil texture on soil CO_2 efflux showed that the inclusion of such variables in the Amazon-wide model analyses, in addition to soil water content and soil temperature, will certainly improve estimates of soil CO_2 efflux for the region. The importance of soil texture has already been pointed by other authors (Silver et al. 2000, Müller and Höper 2004) as well as the importance of the contribution of litter (Luizão and Schubart 1987, Toledo 2002, Chambers et al. 2004), but the quantification of the seasonal litter contribution and topographical variation had been disregarded so far. In these models

Amazon forest is often held as a single ecosystem, which leads to a miscalculation of the effect not only of the soil and vegetation but also of the topography on the fluxes. The topography of the Amazon is quite smooth, however along the seasons the factors influencing soil CO_2 efflux respond differently in each topographic position. The interaction of topographic position in the landscape and time is responsible for a variation of around 30 % in the efflux, and has the same magnitude as the temporal variation.

Predicting whether the soil will be a sink or source of carbon with the expected reduction in precipitation in the Amazon depends not only on the amount of C that is lost from the dried soil but also from the amount of C that is allocated belowground by the plant. This study shows that in the short term, the response to reduced precipitation will mostly depend on the capacity of each soil to supply water to the roots. For example, our sandy Oxisol soil will respond much quicker to low precipitation regime than the clay soil from Santarém (Davidson et al. 2004). The top 0.5 m of soil will be particularly affected by the lower soil water content reducing total soil CO_2 efflux and production, but the deeper soil CO_2 production will mainly depend on the root activity. In the short term, lower CO_2 emissions may signify carbon storage if roots are able to search for water in the soil profile and keep the rates of gross primary productivity (GPP). However, if the soil CO_2 efflux is accompanied by reduction in GPP there may be no change in the net primary productivity (NPP) and thus no change in the allocation of carbon belowground. Declines in GPP and soil CO_2 efflux resulting from soil moisture deficit have been described for temperate European forests (e.g. Ciais et al. 2005) and the processes leading to reduction in both GPP and soil CO_2 efflux seem to be general, though I expect spatial variability in vulnerability to soil moisture stress across the Amazon region.

Accounting for soil diversity along the Amazon basin is also important when predicting the effect of N deposition in the region. The soil with low N availability, as the

sand Oxisols, have lower rates of N cycling, and lower N losses (N_2O and NO), while those with high N availability, as the clay Oxisols, have a high potential for N losses (Figure 5.1). On the other hand, the larger microbial biomass size, available substrate and the higher soil moisture (WFPS) in the clay texture contribute to a higher immobilization of N, hence to a higher N retention in the system. Nevertheless, the mechanisms controlling retention and losses are still not clearly understood.

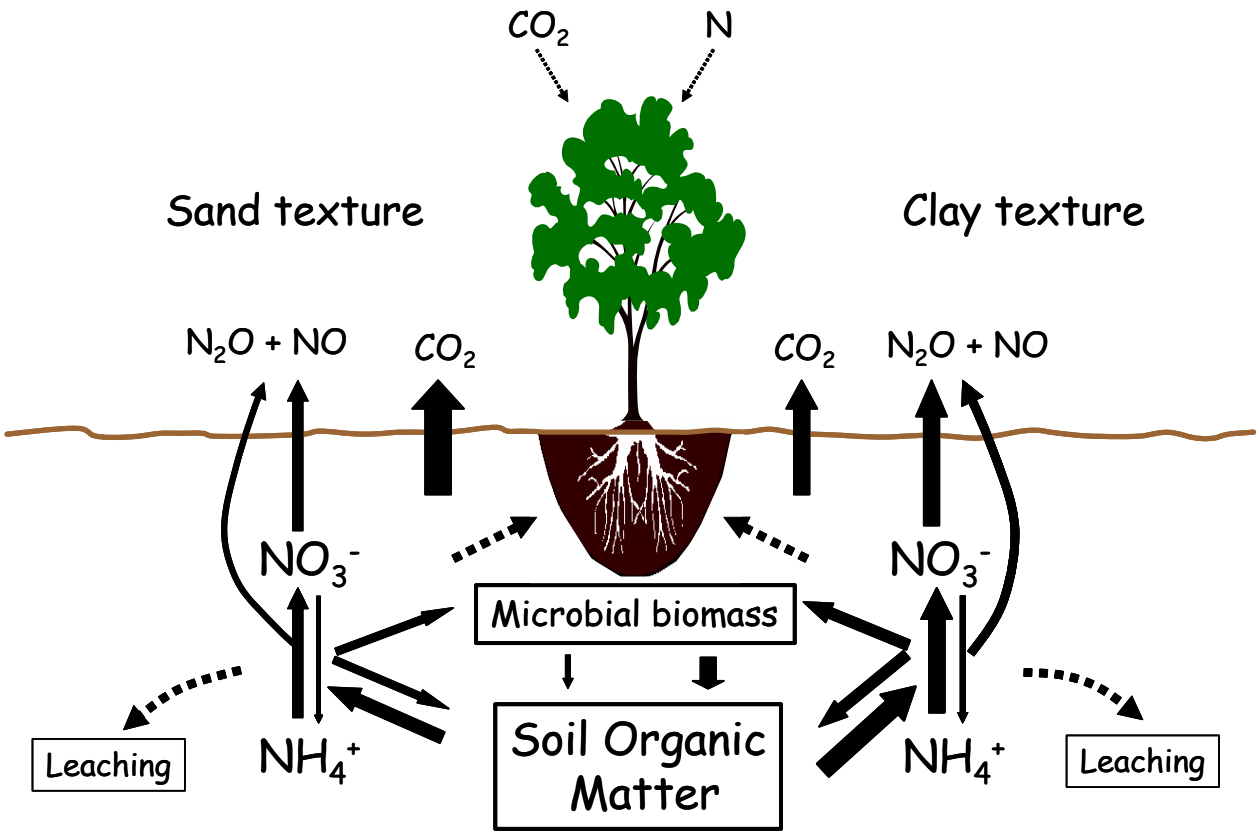

Figure 5.1 - Diagrammatic representation of the carbon and nitrogen cycles, and their interaction in sand and clay soil textures. Line thickness the magnitude of the flux rate and dashed lines fluxes not measured. CO_2 emission is the result of heterotrophic and autotrophic respiration.

With higher soil organic matter and microbial biomass in the clay soil one should expect higher rates of CO_2 efflux resulting from heterotrophic respiration. However, the higher rates of CO_2 efflux were observed in the sand soil. This high rate in sand soil may only be explained by a higher root activity, resultant from the more thorough search for water and nutrients in the coarse soil texture. The larger root biomass in the top 0.3 m of the sand soil (Metcalfe et al. in preparation) may indicate a greater root longevity and a mechanism for using more effectively the photosyntic products. This assumption is corroborated with the linkage between slow root turnover rates and low root tissue N content (Gordon and Jackson 2000).

This study shows that the inclusion of soil and landscape characteristics of the Amazon region in future modelling of global climate change will possibly improve the estimates of C and N belowground processes. That the reduction in soil water will affect some Amazonian forest soils more rapidly than others and that texture will play a big role also on how the forest will react to future N deposition.

6. Zusammenfassung

Es ist noch unbekannt, wie sich Klimaänderungen und steigende N-Einträge auf den Kohlenstoff- und Stickstoffkreislauf tropischer Böden auswirken. Deshalb ist es wichtig, individuelle Prozesse und deren Folgen für das Klima zu identifizieren. In dieser Studie bewertete ich die CO_2-Dynamik im Boden sowie den N-Kreislauf in einem Primärwald in Caxiuana, Ostamazonien. Die Studie gliedert sich in drei Teile: 1) Messung der CO_2 Ausgasungsrate und deren standörtliche Steuergrößen an zwei Oxisol Standorten mit unterschiedlicher Bodentextur und Geländelage, 2) die Untersuchung wie stark sich bei Ausschluss des Bestandesniederschlages (TFE Experiment) die Boden-CO_2 Produktion in einem stark verwitterten sandigen Oxisol in Caxiuana verändert und 3) eine Bewertung des Boden-Stickstoffstatus an zwei stark verwitterten Oxisolen unterschiedlicher Textur (sandig versus tonig). Zwei Jahre lang wurden die Boden-CO_2-Ausgasungsraten, CO_2-Konzentrationen, die Bodentemperatur und die Feuchtigkeit der Profile bis in 3 m Tiefe gemessen. Mittels Isotopenverdünnungsanalyse (^{15}N pool dilution) wurden für beide Böden die Raten der N-Mineralisierung und der Nitrifikation sowie der N-Retention (mikrobielle N-Festlegung, dissimilatorische NO_3 Reduktion zu NH_4 und abiotische N-Festlegung) gemessen. zusätzlich wurden δ^{15}N Werte von der Streu und über das gesamte Profil gemessen, um die ^{15}N-Anreicherung für jeden Bodentyp zu quantifizieren.

Die wichtigsten Ergebnisse sind:

1) Die durchschnittliche CO_2-Ausgasungsrate war im Sand (3.93 ± 0.06 µmol CO_2 $m^{-2}s^{-1}$) 21 % höher als im Ton (3.08 ± 0.07 µmol CO_2 $m^{-2}s^{-1}$). Keine Unterschiede wurden in der Bodentemperatur zwischen beiden Standorten gemessen, während der Bodenwassergehalt im sandigen Boden (23.2 ± 0.33 %) geringer war als im tonigen Boden (34.5 ± 0.98 %). Die Boden-CO_2-Ausgasungsrate unterschied sich nicht zwischen der Trocken – und Regenzeit,

aber ich fand eine signifikante Wechselwirkung zwischen der Jahreszeit und der topografischen Lage. Die durch die Topografie hervorgerufene Variation war in derselben Größenordnung wie die zeitliche Variation. Der mittlere Beitrag der Streu zur CO_2-Ausgasungsrate war 20 % und variierte von 25 % innerhalb der Regenzeit bis nahezu 0 % während der Trockenzeit. Die Beziehung zwischen Bodenwassergehalt und Boden-CO_2-Ausgasungsraten zeigte für beide Bodentexturen ein Optimum aber die Form und das Optimum der Kurve unterschieden sich. Die Ergebnisse unserer Studie zeigen, dass Bodenwasser eine steuernde Größe der zeitlichen Variation der Boden-CO_2-Ausgasungsraten in diesem Primärwald ist. Bei der Extrapolation der CO_2-Ausgasungsraten zu größeren Flachen zeigt der signifikante Einfluss von Bodentextur, Streu und Wechselwirkung der topografischen Lage und Zeit, dass es notwendig, ist diesen Anteil der Landschaftskomplexität mit zu berücksichtigen.

2) TFE reduzierten den Boden von 4.3 ± 0.1 µmol CO_2 m^{-2} s^{-1} (Kontrolle) zu 3.2 ± 0.1 µmol CO_2 m^{-2} s^{-1} (TFE). Der Beitrag des Unterbodens (unterhalb 0.5 m Tiefe) zur der Gesamtproduktion von CO2 war in dem TFE Plot größer (28 %) als in dem Kontrollplot (17 %) und er unterschied sich nicht zwischen den Jahren. Ich unterschied drei Phasen der Trocknung nachdem TFE gestartet war. Die erste Phase war durch die Umschichtung der Wasseraufnahme (und begleitender Wurzelaktivität) zu tieferen Schichten und durch einen zu geringen Wasserstress um die mikrobielle Aktivität und /oder die Wurzelatmung zu beeinflussen charakterisiert. Während der zweiten Phase stand die Aktivität von Boden – und Streuzersetzern mit der Reduzierung der gesamten Boden-CO_2-Ausgasungsrate in dem TFE Plot in Beziehung. Die dritte Trocknungsphase war durch einen kontinuierlichen Abfall der Boden CO_2 Produktion charakterisiert, der durch einen Wasserstress induzierten Abfall in der gesamten Wurzelatmung hervorgerufen wurde. Diese Ergebnisse unterscheiden sich stark von einem Trocknungsexperiment in einem tonigem Oxisol, was ich durch Unterschiede in der

Wasserhaltekapazität und Durchwurzelungstiefe erkläre. Ich folgere, dass Waldökosysteme in Amazonien, die sich auf Böden mit einer groben Textur befinden, sensitiver gegenüber Trockenheit sind als Wälder, die sich auf schwereren Böden befinden. Letztere können die relativ geringe Wasserhaltekapazität der Oberböden mit Wasser aus tieferen Bodenschichten kompensieren.

3) Der tonige Oxisol hatte eine große Bruttorate der N-Mineralisation, Nitrifizierung und des ^{15}N -Anreicherungsfaktors und somit ein großes Potential für N Verluste. Demgegenüber hatte der sandige Oxisol vergleichsweise niedrige Bruttoraten und reagierte ähnlich einem Boden der N limitiert ist. Schnellere Umsatzzeiten von NH_4 im Vergleich zu NO_3 zeigten an, dass NH_4 schneller durch Mikroorganismen umgesetzt wird als NO_3, möglicherweise führt dies zu einer besseren Retention von NH_4 im Vergleich zu NO_3. Jedoch war dieser Prozess bei abiotischen Retentionsprozessen umgekehrt, welcher für NO_3höhere Umwandlung zum organischen N Pool zeigte als NH_4. Die verknüpften Ergebnisse zeigen, dass einige Waldböden in Amazonien höhere N-Verfügbarkeit als andere haben, was entscheidende Konsequenzen für den Kreislauf und Verluste des Bodenstickstoffs hat, wenn der vorhergesagte Anstieg anthropogener N Einträge stattfindet.

7. Summary

The significance of climate changes and of increasing N deposition to the interaction of both carbon and nitrogen cycles in tropical soils is still unknown and deserves more attention. For that, it is important to identify individual processes and their consequences to changes in the climate. In this study I evaluate soil CO_2 dynamics and N cycling in an old-growth forest of Caxiuanã, Eastern Amazonia. The study was divided in three parts: 1) measurement of soil CO_2 efflux and its environmental controls from two Oxisol sites with contrasting soil texture and at different landscape positions, 2) observation of how a throughfall exclusion (TFE) experiment affected soil CO_2 production in a deeply weathered sandy Oxisol of Caxiuanã, and 3) evaluation of the soil N status of two heavily weathered soils which contrast in texture (sand versus clay). Over the course of two years, soil CO_2 efflux and soil CO_2 concentrations, soil temperature and moisture in pits down to 3 m depth was measured. Using ^{15}N pool dilution, for both soils rates of N cycling (gross rates of N mineralization and nitrification) and N retention (microbial N immobilization, dissimilatory NO_3^- reduction to NH_4^+, and abiotic N immobilization) were quantified. To further support the N status assessment, the $\delta^{15}N$ signals from the litter layer down the soil profile was measured, to get an overall measure of the degree of ^{15}N enrichment for each soil type.

The most important results are:

1) Average CO_2 efflux was 21 % higher for sand (3.93 ± 0.06 µmol CO_2 $m^{-2}s^{-1}$) than for the clay (3.08 ± 0.07 µmol CO_2 $m^{-2}s^{-1}$). No difference was detected for soil temperature between sites, while soil water content in sandy soil (23.2 ± 0.33 %) was much lower than the clay soil (34.5 ± 0.98 %), for the two-year period. Soil CO_2 efflux did not differ between dry and wet season, but I detected a significant interaction between season and topographic position. The variation caused by topography was in the same order of magnitude as temporal variation. Mean contribution of the litter layer to the CO_2 efflux rates was 20 % and varied from 25 %

during the wet season to close to 0 % during the dry season. The relation between soil water content and soil CO_2 efflux showed an optimum for both soil textures but the shape and optimum of the curves were different. The results of our study illustrate that soil moisture is an important driver of temporal variations in soil CO_2 efflux in this old-growth forest. When extrapolating soil CO_2 efflux to larger areas, a significant influences of soil texture, litter, and the interaction of topographical position and time illustrate that it is necessary to include some of the complexity of landscapes.

2) TFE reduced soil CO_2 efflux from 4.3 ± 0.1 µmol CO_2 m^{-2} s^{-1} (control) to 3.2 ± 0.1 µmol CO_2 m^{-2} s^{-1} (TFE). The contribution of the subsoil (below 0.5 m depth) to the total soil CO_2 production was higher in the TFE plot (28 %) compared to the control plot (17 %), and it did not differ between years. I distinguished three phases of drying after the TFE was started. The first phase was characterized by a translocation of water uptake (and accompanying root activity) to deeper layers and not enough water stress to affect microbial activity and/or total root respiration. During the second phase a reduction in total soil CO_2 efflux in the TFE plot was related to a reduction of soil- and litter decomposers activity. The third phase of drying, characterized by a continuing decrease in soil CO_2 production was dominated by a water stress-induced decrease in total root respiration. These results strongly contrast to results of a drought experiment on clay Oxisols which I explain with differences in water holding capacity and depth of rooting zone. I conclude that Amazonian forest ecosystems located on soils with coarse texture are more sensitive to drought than forests located on heavier textures because they cannot compensate the relatively low water holding capacity in the top soil with water stored in deeper soil layers.

3) The clay Oxisol had high gross rates of N mineralization, nitrification and ^{15}N enrichment factor and hence high potential for N losses. The sand Oxisol had low gross rates of N cycling and ^{15}N enrichment factor, and reacted more like a soil that is N-limited. Faster turnover rates

of NH_4^+ compared to NO_3^- signified that NH_4^+ cycles faster through microorganisms than NO_3^-, possibly contributing to better retention of NH_4^+ than NO_3^-. However this was opposite to abiotic retention processes, which showed higher conversion of NO_3^- to the organic N pool than NH_4^+. The combined results suggest that some Amazonian forest soils have higher N availability than others which will have important consequences for soil N cycling and losses when projected increases in anthropogenic N deposition will occur.

8. References

Aber JD, Magill A, McNulty SG, Boone RD, Nadelhoffer RJ, Downs M, Hallett R. 1995. Forest biogeochemistry and primary production altered by nitrogen saturation. Water Air and Soil Pollution 85: 1665-1670.

Aber J, McDowell W, Nadelhoffer K, Magill A, Berntson G, Kamakea M, McNulty S, Currie W, Rustad L, Fernandez I. 1998. Nitrogen saturation in temperate forest ecosystems: hypotheses revisited. BioScience 48: 921-934.

Almeida SS, Lisboa PLB, Silva ASL. 1993. Diversidade florística de uma comunidade arbórea na Estação Científica "Ferreira Penna", em Caxiuanã (Pará). Boletim do Museu Paraense Emílio Goeldi – Serie Botânica 9: 99-188.

Amundson R. 2001. The carbon budget in soils. Annual Review of Earth and Planetary Sciences 29: 535-562.

Avissar R, Nobre CA. 2002. Preface to special issue on the Large-Scale Biosphere-Atmosphere Experiment in Amazonia (LBA). Journal of Geophysical Research 107: doi: 10. 1029/2002JD002507.

Azhar E.S, Verhie M, Proot M, Sandra P, Verstraete W. 1986. Binding of nitrite-N on polyphenols during nitrification. Journal of Geophysical Research 99: 16549-16555.

Bartels R. 1982. The rank version of von Neuman's ratio test for randomness. Journal of the American Statistical Association 77: 40-46.

Berntson GM, Aber JD. 2000. Fast nitrate immobilization in N saturated temperate forest soils. Soil Biology and Biochemistry 32: 151-156.

Bobbink R, Hornung M, Roelofs JGM. 1998. The effects of air-borne nitrogen pollutants on species diversity in natural and semi-natural European vegetation. Journal of Ecology 86: 717-738.

Borken W, Davidson EA, Savage K, Gaudinski J, Trumbore SE. 2003. Drying and wetting effects on carbon dioxide release from organic horizons. Soil Science Society of America Journal 67: 1888-1896.

Bowden WB. 1986. Gaseous nitrogen emissions from undisturbed terrestrial ecosystems: An assessment of their impacts on local and global nitrogen budgets. Biogeochemistry 2: 249-279.

Breuer L, Papen H, Butterbach-Bahl K. 2000. N_2O emissions from tropical forest soils of Australia. Journal of Geophysical Research 105: 26353-26367.

Brookes PC, Landman AG, Pruden G, Jenkinson DS. 1985. Chloroform fumigation and the release of soil nitrogen: a rapid direct extraction method to measure microbial biomass nitrogen in soil. Soil Biology and Biochemistry 17: 837-842.

Brumme R, Beese F. 1992. Effects of liming and nitrogen fertilization on emissions of CO_2 and N_2O from a temperate forest. Journal of Geophysical Research 97: 12851-12858.

Cabrera ML, Beare MH. 1993. Alkaline persulfate oxidation for determining total nitrogen in microbial biomass extracts. Soil Science Society of America Journal 57: 1007-1012.

Carswell FE, Costa AL, Palheta M, Malhi Y, Meir P, Costa JPR, Leal LSM, Costa JMN, Clement RJ,Grace J. 2002. Seasonality in CO_2 and H_2O flux at an eastern Amazonian rain forest. Journal of Geophysical Research-Atmospheres 107 (D20): 8076, doi:10.1029/2000JD000284

Cavelier J, Wright SJ, Santamaria J. 1999. Effects of irrigation on litterfall, fine root biomass and production in a semideciduous lowland forest in Panama. Plant and Soil 211: 207-213.

Chambers JQ, Tibuzy ES, Toledo LC, Crispim BF, Iguchi N, dos Santos J, Araujo AC, Kruijt B, Nobre AD, Trumbore SE. 2004. Respiration from a tropical forest ecosystem:

partitioning of sources and low carbon use efficiency. Ecological Applications 14: S72-S88.

Ciais P, Reichstein M, Viovy N, Granier A, Ogee J, Allard V, Aubinet M, Buchmann N, Bernhofer C, Carrara A, Chevallier F, De Noblet N, Friend AD, Friedlingstein P, Grunwald T, Heinesch B, Keronen P, Knohl A, Krinner G, Loustau D, Manca G, Matteucci G, Miglietta F, Ourcival JM, Papale D, Pilegaard K, Rambal S, Seufert G, Soussana JF, Sanz MJ, Schulze ED, Vesala T, Valentini R. 2005. Europe-wide reduction in primary productivity caused by the heat and drought in 2003. Nature 437: 529-533.

Cicerone RJ. 1987. Changes in atmospheric ozone. Science 237: 35-42.

Cochrane MA. 2003. Fire science for rainforests. Nature 421: 913-919.

Corre MD, Beese FO, Brumme R. 2003. Soil nitrogen cycle in high nitrogen deposition forest: changes under nitrogen saturation and liming. Ecological Applications 13: 287-298.

Corre MD, Lamersdorf NP. 2004. Reversal of nitrogen saturation after long-term deposition reduction: impact on soil nitrogen cycling. Ecology 85: 3090-3104.

Corre MD, Dechert G, Veldkamp E. 2006. Soil nitrogen cycling following montane forest conversion in central Sulawesi, Indonesia. Soil Science Society of America Journal 70: 359-366.

Costa AM. 2002. Caracterização e classificação dos solos e dos ambientes da Estação Científica Ferreira Penna, Caxiuanã, Melgaço, Pará. MSc Thesis, FCAP, Belém, Brazil.

Costa MH, Foley JA. 2000. Combined effects of deforestation and doubled atmospheric CO_2 concentrations on the climate of Amazonia. Journal of Climate 13: 18-34.

Costa ML, Kern DC. 1999. Geochemical signatures of tropical soils with archaeological black earth in the Amazon, Brazil. Journal of Geochemical Exploration 66: 369-385.

Cox PM, Betts RA, Jones CD, Spall SA, Totterdell IJ. 2000. Acceleration of global warming due to carbon-cycle feedbacks in a coupled climate model. Nature 408: 184-187.

Cox PM, Betts RA, Collins M, Harris PP, Huntingford C, Jones CD. 2004. Amazonian forest dieback under climate-carbon cycle projections for the 21st century. Theoretical and Applied Climatology 78: 137-156.

Cramer W, Bondeau A, Woodward FI, Prentice IC, Betts RA, Brovkin V, Cox PM, Fisher V, Foley JA, Friend AD, Kucharik C, Lomas MR, Ramankutty N, Sitch S, Smith B, White A, Young-Molling C. 2001. Global response of terrestrial ecosystem structure and function to CO2 and climate change: results from six dynamic global vegetation models. Global Change Biology 7: 357-373

Cuevas E, Medina E. 1986. Nutrient dynamics within Amazonian forest ecosystems .1. Nutrient flux in fine litter fall and efficiency of nutrient utilization. Oecologia 68: 466-472.

Dail BD, Davidson EA, Chorover J. 2001. Rapid abiotic transformation of nitrate in an acid forest soil. Biogeochemistry 54: 131-146.

Davidson ED, Eckert RW, Hart SC, Firestone MK. 1989. Direct extraction of microbial biomass nitrogen from forest and grassland soils in California. Soil Biology and Biochemistry 21: 773-778.

Davidson EA, Hart SC, Shanks CA, Firestone MK. 1991. Measuring gross nitrogen mineralization, immobilization, and nitrification by ^{15}N isotopic pool dilution in intact soil cores. Journal of Soil Science 42: 335-349.

Davidson EA, Trumbore SE. 1995. Gas diffusivity and production of CO_2 in deep soils of the eastern Amazon. Tellus 47B: 550-565.

Davidson EA, Verchot LV, Cattanio JH, Ackerman IL, Carvalho JEM. 2000a. Effects of soil water content on soil respiration in forest and cattle pastures of eastern Amazonia. Biogeochemistry 48: 53-69.

Davidson EA, Keller M, Erickson HE, Verchot LV, Veldkamp E. 2000b. Testing a conceptual model of soil emissions of nitrous and nitric oxides. BioScience 50: 667-680.

Davidson EA, Chorover J, Dail DB. 2003. A mechanism of abiotic immobilization of nitrate in forest ecosystems: the ferrous wheel hypothesis. Global Change Biology 9: 228-236.

Davidson EA, Francoise YI, Nepstad DC. 2004. Effects of an experimental drought on soil emissions of carbon dioxide, methane, nitrous oxide, and nitric oxide in a moist tropical forest. Global Change Biology 10: 718-730.

Davidson EA, Janssens IA, Luo YQ. 2006. On the variability of respiration in terrestrial ecosystems: moving beyond Q_{10}. Global Change Biology 12: 154-164.

De Jong E, Schapert HJV. 1972. Calculation of soil respiration and activity from CO_2 profiles in the soil. Soil Science 119: 328-333.

Dechert G, Veldkamp E, Brumme R. 2005. Are partial nutrient balances suitable to evaluate nutrient sustainability of land use systems? Results from a case study in Central Sulawesi, Indonesia. Nutrient Cycling in Agroecosystems 72: 201-212.

Dise NB, Wright RF. 1995. Nitrogen leaching from European forests in relation to nitrogen deposition. Forest Ecology and Management 71: 153-161.

Drewitt GB, Black TA, Nesic Z, Humphreys ER, Jork EM, Swanson R, Ethier GJ, Griffis T, Morgenstern K. 2002. Measuring forest floor CO_2 fluxes in a Douglas-fir forest. Agricultural and Forest Meteorology 110: 299-317.

Eswaran HE, Vandenberg E, Reich P. 1993. Organic carbon in soils of the world. Soil Science Society of American Journal 57: 192-194.

Fabian P, Kohlpaintner M, Rollenbeck R. 2005. Biomass burning in the Amazon – fertilizer for the mountainous rain forest in Ecuador. Environmental Science and Pollution Research 12: 290-296.

Fan SM, Wofsy SC, Bakwin PS, Jacob DJ, Fitzjarrald DR. 1990. Atmosphere–biosphere exchange of CO_2 and O_3 in the central Amazon forest. Journal of Geophysical Research 95: 16851-16864.

Fearnside PM. 1986. Spatial concentrations of deforestation in the Brazilian Amazon. Ambio 15: 74-81.

Fisher RA, Williams M, do Vale RL, Lola da Costa A, Meir P 2006. Evidence from Amazonian forests is consistent with isohydric control of leaf water potential. Plant, Cell and Environment 29: 151-165.

Fisher RA, Williams M, Pinheiro Ruivo ML, Sombroek WG, Lola da Costa A, Meir P. in review a. The hydraulic properties of a sandy eastern Amazonian oxisol: estimation of unsaturated hydraulic conductivity using tension infiltrometry and instantaneous profiling. Global Change Biology.

Fisher RA, Williams M, Ruivo MLP, Lola da Costa A, Ferreira da Costa R, Meir P. in review b. The response of an Eastern Amazonian rain forest to drought stress: Results and modelling analyses from a through-fall exclusion experiment. Global Change Biology.

Fitzhugh RD, Lovett GM, Venterea RT. 2003. Biotic and abiotic immobilization of ammonium, nitrite, and nitrate in soils developed under different tree species in the Catskill Mountains, New York, USA. Global Change Biology 9: 1591-1601.

Foley JA, Prentice IC, Ramankutty N, Levis S, Pollard D, Sitch S, Haxeltine A. 1996. An integrated biosphere model of land surface processes, terrestrial carbon balance, and vegetation dynamics. Global Biogeochemical Cycles 10: 603-628.

Foley JA, Botta A, Coe MT, Costa MH. 2002. El Nino-Southern oscillation and climate, ecosystems and rivers of Amazonia. Global Biogeochemistry Cycles 16: 1132.

Franzluebbers AJ, Haney RL, Honeycutt CW, Schomberg HH, Hons FM. 2000. Flush of carbon dioxide following rewetting of dried soil relates to active organic pools. Soil Science Society of America Journal 64: 613-623.

Gallardo A, Schlesinger WH. 1994. Factors limiting microbial biomass in the mineral soil and forest floor of a warm-temperate forest. Soil Biology and Biochemistry 26: 1409-1415.

Galloway JN, Levy H, Kasibhatla PS. 1994. Year 2020: consequences of population growth and development on the deposition of oxidized nitrogen. Ambio 23: 120-123.

Galloway JN, Cowling EB, Seitzinger SP, Socolow RH. 2002. Reactive Nitrogen: Too Much of a Good Thing? Ambio 31: 60-63.

Galloway JN, Dentener FJ, Capone DG, Boyer EW, Howarth RW, Seitzinger SP, Asner GP, Cleveland CC, Green PA, Holland EA, Karl DM, Michaels AF, Porter JH, Townsend AR, Vorosmarty CJ. 2004. Nitrogen cycles: past, present, and future. Biogeochemistry 70: 153-226.

Gordon WS, Jackson RB. 2000. Nutrient concentrations in fine root. Ecology 81: 275-280.

Gough CM, Seiler JR. 2004. The influence of environmental, soil carbon, root, and stand characteristics on soil CO_2 efflux in loblolly pine (Pinus taeda L.) plantations located on the South Carolina Coastal Plain. Forest Ecology and Management 191: 353-363.

Goulden ML, Crill PM. 1997. Automated measurements of CO_2 exchange at the moss surface of a black spruce forest. Tree Physiology 17: 537-542.

Grace J, Lloyd J, McIntyre J, Miranda AC, Meir P, Miranda HS, Nobre C, Moncriff J, Massheder J, Malhi Y, Wright I, Gash J. 1995a. Carbon dioxide uptake by an undisturbed tropical rain forest in southwest Amazonia, 1992 to 1993. Science 270: 778-780

Grace J, Lloyd J, McIntyre J, Miranda AC, Meir P, Miranda HS, Moncriff J, Massheder J, Wright I, Gash J. 1995b. Fluxes of carbon dioxide and water vapour over an undisturbed tropical forest in south-west Amazonia. Global Change Biology 1: 1-12.

Hall SJ, Matson PA. 1999. Nitrogen oxide emissions after nitrogen additions in tropical forests. Nature 400: 152-155.

Hall SJ, Matson PA. 2003. Nutrient status of tropical rain forests influences soil N dynamics after N additions. Ecological Society of America 73: 107-129.

Hanson PJ, Wullschleger SD, Bohlman SA, Todd DE. 1993. Seasonal and topographic patterns of forest floor CO_2 efflux from an upland oak forest. Tree Physiology 13: 1-15.

Hart SC, Stark JM, Davidson EA, Firestone MK. 1994a. Nitrogen mineralization, immobilization, and nitrification. Weaver R, editor. Methods of soil analysis, Part 2. Microbiological and biochemical properties. Madison, Wisconsin: American Society of Agronomy, SSSA Book Series, No. 5, p985-1019.

Hart SC, Nason GE, Myrold DD, Perry DA. 1994b. Dynamics of gross nitrogen transformations in an old-growth forest: the carbon connection. Ecology 75: 880-891.

Hedin LO, Vitousek PM, Matson PA. 2003. Nutrient losses over four million years of tropical forest development. Ecology 84: 2231-2255.

Houghton RA, Lawrence KT, Hacker JL, Brown S. 2001. The spatial distribution of forest biomass in the Brazilian Amazon: a comparison of estimates. Global Change Biology 7: 731-746.

Hulme M, Viner D. 1998. A climate change scenario for the tropics. Climatic Change 39: 145-176.

IPCC (Intergovernamental Panel on Climate Change). 1992. Climate Change 1992: the Supplementary Report to the IPCC Scientific Assessment.

IPCC (Intergovernamental Panel on Climate Change). 1995. Scientific Assessments of Climate Change. The Policymaker's Summary of Working Group 1 to the Intergovernamental Panel on Climate Change, WMO/UNEP.

IPCC (Intergovernamental Panel on Climate Change). 1996. Climate Change 1995: the science of climate change. Cambridge University Press, Cambridge, UK.

IPCC (Intergovernamental Panel on Climate Change). 1997. Stabilization of atmospheric Greenhouse gases: physical, biological, and socio- economic implications - IPCC Technical Paper III. WMO/UNEP.

IPCC (Intergovernamental Panel on Climate Change). 2000. Special Report on Land Use, Land-Use Change and Forestry. Cambridge University Press, Cambridge, UK.

Janssens IA, Meiresonne L, Ceulemans R. 2000. Mean soil CO_2 efflux from a mixed forest: temporal and spatial integration. In: Ceulemans RJM, Veroustraete F, Gond V, Van Rensbergen JBHF (eds) Forest ecosystem modelling, up scaling and remote sensing. SPB Academic Publishing bv, The Hague, The Netherlands, pp. 19-31.

Janssens IA, Kowalski AS, Ceulemans R. 2001. Forest floor CO_2 fluxes estimated by eddy covariance and chamber-based model. Agricultural and Forest Meteorology 106: 61-69.

Jobbagy EG, Jackson RB. 2000. The vertical distribution of soil organic carbon and its relation to climate and vegetation. Ecological Applications 10: 423-436.

Joergensen RG. 1996. The fumigation-extraction method to estimate soil microbial biomass: Calibration of the k(EC) value. Soil Biology and Biochemistry 28: 25-31.

Johnson DW, Cheng W, Burke CI. 2000. Biotic and abiotic nitrogen retention in a variety of forest soils. Soil Science Society of America Journal 64: 1503-1514.

Jordan CF. 1985. Soils of the Amazon Rainforest. In: Prance GT, Lovejoy TE (eds) Key environments: Amazonia. Pergamon Press, Oxford, pp. 83-94.

Joslin JD, Wolfe MH, Hanson PJ. 2000. Effects of altered water regimes on forest root systems. New Phytologist 147: 117-129.

Kang S, Kim S, Oh S, Lee D. 2000. Predicting spatial and temporal patterns of soil temperature based on topography, surface cover and air temperature. Forest Ecology and Management 136: 173-184.

Keller M, Kaplan WA, Wofsy SC, Costa JM. 1988. Emissions of N_2O from tropical forest soils: response to fertilization with NH_4^+ and PO_4^{3-}. Journal of Geophysical Research 93: 1600-1604.

Keller M, Veldkamp E, Weitz AM, Reiners WA. 1993. Effect of pasture age on soil trace-gas emissions from a deforested area of Costa Rica. Nature 365: 244-246.

Keller M, Reiners WA. 1994. Soil-atmosphere exchange of nitrous oxide, nitric oxide, methane under secondary succession of pasture to forest in the Atlantic lowlands of Costa Rica. Global Biogeochemistry Cycles 8: 399-409.

Keller M, Alencar A, Asner GP, Brasswell B, Busmante M, Davidson E, Feldpausch T, Fernandes E, Goulden M, Kabat P, Kruijt B, Luizao F, Miller S, Markewitz D, Nobre AD, Nobre CA, Priante Filho N, da Rocha H, Dias PS, von Randow C, Vourlitis GL. 2004. Ecological research in the large-scale biosphere-atmosphere experiment in Amazonia: early results. Ecological Applications 14: S3:S16.

Kern DC. 1996. Geoquimica e pedoquimica em sitios arqueológicos com terra preta na Floresta Nacional de Caxiuana (Portel-PA). Universidade Federal do Pará, Belém, Pará, PhD. Thesis, 119p.

Kiese R, Butterbach-Bahl K. 2002. N_2O and CO_2 emissions from three different tropical forest sites in the wet tropics of Queensland, Australia. Soil Biology and Biochemistry 34: 975-987.

King AW, Post WM, Wullschleger SD. 1997. The potential response of terrestrial carbon storage to changes in climate and atmospheric CO_2. Climate Change 35: 199-227.

Kirkham D, Bartholomew WV. 1954. Equations for following nutrient transformations in soil, utilization tracer data. Soil Science Society of America Proceedings 18: 33-34.

Kirschbaum MUF. 1993. A modeling study of the effects of changes in atmospheric CO_2 concentration, temperature and atmospheric nitrogen input on soil organic carbon storage. Tellus 45B: 321-334.

Klinge R, Martins ARA, Mackensen J, Folster H. 2004. Element loss on rain forest conversion in East Amazonia: comparison of balances of stores and fluxes. Biogeochemistry 69: 63-82.

Lavine MB, Foster RJ, Goodine G. 2004. Seasonal and annual changes in soil respiration in relation to soil temperature, water potential and trenching. Tree Physiology 24: 415-424.

Li YQ, Xu M, Zou XM, Xia Y. 2005. Soil CO_2 efflux and fungal and bacterial biomass in a plantation and a secondary forest in wet tropics in Puerto Rico Plant and Soil 268: 151-160.

Lisboa PLB, Ferraz MG. 1999. Estacao Cientifica Ferreira Penna. CNPq / Museu Paraense Emilio Goeldi, Belem, Para, pp. 151.

Lisboa PLB, Silva ASL, Almeida SS. 1997. Floristica e estrutura dos ambientes. In: Lisboa PLB (ed). Caxiuana: pesquisa e desenvolvimento sustentavel. CNPq / Museu Paraense Emilio Goeldi, Belem, pp. 163-193.

Liu HS, Li FM, Xu H. 2004. Deficiency of water can enhance root respiration rate of drought-sensitive but not drought-tolerant spring wheat. Agricultural Water Management 64: 41-48.

Loftfield N, Flessa H, Augustin J, Beese F. 1997. Automated gas chromatographic system for rapid analysis of the atmospheric trace gases methane, carbon dioxide, and nitrous oxide. Journal of Environmental Quality 26: 560-564.

Lourdes Pinheiro Ruivo M, Quantz B, Pereira Baia S, Busseti EPC, Nagaishi TY. 2002. The soils of the LBA experimental sites (Caxiuanã, Para State, Brazil). Symposia of the 17th World Congress of Soil Science, 14-21 August 2002, Thailand.

Luizão FJ, Schubart HOR.1987. Litter production and decomposition in a terra-firme forest of Central Amazonia. Experientia 43: 259-265.

Luizão RCC, Luizão FJ, Paiva RQ, Monteiro TF, Sousa LS, Kruijt B. 2004. Variation of carbon and nitrogen cycling processes along a topographic gradient in a central Amazonian forest. Global Change Biology 10: 592-600.

Malhi Y, Grace J. 2000. Tropical forests and atmospheric carbon dioxide. Trends in Ecology and Evolution 15: 332-337.

Mariotti A, Germon JC, Hubert P, Kaiser P, Letolle R, Tardieux A, Tardieux P. 1981. Experimental determination of nitrogen kinetic isotope fractionation: some principles, ilustration for the denitrification and nitrification processes. Plant and Soil 62: 413-430.

Martinelli LA, Piccolo MC, Townsend AR, Vitousek PM, Cuevas E, McDowell WA, Robertson GP, Santos OC, Treseder K. 1999. Nitrogen stable isotope composition of leaves and soil: Tropical versus temperate forests. Biogeochemistry 46: 45-55.

Mason EA, Monchick L. 1962. Transport properties of polar-gas mixtures. The Journal of Chemical Physics 36: 2746-2757.

Mathieu GG, Biscaye PE, Lupton RA, Hammond DE. 1988 System for measurement of ^{222}Rn at low levels in natural waters. Health Physics 55: 989-992.

Matson PA, McDowell WH, Townsend AR, Vitousek PM. 1999. The globalization of N deposition: ecosystem consequences in tropical environments. Biogeochemistry 46: 67-83.

Matson PA, Vitousek PM. 1987. Cross-system comparisons of soil nitrogen transformations and nitrous-oxide flux in tropical forest ecosystems. Global Biogeochemistry Cycles 1: 163-170.

McGuire AD, Melillo JM, Kicklighter DW, Joyce LA. 1995. Equilibrium responses of soil carbon to climate change: Empirical and process-based estimates. Journal of Biogeography 22: 785-796.

Meir P, Grace J. 2005. The response of drought by tropical rainforest ecosystems. In: Malhi Y, Grace J (eds) Tropical Forests and global atmospheric change. Oxford University Press, Oxford, UK, pp. 75-84.

Melillo M, Steudler PA, Feigl BJ, Neill C, Garcia D, Piccolo MC, Cerri C, Tian H. 2001. Nitrous oxide emissions from forests and pastures of various ages in the Brazilian Amazon. Journal of Geophysical Research 106: 179-188.

Metcalfe DB, Meir P, Aragao LEOC, Costa ACL, Braga A, Goncalves PHL, Athaydes J, Dawson LA, Malhi Y, Williams M. in preparation. Root responses to soil moisture variation at an eastern Amazon rainforest site.

Millington RJ, Quirk JM. 1961. Permeability of porous solids. Transactions of the Faraday Society 57: 1200-1207.

Millington RJ, Shearer RC. 1971. Diffusion in aggregated porous media. Soil Science 3: 372-378.

Moldrup P, Olesen T, Schjønning P, Yamaguchi T, Rolston DE. 2000. Predicting the gas diffusion coefficient in undisturbed soil from soil water characteristics. Soil Science Society 64: 94-100.

Moraes JC, Costa JPR, Rocha EJP, Silva IMO. 1997. Estudos hidrometeorológicos na bacia do rio Caxiuanã. In: Lisboa PLB (ed) Caxiuanã. CNPq/Museu Paraense Emílio Goeldi, Belém, p. 85-95.

Müller T, Höper H. 2004. Soil organic matter turnover as a function of the soil clay content: consequences for model applications. Soil Biology and Biochemistry 36: 877-888.

Myers N. 1980. Conversion of tropical moist forest. National Academy of Sciences, Washington, D.C., 205 p.

Nadelhoffer KJ, Fry B. 1988. Controls on natural nitrogen-15 and carbon-13 abundances in forest soil organic matter. Soil Science Society of America Journal 52: 1633-1640.

Neill C, Piccolo MC, Melillo JM, Steudler PA, Cerri CC. 1999. Nitrogen dynamics in Amazon forest and pasture soils measured by ^{15}N pool dilution. Soil Biology Biochemistry 31: 567-572.

Nepstad DC, Carvalho CR, Davidson EA, Jipp PH, Lefebvre PA, Negreiros GH, da Silva ED, Stone TA, Trumbore SE, Vieira S. 1994. The role of deep roots in the hydrological and carbon cycles of Amazonian forests and pastures. Nature 372: 666-669.

Nepstad DC, Verissimo A, Alencar A, Nobre C, Lima E, Lefebvre P, Schlesinger P, Potter C, Moutinho P, Mendoza E, Cochrane M, Brooks V. 1999. Large-scale impoverishment of Amazonian forests by logging and fire. Nature 398: 505-508.

Nepstad DC, Moutinho P, Dias-Filho MB, Davidson E, Cardinot G, Markewitz D, Figueiredo R, Vianna N, Chambers J. 2002. The effects of partial throughfall exclusion on canopy processes, aboveground production, and biogeochemistry of an Amazon forest. Journal of Geophysical Research 107: 8085, doi:10.1029/2001JD000360.

Nobre CA, Sellers PJ, Shukla J. 1991. Amazonian deforestation and regional climate change. Journal of Climate 4: 957-988

Nömmik H. 1970. Non-exchangeable binding of ammonium and amino nitrogen by Norway spruce raw humus. Plant and Soil 33: 581-595.

Nömmik H, Vahtras K. 1982. Retention and fixation of ammonium and amonia in soils. Stevenson FJ, editor. Nitrogenin agricultural soils. Madison, Wisconsin, USA: ASA-CSSA-SSSA Agronomy Monograph 22. p123-172.

Norby RJ, Jackson RB. 2000. Root dynamics and global change: seeking an ecosystem perspective. New Phytologist 147: 3-12.

Norman JM, Garcia R, Verma SB. 1992. Soil surface CO_2 fluxes and the carbon budget of a grassland, Journal of Geophysical Research 97: 18845-18853.

Parkinson KJ. 1981. An improved method for measuring soil respiration in field. J. Applied Ecology 18: 221-228.

Paul EA, Clark FE. 1996. Soil Microbiology and Biochemistry. 2 ed., California, USA: Elsevier Science and Technology Books. 340p.

Piccolo MC, Neill C, Cerri CC. 1994. Natural abundance of ^{15}N soils along forest-to-pasture chronosequences in the western Brazilian Amazon Basin. Oecologia 99: 112-117.

Piccolo MC, Neill C, Melillo JM, Cerri CC, Steudler PA. 1996. ^{15}N natural abundance in forest and pasture soils of the Brazilian Amazon Basin. Plant and Soil 182: 249-258.

Potter CS, Randerson JT, Field CB, Matson PA, Vitousek PM, Money HA, Klooster S. 1993. Terrestrial ecosystem production: A process model based on global satellite and surface data. Global Biogeochemical Cycles 7: 811-842.

Potter CS, Matson PA, Vitousek PM, Davidson EA. 1996. Process modelling of controls on nitrogen trace gas emissions from soils worldwide. Journal Geophysical Research 101: 1361-1377.

Prather M, Derwent R, Ehhalt D, Fraser P, Sanhueza E, Zhou X. 1995. Other trace gases and atmospheric chemistry. In: Houghton JT, Meira Filho LG, Bruce J, Lee H, Callander

BA, Haites E, Harris N, Maskell K (eds) Climate change 1994: Radiative Forcing of Climate Change and an Evolution of the IPCC IS 92 Emission Scenarios. Cambridge University Press, New York, pp. 77-126.

Prather M, Ehalt D. 2001. Atmospheric chemistry and greenhouse gases. In: Houghton JT, Ding Y, Griggs DJ, Noguer PJ, van der Linden PJ, Dai X, Maskell K, Johnson CA (eds) Climate change 2001: The Scientific Basis. Cambridge University Press, Cambridge, UK, pp. 239-288.

Prentice C, Heimann M, Sitch S. 2000. The carbon balance of the terrestrial biosphere: ecosystem models and atmospheric observations. Ecological Applications 10: 1553-1573.

Purbopuspito J, Veldkamp E, Brumme R. 2006. Trace gas fluxes and nitrogen cycling along an elevation sequence of tropical mountain forests in Central Sulawesi, Indonesia. Global Biogeochemical Cycles, in press.

Riley RH, Vitousek PM. 1995. Nutrient dynamics and trace gas flux during ecosystem development in Hawaiian montane rainforest. Ecology 76: 292-304.

Ruivo MLP, Cunha ES. 2003. Mineral and organic components in archaeological black earth and yellow latosol in Caxiuanã, Amazon, Brazil. In: Tiezzi E, Brebbia CA, Uso JL (eds) Ecosystems and Sustainable Development, WITT Press, Southhampton, UK, pp.1113-1121.

Running SW, Nemani RR, Hungerford RD. 1987. Extrapolation of synoptic meteorological data in mountainous terrain and its use for simulating forest evapotranspiration and photosynthesis. Canadian Journal of Forest Research 17: 472-483.

Rustad LE, Huntington TG, Boone RD. 2000. Controls on soil respiration: implications for climate change. Biogeochemistry 48: 1-6.

Salamanca EF, Kaneko N, Katagiri S. 2003. Rainfall manipulation effects on litter decomposition and the microbial biomass of the forest floor. Applied Soil Ecology 22: 271-281.

Saleska SR, Miller SD, Matross DM, Goulden ML, Wofsy SC, da Rocha HR, de Camargo PB, Crill P, Daube BC, de Freitas HC, Hutyra L, Keller M, Kirchhoff V, Menton M, Munger JW, Pyle EH, Rice AH, Silva H. 2003. Carbon in Amazon forests: Unexpected seasonal fluxes and disturbance-induced losses. Science 302: 1554-1557.

Schimel DS. 1988. Carbon and nitrogen turnover in adjacent grassland and cropland ecosystems. Biogeochemistry 2: 345-357.

Schimel DS, Braswell BH, Holland EA, McKeown R, Ojima DS, Painter TH, Parton WJ, Townsend AR. 1994. Climatic, edaphic, and biotic controls over storage and turnover of carbon in soils. Global Biogeochemistry Cycles 8: 279-293.

Schlesinger WH. 1977. Carbon Balance in Terrestrial Detritus. Annual Review of Ecology and Systematics 8: 51-81.

Schlesinger WH, Winkler Palmer J, Megonigal JP. 2000. Soils and the global carbon cycle. In: Wigley TML, Schimel DS (eds) The carbon cycle. Cambridge University Press, Cambridge, pp 93-101.

Schulze ED.1989. Air-pollution and forest decline in a spruce (*Picea-abies*) forest. Science 244: 776-783.

Schwendenmann L, Veldkamp E, Brenes T, O'Brien JJ, Mackensen J. 2003. Spatial and temporal variation in soil CO_2 efflux in an old-growth neotropical rain forest, La Selva, Costa Rica. Biogeochemistry 64: 111-128.

Schwendenmann L, Veldkamp E. 2005. The role of dissolved organic carbon, dissolved organic nitrogen and dissolved inorganic nitrogen in a tropical wet forest ecosystem. Ecosystems 8: 339-351.

Schwendenmann L, Veldkamp E 2006. Long-term CO_2 production from deeply weathered soils of a tropical rain forest: evidence for a potential feedback to climate warming. Global Change Biology, in press

Shen SM, Pruden G, Jenkinson DS. 1984. Mineralization and immobilization of nitrogen in fumigated soil and the measurement of the microbial biomass nitrogen. Soil Biology and Biochemistry 16: 437-444.

Shine KP, Derwent RG, Wuebble DJ, Morcrette JJ. 1990. Radiative forcing of climate. In: Houghton JT, Jenkins GJ, Ephraums JJ (eds). Climate Change 1992. The IPCC Scientific Assessment. Cambridge University Press, Cambridge, pp. 41-68.

Shine KP. 1995. The roles of carbon-dioxide and water-vapor in warming and cooling the earth's troposphere – comment. Spectrochimica Acta Part A: Molecular and Biomolecular Spectroscopy 51: 1393-1394.

Shukla J, Nobre CA, Sellers P. 1990. Amazon deforestation and climate change. Science 247: 1322-1325.

Silver WL, Keller M, Lugo AE. 1999. Soil oxygen availability and biogeochemical cycling along elevation and topographic gradients in Puerto Rico. Biogeochemistry 44: 301-328.

Silver WL, Donald JH, Firestone MK. 2001. Dissimilatory nitrate reduction to ammonium in upland tropical forest soils. Ecological Society of America 82: 2410-2416.

Silver WL, Neff J, McGroddy M, Veldkamp E, Keller M, Cosme R. 2000. Effects of soil texture on belowground carbon and nutrient storage in a lowland Amazonian forest ecosystem. Ecosystems 3: 193-209.

Silver WL, Thompson AW, Reich A, Ewel JJ, Firestone MK. 2005. Nitrogen cycling in tropical plantation forests: potential controls on nitrogen retention. Ecological Applications 15: 1604-1614.

Smith CJ, Chalk FE. 1980. Gaseous nitrogen evolution during nitrification of ammonia fertilizer and nitrite transformations in soil. Soil Science Society America Journal 44: 277-282.

Sokal RR, Rohlf FJ. 1981. Biometry. New York, USA: W. H. Freeman and Co.

Sombroek WG. 1966. Amazon soils: A reconnaissance of the soils of the Brazilian Amazon region. Center of Agricultural Publication and Documentation, Wageningen.

Sombroek WG, Nachtergaele FO, Hebel A. 1993. Amounts, dynamics and sequestering of carbon in tropical and subtropical soils. Ambio 22: 417-426.

Sotta ED, Meir P, Malhi Y, Nobre AD, Hodnett M, Grace J. 2004. Soil CO_2 efflux in a tropical forest in central Amazon. Global Change Biology 10: 601-617.

Sotta ED, Veldkamp E, Guimaraes B, Paixao RK, Ruivo MLP. in review. Landscape and climatic controls on spatial and temporal variation in soil CO_2 efflux in an Eastern Amazonian Rainforest, Caxiuanã, Brazil. Forest Ecology and Management

Souza JS. 2004. Dinamica espacial e temporal do fluxo de CO_2 do solo em floresta de terra firme na Amazonia central. MSc.Thesis, INPA, Manaus, Brazil.

Spalding RF, Exner ME. 1993. Occurrence of nitrate in groundwater, a review. Journal of Environmental Quality 22: 393-402.

Stark JM, Hart SC. 1996. Diffusion technique for preparing salt solutions, Kjeldahl digests, and persulfate digests for nitrogen-15 analysis. Soil Science Society America Journal 60: 1846-1855.

Stokstad E. 2005. Ecology - Experimental drought predicts grim future for rainforest. Science 308: 346-347.

Thorn KA, Mikita MA. 2000. Nitrite fixation by humic substances: nitrogen-15 nuclear magnetic resonance evidence for potential intermediates of chemodenitrification. Soil Science Society of America Journal 64: 568-582.

Timmerman A, Oberhuber J, Bacher A, Esch M, Latif M, Roeckner E. 1999. Increased El Nino frequency in a climate model forced by future greenhouse warming. Nature 398: 694-697.

Toledo LC. 2002. Efeito da umidade na respiracao de liteira grossa e fina em uma floresta tropical de terra-firme a Amazonia central. MSc Thesis, INPA, Manaus, Brazil.

Trumbore SE, Bonani G, Wölfli W. 1990. The rates of carbon cycling in several soils from AMS ^{14}C measurements of fractionated soil organic matter. In: Bouwman AF. (ed) Soils and the greenhouse effect. John Wiley Publishers, New York, pp. 405-414.

Trumbore SE, Davidson EA, Camargo PB, Nepstad DC, Martinelli LA. 1995. Belowground cycling of carbon in forests and pastures of Eastern Amazonia. Global Biogeochemical Cycles 9: 515-528.

Trumbore SE, Chadwick OA, Amundson R. 1996. Rapid exchange between soil carbon and atmospheric carbon dioxide driven by temperature change. Science 272: 393-396.

Trumbore SE. 2000. Age of soil organic matter and soil respiration: Radiocarbon constraints on belowground C dynamic. Ecological Applications 10: 399-411.

Uchida M, Nojiri Y, Saigusa N, Oikawa T. 1997. Calculation of CO_2 flux from forest soil using ^{222}Rn calibrated method. Agricultural and Forest Meteorology 87: 301-311.

Van Breemen N, Burrough PA, Velthorst EJ, Dobben van HF, de Wit T, Ridder TB, Reijnders HFR. 1982. Soil acidification from atmospheric ammonium sulphate in forest canopy throughfall. Nature 299: 548–550.

Van Cleemput O, Samater AH. 1996. Nitrite in soils: accumulation and role in the formation of gaseous N compounds – mini review. Fertilizer Research 45: 81-89.

Veldkamp E, Davidson E, Erickson H, Keller M, Weitz A. 1999. Soil nitrogen cycling and nitrogen oxide emissions along a pasture chronosequence in the humid tropics of Costa Rica. Soil Biology and Biochemistry 31: 387-394

Veldkamp E, Becker A, Schwendenmann L, Clark DA, Schulte-Bisping H. 2003. Substantial labile carbon stocks and microbial activity in deeply weathered soils below a tropical wet forest. Global Change Biology 9: 1171-1184.

Verchot LV, Davidson EA, Cattanio JH, Ackerman IL, Erickson HE, Keller M. 1999. Land use change and biogeochemical controls of nitrogen oxide emissions from soils of eastern Amazonia. Global Biogeochemical Cycles 13: 31-46.

Vervaet H, Massart B, Boeckx P, Van Cleemput O, Hofman G. 2002. Can $\delta^{15}N$ profiles in forest soils predict loss and net N mineralization rates? Biology and Fertility of Soils 36: 143-150.

Vitousek PM. 1984. Litterfall, Nutrient Cycling, and Nutrient Limitation in Tropical Forests. Ecology 65: 285-298.

Vitousek PM, Howarth R. 1991. Nitrogen limitation on land and in the sea: how can it occur? Biogeochemistry 13: 87-115.

Vitousek PM, Aber JD, Howarth RW, Likens GE, Matson PA, Schindler DW, Schlesinger WH, Tilman DG. 1997. Human Alteration of the Global Nitrogen Cycle: Sources and Consequences. Ecological Applications 7: 737-750.

Vitousek PM, Farrington H. 1997. Nutrient limitation and soil development: experimental test of a biogeochemical theory. Biogeochemistry 37: 63-75.

Werth D, Avissar R. 2002. The local and global effects of Amazon deforestation. Journal of Geophysical Research 107: 8087, doi: 10.1029/2001JD000717.

Wofsy SC, Harriss RC, Kaplan WA. 1988. Carbon dioxide in the atmosphere over the Amazon basin. Journal of Geophysical Research 93: 1377-1387.

Wollast R. 1993. Interactions of carbon and nitrogen cycles in the costal zone. In: Wollast R, MacKenzie FR, Chou L. (eds) Interactions of C, N, P and S Biogeochemical Cycles and Global Change. Spring-Verlag, New York, pp.195-210.

Wong PTW, Griffin DM. 1976. Bacterial movement at high matric potentials.1. Artificial and natural soils. Soil Biology and Biochemistry 8: 215-218.

Xu M, Qi Y. 2001. Spatial and seasonal variations of Q(10) determined by soil respiration measurements at a Sierra Nevadan forest. Global Biogeochemical Cycles 15: 687-696.

9. Appendix

Table A1 – Soil CO_2 efflux, soil temperature at 0.05 m depth (*Ts*) and soil water content (*swc*) at 0.3 m depth in sand and clay soil textures at the Caxiuanã National Forest, Brazil (n = 16).

Date	Sand						Clay					
	CO_2 efflux (μmol CO_2 m^{-2} s^{-1})		*Ts* (°C)		*swc* (%)		CO_2 efflux (μmol CO_2 m^{-2} s^{-1})		*Ts* (°C)		*swc* (%)	
dd/mm/yyyy	mean	(SE)	mean	(SE)	mean	(SE)	mean	(SE)	mean	(SE)	mean	(SE)
12/11/2001	3.8	(0.3)	24.6	(0.1)	16.2	(0.4)	-		-		-	
16/12/2001	4.8	(0.5)	24.3	(0.8)	24.7	(0.5)	-		-		-	
11/01/2002	4.3	(0.2)	-		24.4	(0.4)	-		-		-	
24/01/2002	4.5	(0.3)	22.7	(0.1)	24.7	(0.2)	3.6	(0.5)	20.5	(0.2)	40.6	(0.7)
07/02/2002	5.1	(0.4)	-		24.2	(0.4)	3.3	(0.5)	-		39.5	(2.7)
21/02/2002	4.0	(0.3)	-		26.4	(0.3)	4.3	(0.1)	-		39.2	(1.3)
07/03/2002	3.9	(0.2)	20.4	(0.0)	25.4	(0.4)	3.4	(0.1)	20.7	(0.1)	38.8	(0.6)
23/03/2002	2.9	(0.4)	23.4	(0.3)	28.4	(0.7)	2.8	(0.0)	21.4	(0.6)	41.2	(1.5)
07/04/2002	3.1	(0.2)	22.5	(0.1)	27.2	(0.3)	2.0	(0.2)	20.1	(0.8)	43.1	(0.1)
28/04/2002	3.3	(0.1)	23.3	(0.0)	28.2	(0.2)	2.7	(0.1)	23.3	(0.0)	43.3	(0.4)
25/05/2002	4.1	(0.1)	23.8	(0.4)	26.4	(0.6)	2.6	(0.2)	22.7	(0.4)	41.4	(1.3)
03/06/2002	3.6	(0.2)	22.9	(0.1)	28.3	(0.4)	2.9	(0.5)	23.8	(0.4)	41.9	(0.6)
16/06/2002	3.0	(0.1)	23.1	(0.2)	28.8	(0.2)	2.5	(0.4)	23.3	(0.8)	43.5	(0.1)
01/07/2002	3.7	(0.3)	24.9	(0.2)	26.9	(0.2)	3.1	(0.4)	24.4	(0.1)	39.1	(3.1)
15/07/2002	4.3	(0.3)	24.6	(0.1)	21.0	(0.7)	3.4	(0.2)	24.1	(0.4)	29.8	(3.3)
26/07/2002	4.6	(0.4)	24.3	(0.1)	22.4	(0.9)	2.8	(0.4)	24.3	(0.4)	41.3	(1.8)
09/08/2002	4.2	(0.3)	24.8	(0.1)	23.4	(0.5)	3.3	(0.4)	24.1	(0.1)	37.1	(2.0)
24/08/2002	4.1	(0.1)	24.6	(0.1)	23.2	(0.8)	3.2	(0.3)	25.1	(0.2)	35.4	(2.2)
06/09/2002	3.8	(0.3)	24.6	(0.1)	21.5	(0.6)	2.8	(0.1)	24.8	(0.1)	29.7	(2.6)
20/09/2002	3.3	(0.2)	24.3	(0.1)	19.2	(0.4)	2.2	(0.1)	25.3	(0.3)	24.1	-
04/10/2002	3.1	(0.1)	24.0	(0.0)	18.4	(0.4)	2.8	(0.1)	24.2	(0.3)	23.2	(1.0)
18/10/2002	3.8	(0.1)	24.2	(0.1)	20.7	(0.7)	2.5	(0.2)	23.8	(0.1)	35.7	(2.6)
03/11/2002	3.4	(0.1)	24.3	(0.1)	15.9	(0.4)	3.1	(0.2)	24.0	(0.0)	27.5	(2.9)
15/11/2002	4.4	(0.2)	23.5	(0.0)	20.7	(0.5)	2.9	(0.3)	23.3	(0.2)	25.0	(2.0)
29/11/2002	4.0	(0.2)	24.4	(0.1)	16.3	(0.4)	-		24.4	(0.3)	21.6	-
13/12/2002	3.6	(0.3)	23.6	(0.1)	22.7	(0.8)	2.7	(0.4)	22.4	(0.6)	35.5	(1.8)
13/01/2003	4.2	(0.1)	24.0	(0.2)	22.3	(0.7)	3.6	(0.1)	22.9	(0.0)	26.3	(2.9)
07/02/2003	3.9	(0.1)	22.5	(0.2)	24.9	(0.7)	3.6	(0.1)	23.6	(0.1)	36.4	(1.8)
20/03/2003	4.9	(0.3)	24.2	(0.1)	24.7	(0.3)	3.9	(0.6)	24.4	(0.0)	35.2	(2.3)
03/04/2003	3.8	(0.2)	25.3	(0.3)	27.8	(0.1)	3.5	-	24.1		39.8	-
15/05/2003	3.3	(0.2)	24.5	(0.2)	26.4	(0.2)	2.4	(0.4)	25.0	(0.1)	43.3	(0.7)
03/07/2003	5.2	(0.3)	24.5	(0.3)	23.1	(0.5)	3.6	(0.1)	24.8	(0.1)	36.8	(4.0)
13/09/2003	4.8	(0.1)	24.4	(0.2)	19.0	(0.5)	3.2	(0.0)	24.3	(0.1)	24.4	(2.2)
26/10/2003	3.5	(0.3)	24.1	(0.4)	19.0	(0.6)	3.8	(0.1)	24.4	(0.2)	22.7	(1.8)
01/11/2003	3.3	(0.3)	24.5	(0.1)	15.4	(0.2)	3.2	(0.2)	24.6	(0.2)	20.2	(2.4)

Table A2 – Soil CO_2 production (P_{CO2}), soil temperature (*Ts*) and soil water content (*swc*) in control and throughfall exclusion (TFE) plot at the Caxiuanã National Forest, Brazil (n = 4).

Date	Depth	Control			TFE		
		P_{CO2}	*Ts*	*swc*	P_{CO2}	*Ts*	*swc*
	(m)	(µmol CO_2 m^{-2} s^{-1})	(°C)	(%)	(µmol CO_2 m^{-2} s^{-1})	(°C)	(%)
dd/mm/yyyy		mean (SE)	mean (SE)	mean (SE)	mean (SE)	mean (SE)	mean (SE)
11/01/2002	0-0.5	4.1 (0.4)	20.4 (0.3)	22.7 (0.8)	3.9 (0.4)	20.2 (0.5)	19.8 (1.2)
24/01/2002	0-0.5	4.1 (0.3)	22.6 (0.1)	23.2 (1.2)	3.5 (0.1)	19.7 (0.6)	19.5 (0.5)
07/02/2002	0-0.5	4.5 (0.4)	18.7 (0.9)	-	2.9 (0.1)	17.9 (0.3)	-
21/02/2002	0-0.5	3.4 (0.5)	18.3 (0.2)	25.1 (1.2)	2.8 (0.3)	18.6 (0.3)	18.9 (1.1)
07/03/2002	0-0.5	3.1 (0.3)	21.2 (0.2)	25.5 (0.7)	2.5 (0.1)	21.6 (0.3)	17.2 (1.3)
23/03/2002	0-0.5	2.4 (0.4)	24.0 (0.1)	27.3 (0.7)	2.2 (0.2)	22.4 (0.2)	19.9 (1.7)
07/04/2002	0-0.5	2.5 (0.3)	22.7 (0.1)	28.0 (0.6)	2.2 (0.3)	21.9 (0.7)	19.6 (1.6)
28/04/2002	0-0.5	2.6 (0.2)	23.7 (0.2)	26.8 (0.7)	2.5 (0.2)	24.1 (0.3)	20.4 (1.1)
25/05/2002	0-0.5	3.2 (0.4)	25.5 (0.4)	28.2 (0.5)	3.3 (0.3)	24.3 (0.3)	20.0 (1.0)
03/06/2002	0-0.5	3.0 (0.3)	22.7 (0.2)	26.7 (0.8)	2.7 (0.2)	24.0 (0.1)	18.1 (0.9)
16/06/2002	0-0.5	2.1 (0.3)	24.4 (0.1)	27.9 (0.4)	2.2 (0.1)	23.1 (0.2)	17.8 (1.9)
01/07/2002	0-0.5	2.8 (0.5)	24.9 (0.1)	26.3 (1.0)	2.7 (0.2)	25.0 (0.2)	17.9 (1.3)
15/07/2002	0-0.5	3.5 (0.3)	24.9 (0.0)	-	2.2 (0.1)	24.9 (0.1)	-
26/07/2002	0-0.5	3.5 (0.4)	25.1 (0.1)	24.2 (1.1)	1.9 (0.2)	25.1 (0.2)	16.3 (0.3)
09/08/2002	0-0.5	3.4 (0.3)	25.1 (0.1)	23.5 (0.9)	1.9 (0.1)	24.8 (0.1)	15.5 (0.7)
24/08/2002	0-0.5	3.3 (0.1)	24.9 (0.1)	20.1 (0.7)	1.9 (0.1)	24.7 (0.2)	14.0 (0.3)
06/09/2002	0-0.5	2.9 (0.3)	25.2 (0.1)	18.5 (0.6)	1.2 (0.2)	24.9 (0.2)	13.5 (0.3)
20/09/2002	0-0.5	2.4 (0.3)	24.6 (0.0)	17.5 (0.7)	1.3 (0.1)	24.4 (0.1)	13.6 (0.3)
04/10/2002	0-0.5	1.8 (0.4)	24.2 (0.0)	16.0 (0.5)	1.1 (0.2)	24.3 (0.1)	13.1 (0.2)
18/10/2002	0-0.5	2.8 (0.1)	24.0 (0.1)	19.4 (1.1)	1.9 (0.6)	24.1 (0.1)	17.7 (0.6)
03/11/2002	0-0.5	2.2 (0.4)	24.3 (0.1)	19.0 (0.8)	2.0 (0.2)	24.4 (0.1)	13.1 (0.5)
15/11/2002	0-0.5	3.7 (0.2)	24.1 (0.1)	21.1 (0.8)	2.5 (0.1)	24.0 (0.1)	13.3 (0.5)
29/11/2002	0-0.5	3.3 (0.1)	24.8 (0.1)	17.2 (1.0)	1.2 (0.1)	24.6 (0.1)	13.7 (0.2)
13/12/2002	0-0.5	2.4 (0.3)	23.7 (0.1)	18.0 (1.8)	2.0 (0.3)	23.5 (0.1)	14.3 (1.4)
13/01/2003	0-0.5	3.6 (0.1)	24.2 (0.1)	22.5 (1.0)	2.7 (0.2)	24.2 (0.1)	13.3 (1.0)
07/02/2003	0-0.5	3.1 (0.2)	23.5 (0.1)	25.3 (0.7)	3.0 (0.2)	23.6 (0.1)	17.9 (1.5)
20/03/2003	0-0.5	4.1 (0.4)	24.0 (0.1)	25.2 (0.6)	3.0 (0.3)	24.3 (0.0)	15.5 (1.6)
03/04/2003	0-0.5	2.1 (0.1)	23.8 (0.1)	27.3 (0.8)	3.4 (0.2)	25.7 (0.4)	19.2 (2.3)
15/05/2003	0-0.5	2.5 (0.3)	24.0 (0.2)	26.1 (0.6)	2.4 (0.3)	25.2 (0.2)	18.4 (1.8)
03/07/2003	0-0.5	4.4 (0.3)	24.8 (0.1)	24.2 (0.9)	2.5 (0.2)	18.0 (2.4)	15.4 (1.3)
13/09/2003	0-0.5	3.8 (0.2)	25.2 (0.1)	18.2 (1.1)	1.4 (0.2)	24.8 (0.1)	14.0 (2.0)
26/10/2003	0-0.5	2.7 (0.2)	23.9 (0.2)	17.5 (0.9)	1.6 (0.2)	24.4 (0.1)	13.6 (0.5)
01/11/2003	0-0.5	2.4 (0.3)	24.6 (0.1)	17.9 (0.3)	1.7 (0.1)	24.8 (0.1)	12.9 (0.9)

Table A2 – (continued).

Date	Depth	Control			TFE		
		P_{CO2}	*Ts*	*swc*	P_{CO2}	*Ts*	*swc*
	(m)	(µmol CO_2 m^{-2} s^{-1})	(°C)	(%)	(µmol CO_2 m^{-2} s^{-1})	(°C)	(%)
dd/mm/yyyy		mean (SE)	mean (SE)	mean (SE)	mean (SE)	mean (SE)	mean (SE)
11/01/2002	0.6-2.0	0.4 (0.1)	20.5 (0.5)	22.6 (0.8)	0.6 (0.1)	20.4 (0.5)	20.7 (1.1)
24/01/2002	0.6-2.0	0.3 (0.1)	23.0 (0.1)	23.9 (0.7)	0.9 (0.2)	20.7 (0.1)	19.9 (0.8)
07/02/2002	0.6-2.0	0.5 (0.0)	18.8 (0.9)	-	1.4 (0.3)	18.3 (0.3)	-
21/02/2002	0.6-2.0	0.5 (0.1)	18.2 (0.2)	23.4 (0.7)	1.0 (0.1)	18.0 (0.4)	19.5 (0.5)
07/03/2002	0.6-2.0	0.6 (0.1)	21.1 (0.2)	24.3 (0.6)	0.9 (0.1)	21.9 (0.3)	19.1 (0.6)
23/03/2002	0.6-2.0	0.4 (0.1)	23.8 (0.1)	25.3 (0.6)	1.0 (0.2)	22.2 (0.2)	18.1 (1.1)
07/04/2002	0.6-2.0	0.4 (0.2)	22.4 (0.1)	24.8 (0.4)	0.6 (0.1)	22.1 (0.4)	19.4 (0.7)
28/04/2002	0.6-2.0	0.5 (0.1)	24.1 (0.1)	25.1 (0.6)	0.8 (0.1)	24.6 (0.3)	19.5 (0.7)
25/05/2002	0.6-2.0	0.7 (0.2)	25.4 (0.5)	23.7 (0.5)	0.6 (0.1)	24.6 (0.5)	19.0 (0.5)
03/06/2002	0.6-2.0	0.5 (0.1)	22.9 (0.2)	24.6 (0.8)	0.7 (0.1)	24.2 (0.0)	19.0 (0.7)
16/06/2002	0.6-2.0	0.8 (0.2)	24.9 (0.1)	24.8 (0.6)	1.1 (0.2)	23.8 (0.2)	16.9 (1.1)
01/07/2002	0.6-2.0	0.7 (0.1)	25.0 (0.1)	23.4 (0.7)	0.8 (0.1)	25.1 (0.1)	18.0 (1.0)
15/07/2002	0.6-2.0	0.6 (0.1)	25.0 (0.1)	-	0.5 (0.1)	25.2 (0.1)	-
26/07/2002	0.6-2.0	0.6 (0.1)	25.2 (0.1)	21.2 (0.4)	0.7 (0.2)	25.6 (0.3)	17.1 (0.5)
09/08/2002	0.6-2.0	0.5 (0.1)	25.3 (0.1)	22.3 (0.4)	0.5 (0.1)	25.2 (0.1)	17.2 (0.1)
24/08/2002	0.6-2.0	0.4 (0.0)	24.8 (0.1)	21.3 (0.3)	0.5 (0.1)	24.7 (0.2)	16.5 (0.2)
06/09/2002	0.6-2.0	0.6 (0.1)	25.2 (0.2)	20.1 (0.3)	0.8 (0.1)	25.1 (0.2)	15.9 (0.8)
20/09/2002	0.6-2.0	0.5 (0.1)	24.8 (0.1)	19.5 (0.6)	0.5 (0.0)	24.6 (0.1)	16.2 (0.3)
04/10/2002	0.6-2.0	0.5 (0.0)	24.3 (0.0)	18.9 (0.4)	0.4 (0.1)	24.4 (0.1)	16.6 (0.4)
18/10/2002	0.6-2.0	0.6 (0.1)	24.3 (0.1)	18.8 (0.2)	1.0 (0.4)	24.4 (0.1)	16.4 (0.3)
03/11/2002	0.6-2.0	0.8 (0.4)	24.1 (0.1)	18.3 (0.6)	0.5 (0.1)	24.5 (0.1)	15.5 (0.3)
15/11/2002	0.6-2.0	0.5 (0.1)	24.2 (0.1)	20.3 (1.7)	0.4 (0.1)	24.4 (0.2)	16.2 (0.1)
29/11/2002	0.6-2.0	0.5 (0.1)	24.7 (0.1)	19.2 (1.0)	0.4 (0.1)	24.8 (0.0)	16.0 (0.3)
13/12/2002	0.6-2.0	0.7 (0.0)	24.0 (0.2)	18.0 (0.9)	0.6 (0.1)	24.0 (0.1)	15.9 (0.3)
13/01/2003	0.6-2.0	0.5 (0.0)	24.5 (0.2)	20.4 (1.6)	0.6 (0.0)	24.5 (0.1)	14.9 (0.4)
07/02/2003	0.6-2.0	0.6 (0.1)	24.3 (0.1)	23.3 (1.2)	0.6 (0.1)	24.2 (0.1)	15.8 (0.6)
20/03/2003	0.6-2.0	0.5 (0.1)	24.2 (0.0)	24.7 (0.5)	0.6 (0.2)	24.6 (0.1)	17.7 (1.4)
03/04/2003	0.6-2.0	1.1 (0.2)	24.3 (0.0)	26.2 (0.4)	0.5 (0.2)	25.9 (0.6)	19.5 (1.7)
15/05/2003	0.6-2.0	0.7 (0.1)	23.9 (0.1)	23.9 (0.9)	0.7 (0.1)	25.7 (0.2)	18.9 (1.5)
03/07/2003	0.6-2.0	0.7 (0.0)	25.0 (0.1)	23.4 (0.3)	0.7 (0.1)	18.5 (2.4)	17.2 (0.8)
13/09/2003	0.6-2.0	0.5 (0.1)	25.5 (0.1)	19.9 (0.5)	0.6 (0.1)	25.1 (0.1)	17.2 (0.9)
26/10/2003	0.6-2.0	0.5 (0.1)	24.0 (0.1)	18.1 (0.6)	0.7 (0.1)	24.8 (0.1)	15.1 (0.7)
01/11/2003	0.6-2.0	0.5 (0.1)	24.3 (0.1)	19.0 (0.5)	0.4 (0.0)	25.2 (0.4)	16.8 (0.5)

Table A2 - (continued).

Date	Depth	Control						TFE					
		P_{CO2}		*Ts*		*swc*		P_{CO2}		*Ts*		*swc*	
	(m)	(µmol CO_2 m^{-2} s^{-1})		(°C)		(%)		(µmol CO_2 m^{-2} s^{-1})		(°C)		(%)	
dd/mm/yyyy		mean	(SE)	mean	(SE)	mean	(SE)	mean	(SE)	mean	(SE)	mean	(SE)
11/01/2002	2.1-3.0	0.1	(0.0)	19.9	(0.7)	18.6	(1.3)	0.1	(0.0)	20.3	(0.5)	18.2	(0.6)
24/01/2002	2.1-3.0	0.1	(0.0)	23.3	(0.1)	23.9	(1.7)	0.1	(0.0)	20.9	(0.2)	18.4	(1.2)
07/02/2002	2.1-3.0	0.1	(0.0)	19.1	(0.9)	-		0.1	(0.0)	18.1	(0.3)	-	
21/02/2002	2.1-3.0	0.1	(0.1)	18.4	(0.2)	24.6	(1.2)	0.1	(0.1)	18.0	(0.4)	19.7	(1.5)
07/03/2002	2.1-3.0	0.1	(0.0)	21.4	(0.4)	23.8	(0.9)	0.1	(0.0)	22.5	(0.1)	19.9	(1.5)
23/03/2002	2.1-3.0	0.1	(0.0)	23.7	(0.1)	25.0	(1.3)	0.2	(0.1)	22.1	(0.2)	17.1	(2.7)
07/04/2002	2.1-3.0	0.1	(0.1)	22.3	(0.1)	25.0	(1.2)	0.2	(0.1)	22.3	(0.3)	18.9	(1.3)
28/04/2002	2.1-3.0	0.1	(0.0)	24.1	(0.1)	25.1	(1.3)	0.1	(0.0)	24.7	(0.3)	20.1	(0.7)
25/05/2002	2.1-3.0	0.1	(0.1)	25.3	(0.4)	23.4	(1.4)	0.2	(0.0)	24.8	(0.5)	20.1	(0.7)
03/06/2002	2.1-3.0	0.1	(0.0)	22.8	(0.2)	25.1	(1.2)	0.2	(0.0)	24.2	(0.0)	17.8	(1.9)
16/06/2002	2.1-3.0	0.1	(0.1)	25.0	(0.1)	24.2	(1.3)	0.2	(0.0)	24.0	(0.1)	16.0	(1.2)
01/07/2002	2.1-3.0	0.1	(0.1)	24.9	(0.1)	24.1	(1.2)	0.2	(0.1)	25.2	(0.0)	17.1	(1.8)
15/07/2002	2.1-3.0	0.2	(0.0)	24.9	(0.1)	-		0.3	(0.1)	25.1	(0.1)	-	
26/07/2002	2.1-3.0	0.3	(0.1)	25.1	(0.1)	23.1	(1.0)	0.3	(0.1)	25.8	(0.2)	16.7	(1.6)
09/08/2002	2.1-3.0	0.2	(0.1)	25.1	(0.1)	22.9	(0.8)	0.2	(0.0)	25.3	(0.1)	18.9	(0.6)
24/08/2002	2.1-3.0	0.2	(0.1)	24.6	(0.0)	22.1	(0.9)	0.3	(0.1)	24.6	(0.2)	18.7	(0.4)
06/09/2002	2.1-3.0	0.3	(0.1)	25.1	(0.2)	22.3	(1.0)	0.3	(0.0)	25.0	(0.2)	19.1	(0.4)
20/09/2002	2.1-3.0	0.3	(0.1)	24.6	(0.0)	20.8	(0.8)	0.2	(0.0)	24.6	(0.1)	18.2	(0.3)
04/10/2002	2.1-3.0	0.2	(0.1)	24.2	(0.0)	17.3	(2.7)	0.3	(0.1)	24.4	(0.1)	16.1	(1.6)
18/10/2002	2.1-3.0	0.3	(0.1)	24.4	(0.1)	19.1	(0.3)	0.2	(0.1)	24.5	(0.1)	15.5	(1.4)
03/11/2002	2.1-3.0	0.3	(0.1)	24.2	(0.0)	18.3	(0.6)	0.2	(0.0)	24.5	(0.1)	17.0	(0.6)
15/11/2002	2.1-3.0	0.2	(0.1)	24.2	(0.1)	18.4	(0.6)	0.1	(0.0)	24.5	(0.1)	17.8	(0.4)
29/11/2002	2.1-3.0	0.2	(0.1)	24.6	(0.1)	19.3	(0.9)	0.2	(0.0)	24.8	(0.0)	17.8	(0.4)
13/12/2002	2.1-3.0	0.4	(0.1)	24.1	(0.1)	19.3	(0.5)	0.2	(0.0)	24.2	(0.1)	17.6	(0.9)
13/01/2003	2.1-3.0	0.0	(0.0)	24.5	(0.3)	18.8	(0.8)	0.2	(0.0)	24.6	(0.1)	16.0	(0.8)
07/02/2003	2.1-3.0	0.1	(0.1)	24.4	(0.2)	18.0	(1.9)	0.1	(0.0)	24.5	(0.1)	16.5	(1.2)
20/03/2003	2.1-3.0	0.1	(0.0)	24.4	(0.1)	25.2	(1.2)	0.1	(0.0)	24.9	(0.0)	19.0	(0.8)
03/04/2003	2.1-3.0	0.4	(0.1)	24.2	(0.3)	25.1	(1.2)	0.1	(0.0)	26.6	(0.2)	20.1	(1.4)
15/05/2003	2.1-3.0	0.1	(0.0)	23.9	(0.1)	26.4	(1.3)	0.1	(0.0)	25.8	(0.1)	19.0	(1.8)
03/07/2003	2.1-3.0	0.1	(0.0)	24.9	(0.1)	24.9	(1.1)	0.2	(0.0)	18.5	(2.4)	20.0	(1.3)
13/09/2003	2.1-3.0	0.3	(0.1)	25.4	(0.1)	19.5	(0.7)	0.2	(0.1)	25.0	(0.1)	18.2	(0.6)
26/10/2003	2.1-3.0	0.2	(0.1)	23.6	(0.2)	18.8	(1.3)	0.2	(0.0)	24.7	(0.1)	18.0	(0.6)
01/11/2003	2.1-3.0	0.2	(0.1)	24.1	(0.1)	19.5	(1.0)	0.2	(0.0)	25.0	(0.3)	18.2	(0.5)

Acknowledgements

I want to thank God for the strength and perseverance He has put in my heart to achieve this goal in my life. I also want to thank my family, specially my husband, for their support and love in all times.

I am grateful to Dr. Michel Keller who trusted my work and presented me as a candidate to the PhD position offered by the University of Göttingen in the LBA project.

I would like to thank Prof. Dr. Edzo Veldkamp from the Institute of Soil Science and Forest Nutrition for supervising the thesis, for his support during the study and for his critical input during the development of the field work, data analysis and writing of the thesis.

I would also like to thank Dr. Luitgard Schwendenmann for her unconditional support and supervision in the field work, as well as during the analysis and discussion of the data.

In the same way I want to thank Dr. Marife Corre for her continuous support and supervision during the field and lab work, as well as during the analysis and writing of the thesis.

Many thanks to the Caxiuanã LBA-EU team, especially Prof. Antonio Carlos Lola da Costa for his constant support in field work, Dr. Patrick Meir for his encouragement, and Rafael Ferreira da Costa, Alan Pantoja and Joao Athayde for their companionship and helpful ideas and work force in difficult times.

I gratefully acknowledge the help of Dr Maria de Lourdes Ruivo, and the valuable work of Brenda Rocha Guimaraes, Rosiene Keila Paixao and Alessandro Rosario.

And finally I want to thank CNPq/DAAD for the financial support through the scholarship.

Curriculum vitae

Eleneide Doff Sotta
Forest Engineer
born on the 28 May 1972 in Curitiba, Paraná, Brazil

1991 - 1995 Graduation in Forest Engineering - Federal University of Parana - UFPR, Curitiba, Paraná, Brazil.

1996 - 1998 Masters in Tropical Forest Science, National Research Institute of Amazon - INPA, Manaus, Amazonas, Brazil. CO_2 flux between soil and atmosphere in tropical rain forest of central Amazonia.

1999 - 2000 Researcher in Instituto do Homem e Meio Ambiente da Amazonia – IMAZON, in Belém, Pará, Brazil. Indicators for Sustainable Development in Eastern Amazon. Project coordination and execution.

2001 - 2002 Research Assistant in Institute of Soil Science and Forest Nutrition – IBW, University of Göttingen, Germany. Soil CO_2 dynamics in Eastern Amazon, Para, Brazil. Project execution.

2003 - 2006 PhD student in University of Göttingen, Germany. Soil CO_2 dynamics and N cycling in an Eastern Amazon Rainforest, Caxiuanã, Brazil.

Sotta ED, Corre M, Veldkamp E. (in preparation). Mechanisms of soil N retention in an Eastern Amazonian Rainforest, Caxiuanã, Brazil. Ecosystems

Sotta ED, Veldkamp E, Schwendenmann L, Guimarães BR, Paixão RK, Meir P, Ruivo MLP, da Costa ACL. (in preparation) Effects of an induced drought on the soil CO_2 production and soil CO_2 efflux in an Eastern Amazonian Rainforest, Brazil.

Sotta ED, Veldkamp E, Guimarães BR, Ruivo MLP, Almeida S. (in review) Landscape and climatic controls on spatial and temporal variation in soil CO_2 efflux in an Eastern Amazonian Rainforest, Caxiuanã, Brazil. Forest Ecology and Management.

Sotta ED, Meir P, Malhi Y, Nobre AD, Hodnett M Grace J. (2004) Soil CO_2 efflux in a tropical forest in the central Amazon. Global Change Biology, 10: 601-617.